Department of Electrical and Computer Engineering
Lisbon, Portugal

Higher Technical School of Telecommunication Engineering
Valencia, Spain

Graduation Project

Adaptive Beamforming in UTRA-TDD Applying the Recursive Least Squares Algorithm

Juan Luis Méndez Fernández

Lisbon, Portugal

June 2001

This work has been carried out under the supervision of:

Prof. Luís M. Correia

Department of Electrical and Computer Engineering
Instituto Superior Técnico
Technical University of Lisbon

To my parents

Acknowledgements

There are so many people present in my life that I cannot refer everyone, but at least a brief mention has to be done in this work to show that all are very important to me, and that without them this objective would have never achieved.

In the first place, I want to thank my parents, because this moment is more for them than for me. I know the much they have fought for their son to become an Engineer, with their presence and love near to me in my bad days.

Thanks to Prof. Correia, for his attention and dedication to make my stay in Lisbon easier, spending his time and always offering his help to me.

Thanks to João, for illustrating my life in Portugal and for his continuous classes to teach Portuguese, something that I did not get as much as I had wished.

Thanks to Gabriela and Lucio, colleagues of the Asilum project where my project is integrated: their help, support and kindness are the best regards I will never forget.

During my stay in Lisbon I met many people who made my stay in Lisbon easier: Krzysztof, Hugo, Zé, Rui, Pedro, Ramon, Chiara, Teresa, Jochan, and specially Claudia.

Thanks to my colleagues of the Figanier's laboratory, with whom I spent nice moments and made the work more pleasant; thanks Hugo, Rui, David and Alberto.

Thanks to my colleagues of my stay in Valencia, without them those long years in Valencia would had not been the same; Fabi, Joaquin, Manolo, Polo, Gines, Sergio, Frano, Zaplana, Samu, thanks.

Thanks to the friends from my home town, in spite of so much time out of home I go on enjoying their friendship, sharing a lot of things together, Vargas, Reina, Ramon, Jose Miguel, Eric, Carri, Soto... Forgive me if I miss anyone, but it is impossible to remember all the names that were important in my life.

Francis and Loli, my brothers, you are a very important part in my life, and I want to remember you in this day so important for me.

Abstract

This document presents the study of an application of a non-blind adaptive algorithm, Recursive Least Squares, at the base station, in a UTRA-TDD perspective, for the up- and downlinks. Since smart antenna technologies have been recommended as a way to increase capacity in UMTS, their application will be a reality in the future, when the improvement of UMTS will be needed. Beamforming is a technique where an adaptive algorithm updates the weights after each iteration, ideally locating nulls in the directions of the arriving interfering signals.

Since a non-blind adaptive algorithm is implemented, a reference acquisition method for CDMA is used. This work being a joint algorithm-propagation performance problem, specific propagation scenarios are considered and adequate Wideband Directional Channel Models are applied, with several mobile interfering terminals present. The algorithm is applied to a street where various mobile terminals are distributed. The algorithm convergence analysis, a specific channel cluster model is used, based on the Geometrically Based Single Bounce models.

For all simulated scenarios a beamforming processing gain has been found, 7 dB for the worst cases with 16 MTs close to base station. The number of needed iterations is small and the complexity cost to add a new user in terms of *Flops* is low.

Keywords

UMTS, Adaptive Antennas, Recursive Least Squares, TDD mode, Up-link.

Table of Contents

Acknowledgments ..... **v**

Abstract ..... **vii**

Table of Contents ..... **ix**

List of Figures ..... **xi**

List of Tables ..... **xv**

List of Acronyms ..... **xvii**

List of Symbols ..... **xxi**

1 Introduction **1**

2 The Universal Mobile Telecommunications System **3**

2.1 INTRODUCTION 3
2.2 WCDMA 5
2.2.1 General Concepts *5*
2.2.2 The FDD Mode *7*
2.2.3 The TDD Mode *13*
2.3 CELL STRUCTURE 15

3 Adaptive Beamforming **17**

3.1 INTRODUCTION 17
3.2 BEAMFORMING AND SPATIAL FILTERING 20
3.3 RECURSIVE LEAST SQUARES ALGORITHM 23

4 RLS Adaptive Beamforming Implementation **29**

4.1 ALGORITHM IMPLEMENTATION 29
4.1.1 Assupmtions *29*
4.1.2 Wideband Directional Channel Model *30*
4.1.3 Application to UTRA-TDD *32*
4.1.3 RLS Problem Description 33
4.2 RLS PERFORMANCE 35
4.2.1 Description of Evaluated Quantities *35*
4.2.2 Initialisation and Transient Phase Analysis *36*
4.2.3 Test Cases *38*
4.2.4 RLS Performance Results on Average WDCM *40*
4.2.5 RLS Performance Results on one WDCM Concretisation *46*

5 Application of the RLS Algorithm to Specific Scenarios **57**

5.1 SCENARIOS DESCRIPTION ..... **ERROR! BOOKMARK NOT DEFINED.**
5.2 ANALYSIS OF RESULTS ..... **ERROR! BOOKMARK NOT DEFINED.**

6 Conclusions 68

Appendix A Criteria and Algorithms for Adaptive Beamforming 71

A.1 CRITERIA 71
A.1.1 Method of Least Squares 71
A.1.2 Method of Steepest Descent 72
A.2 ADAPTIVE ALGORITHMS 73
A.2.1 Least Mean Square Algorithm 74
A.2.2 Direct Sample Covariance Matrix Inversion 75
A.2.3 Conjugate Gradient Algorithm 77
A.2.4 Constant Modulus Algorithm 78
A.2.5 Other Algorithms 78

Appendix B Plots of the Cases Under Study of Chapter 4 79

Appendix C Plots of other Scenarios of Simulation 85

References 88

List of Figures

Figure 2.1. UMTS coverage is universal (extracted from [UMTS98a]). 3

Figure 2.2. Frequency bands for IMT-2000 (extracted from [Fern00]). 5

Figure 2.3. Principles of FDD and TDD operation (extracted from [HoTo00]). 6

Figure 2.4. Relation between spreading and scrambling (extracted from [HoTo00]). 7

Figure 2.5. Channelisation code tree (extracted from [HoTo00]). 8

Figure 2.6. Closed-loop power control in CDMA (extracted from [HoTo00]). 9

Figure 2.7. Softer handover (extracted from [HoTo00]). 11

Figure 2.8. Soft handover (extracted from [HoTo00]). 12

Figure 2.9. Frame structure of UTRA TDD (extracted from [HoTo00]). 14

Figure 2.10. UL/DL asymmetries in TDD (extracted from [HoTo00]). 14

Figure 2.11. Example of UMTS layer network (extracted from [UMTS98b]). 16

Figure 3.1. Generic adaptive beamforming scheme (extracted from [LiLo96]). 18

Figure 3.2. Spatial filtering elements. 20

Figure 3.3. Representation of the NB and WB basic beamforming structures (extracted from [LiRa99]). 22

Figure 4.1. General Block Diagram of the Adaptive beamforming implementation 29

Figure 4.2. Square error representation vs. number of iterations for several δ_{RLS} 37

Figure 4.3. Plot of the residual error norms vs. the number of RLS iterations for all active links 42

Figure 4.4. Average SINR vs. the number of RLS iterations, for link MT1-BS. 44

Figure 4.5. Average BER vs. the number of RLS iterations for all active links, Cs #6. 45

Figure 4.6. Residual norm vs. number of RLS iterations for all links, cases #5 and #6. 46

Figure 4.7. SINR vs. the number of iterations for all links, cases #3 and #6. 48

Figure 4.8. BER vs. the number of iterations for all links, Cs #6. 49

Figure 4.9. Number of RLS flops per iteration vs. the number of antenna elements. 51

Figure 4.10. Number of RLS flops per iteration vs. the number of antenna elements, function of the number of users. 52

Figure 4.11. The final antenna patterns, for all links, Cs #1, with the indication of the angular position of clusters. 55

Figure 4.12. The final antenna patterns all links, Cs #6, with the indication of the angular position of clusters. 56

Figure 5.1. Spatial distribution of scatterers within a street (extracted from [Marqu01]).... 57

Figure 5.2. DCIR results for 50 and 500m. 58

Figure 5.3. Environment for simulation. 59

Figure 5.4. Beampattern vs. the DCIR for $d_{\text{BS-MT}}$=500m. 63

Figure 5.5. Beampattern vs. the DCIR for $d_{\text{BS-MT}}$=1000m. 64

Figure 5.6. SINR vs. the number of iterations, for L=4 at 50 m..... 64

Figure 5.7. SINR vs. the number of iterations, for L=8 at 50 m..... 65

Figure B.1. Average SINR vs. the number of iterations, for link MT2-BS. 77

Figure B.2. Average SINR vs. the number of iterations, for link MT3-BS 77

Figure B.3. Average SINR vs. the number of iterations, for link MT4-BS 78

Figure B.4. Residual error norm for Cs #1. 78

Figure B.5. Residual error norm for Cs #2. 79

Figure B.6. Residual error norm for Cs #3. 79

Figure B.7. Residual error norm for Cs #4. 80

Figure B.8. SINR for Cs #1. 80

Figure B.9. SINR for Cs #2. 81

Figure B.10. SINR for Cs #4. 81

Figure B.11. SINR for Cs #5. 82

Figure C.1. SINR vs. the number of iterations for L=16 and M=4..... 83

Figure C.2. G_{bf} vs. the number of iterations for L=16 and M=4..... 83

Figure C.3. SINR vs. the number of iterations for L=16 and M=12..... 84

Figure C.4. G_{bf} vs. the number of iterations for L=16 and M=12..... 84

Figure C.1. SINR vs. the number of iterations for L=16 and M=6..... 85

List of Tables

Table 2.1. Main WCDMA parameters (extracted from [HoTo00]) 6

Table 2.2. Functionality of the channelisation and scrambling codes (extracted from [HoTo00]). 8

Table 2.3. Maximum available data rates (extracted from [UMTS98b]). 15

Table 4.1. Representation of the weight values at iteration 5, 20 and the optimal weight... 38

Table 4.2. Parameters for the simulations. 39

Table 4.3. Number of iterations for RLS convergence. 43

Table 4.4. Final beamforming gain for the RLS. 44

Table 4.5. Number of RLS iterations after which the 1% variation criterion is met. 47

Table 4.7. The weights vectors calculated, along iterations, for link 1, Cs #1. 53

Table 4.8. The weight vectors calculated, along iterations, for link 1, Cs #6. 54

Table 5.1. Simulation results for L=4. 61

Table 5.2. Simulation results for L=8. 61

Table 5.3. Simulation results for L=16. 61

Table 5.4. Simulation average results for 100 WDCM concretisations, for L=16. 62

Table 5.5. Simulation results for L=16 and $d_{\text{BS-MT}}$=50 m. 62

Table 5.6. Simulation results for L=8 and M=12. 63

List of Acronyms

3GPP	3rd Generation Partnership Project
AoA	Angle-of-Arrival
AWGN	Additive White Gaussian Noise
BA	Beamforming Antennas
BER	Bit Error Rate
BS	Base Station
CDMA	Code Division Multiple Access
CG	Conjugate Gradient
CMA	Constant Modulus Algorithm
Cs	Case under study
DBF	Digital Beamforming
DCIR	Directional Channel Impulse Response
DesS	Desired Signal
DoA	Direction-of-Arrival
DoF	Degree-of-Freedom
DTX	Discontinuous Transmission
DL	Down-Link
DS-CDMA	Direct Sequence Code Division Multiple Access
DSP	Digital Signal Processing
FDD	Frequency Division Duplex
FDMA	Frequency Division Multiple Access
FER	Frame Error Rate
Flops	Floating Point Operations
GBSB	Geometrically-Based Single Bounce
GPS	Global Position System
GSM	Global System for Mobile communications
IMT-2000	International Mobile Telecommunications-2000
ISI	Inter-Symbol Interference
LMS	Least-Mean-Square
LoS	Line-of-Sight
LS	Least Squares
MAI	Multiple Access Interference

MMSE	Minimum Mean-Square-Error
MSE	Minimum Square Error
MT	Mobile Terminal
NB	Narrowband
NDesI	Non-Desired Interference
NN	Neural Networks
OVSF	Orthogonal Variable Spreading Factor
PDF	Probability Density Function
PN	Pseudo Noise
PSCH	Physical Synchronisation CHannel
QPSK	Quadrature-Phase Shift Keying
QoS	Quality of Service
RF	Radio Frequency
RLS	Recursive Least Squares
RNC	Radio Network Controller
Rx	Receiver
SA	Smart Antennas
SF	Spreading Factor
SINR	Signal to Interference-plus-Noise Ratio
SIR	Signal to Interference Ratio
SMI	Sample Matrix Inversion
SNR	Signal to Noise Ratio
SoI	Signal-of-Interest
SD	Steepest Descent
TDD	Time Division Duplex
TDMA	Time Division Multiple Access
ToA	Time-of-Arrival
Tx	Transmitter
UL	Up-Link
ULA	Uniform Linear Array
UMTS	Universal Mobile Telecommunication System
UTRA	UMTS Terrestrial Radio Access
VHE	Virtual Home Environment
WB	Wideband
WCDMA	Wideband Code Division Multiple Access

WDCM	Wideband Directional Channel Model

List of Symbols

α_{n_c}	Overall equivalent attenuation of signals from the n_cth cluster
Γ_{i_s,n_c}	Reflection coefficient of the i th scatterer within the n_cth cluster
$\beta_e(n,i)$	Error weight, obtained at iteration I, used for instant n.
δ_{RLS}	Initial value for the inverse correlation matrix, for the RLS
ϕ	Azimuth coordinate
ϕ_{n_c}	Azimuth corresponding to the n_c clsuter
ϕ_{i_s,n_c}	Azimuth corresponding to the i_sth scatterer within the n_cth cluster
$\phi_{i_s,n_c,l}$	Azimuth corresponding to the i_sth scatterer within the n_cth cluster, from link l
$\mathbf{\Phi}(n)$	Auto-correlation matrix with past correlation contributions
λ	Wavelength
λ_{RLS}	Exponential weighting factor for RLS
λ_{max}	Maximum eigenvalue of $\mathbf{R_x}$
μ	Convergence step constant
σ_x^2	Variance of the signal samples $\mathbf{x}(n)$
σ_e^2	Variance of the error measurement process
τ	Time delay
τ_{n_c}	Sampling instant/Delay time, corresponding to cluster n_c
$\xi(n)$	A priori estimation error at instant n
$\xi_l(n)$	A priori estimation error at instant n, corresponding to link l
$a_l(m)$	Steering vector mth element
$\mathbf{c}_{\mathrm{d}}^{(l)}$	Code vector corresponding to the desired signal, from link l
$c_d^{(l)}$	Code symbol corresponding to the desired signal, from link l
$\hat{c}_d^{(l)}$	Estimated code symbol corresponding to the desired signal, from link l
$\hat{c}_{\mathrm{d}}^{(l)}(n\|X_{nn})$	Beamformer code symbol estimate corresponding to $\mathbf{x}(n)$, from link l
$d(n)$	Desired signal at instant n
d_{el}	Distance between antenna array elements
$\mathbf{dir}(n)$	Direction vector
$\mathbf{d}_l$	Desired vector, corresponding to link l

$d_l(n)$	Desired symbol, at instant n, corresponding to link l
$\mathbf{e}_l$	Weight estimation error vector from link l
$\mathbf{e}_0(i)$	Measurement error at iteration i for Least Square
E_b	Energy per bit
$\mathbf{e}_{opt}$	Weight estimation error vector at optimum
$f(n)$	General cost function, function of n
$f(\mathbf{w})$	General cost function, function of $\mathbf{w}$
$\mathbf{g}_{\mathrm{RLS}}(n)$	Convergence step gain vector at instant n
G_{bf}	Beamforming processing gain
G_{bfm}	Mean Beamforming processing gain
G_p	Processing gain
$h_l(\tau;\phi)$	Channel impulse response, function of τ and ϕ, for link l
i	Sub-iteration index, lower than n
i_s	Scatterer index
I_s	Number of scatterers per cluster, per link
$\mathbf{I}$	Identity matrix
l	Link index
L	Total number of links
L_{T}	Total number of orthogonal arriving signals
m	Antenna element index
M	Number of antenna array elements
n	Sampling instant or present iteration index
n_c	Cluster index
N_{b}	Number of correlation data samples
N_c	Total number of clusters
N_0	Spectral Noise Power Density
N_s	Total number of samples
$\overline{n_{n,m}}$	Complex noise signal contribution, at instant n and antenna element m
$\mathbf{P}(n)$	Estimate of the inverse of the correlation matrix at iteration n
P_{DesS}	Desired signal power
P_{NDesI}	Non-desired interference power
Q	Q-function
$\mathbf{r}$	Cross-correlation between input signal and desired signal

$\mathbf{res}$	Residual error vector
$\mathbf{res}_l$	Residual error vector, corresponding to link l
$\mathbf{R_x}$	Auto-correlation matrix of $\mathbf{x}$
$res(i)$	Residual error at iteration i
$\mathbf{res}_{opt}$	Residual error vector at optimum
T_b	Chip period
ts	Number of time slots
$\mathbf{U}$	Array input signal matrix
$u_{n,m}$	Baseband signal, at instant n and antenna element m
$\mathbf{W}$	Weight vector
$\mathbf{w}_l$	Weight vector for link l
$\mathbf{w}_{opt,l}$	Optimum weight vector from link l
$\mathbf{x}(n)$	Input vector to the Rx antenna, at instant n
$\mathbf{X}$	Matrix of consecutive arry inputs
$y(n)$	Output signal, at instant n
$\mathbf{z}(n)$	Cross-correlation vector with past correlation contributions
tr[$\mathbf{R}$]	Trace of matrix $\mathbf{R}$
$\mathbf{R}_x^{-1}$	Inverse of autocorrelation matrix
$\hat{\mathbf{w}}(n)$	Estimate of $\mathbf{w}$
$\mathbf{w}^{\mathrm{H}}$	Hermitian transpose of vector $\mathbf{w}$
ξ^*	Conjugate of ξ
$\nabla\left\{\xi^2(n)\right\}$	Gradient vector of function ξ, at instant n

1 Introduction

This report shows the result of eight long months of work, a difficult work for the study of a new telecommunications system, nevertheless, well known for everyone, the Universal Mobile Telecommunications System, UMTS. Europe has put a lot of expectations and money into the development of UMTS, although, today, nobody knows what will be the penetration of the system in the population, will be and not even the success is ensured. However, many applications and services are being studied and modelled to be used in UMTS.

Although UMTS is not a reality yet, because the terminals are not for sale, in fact there are many technical efforts to improve it, e.g., to increase the capacity or coverage when the high demand for high data rates will require it. Within so many applications and services that are being studied to be implemented under the support of UMTS, the technical part must provide an adequate platform for their utilisation. In order to support these high demands, it is expected that the system will need techniques such as Adaptive Antennas or Smart Antennas (SA). Adaptive Antennas is a current topic that is being developed to be used in wide radio areas. This work addresses a mechanism that can be included in Adaptive Antennas, but the concept of Adaptive Antennas is larger than the one studied in this report, where only a non-blind Adaptive Beamforming implementation is studied.

The subject of SA has been widely studied for many decades, always very close together to radar techniques. Its early use in radar applications has quickly evolved with the explosive growth of mobile and satellite communications. In the mobile field, smart technologies are not only being applied at the antenna level, but also at the receiver and at baseband processing software ones. The ultimate benefit of these techniques is to increase cellular capacity and range. Furthermore, with the use of Code Division Multiple Access (CDMA), where Multiple Access Interference (MAI) power is a fundamental capacity limiting factor, adaptive beamforming reveals to be another complementary means for Signal-to-Interference-plus-Noise Ratio (SINR) optimisation.

The problem studied in this work is limited to the antenna array level, dealing with the formation of a lobe structure that results from the dynamic variation of an element-space processing weight vector. The beamforming is controlled by an adaptive algorithm, the Recursive Least Squares (RLS), minimising a particular cost function, ideally directing beams

towards the Signal-of-Interest (SoI) and nulls into the directions of interference, resulting in the increase of a link's SINR.

Additionally, the study of an adaptive algorithm within a beamforming solution needs to be verified together with a well-defined propagation channel. A Wideband Directional Channel Model (WDCM) is applied to the street canyon, without and with single and several mobile interfering terminals, and studying how the propagation channel characteristics and the distance of the users affect the convergence.

Maybe the extraordinary advances in processor speed and power consumption reduction will result in that the algorithm complexity and speed will not be a determinant factor, the key issue being the largest SINR gain, for critical traffic areas and high data services. Nevertheless, it is of interest to study the complexity of this implementation, for which a study on the number of Floating point operations (*Flops*) required for the implementation of the algorithm is presented.

In order to understand the importance of an implementation like this, the knowledge of the radio mechanisms in radio propagation is required, since the major part of these mechanisms can be improved with the use of adaptive techniques, like Adaptive Beamforming. The development of techniques that enable to exploit the reduction of the power required to implement the system will affect UMTS services, since in CDMA the limitation is directly related to the interfering power. All the efforts to reduce interference imply more relaxed power requirements, affecting UMTS especially in terms of capacity and Quality of Service (QoS).

In Chapter 2, an overview on UMTS is presented, mainly for the most important radio and coding aspects. The radio aspects are important, since they form the physical group of parameters that are directly improved by the use of Adaptive Beamforming. The part of coding in UMTS also needs to be clarified, since a non-blind implementation is used, therefore, a reference signal being required, the code. Chapter 3 covers a brief description about the concept of Beamforming Antennas (BA), narrow- and wideband approaches, and an in- depth description of the RLS algorithm, which is the algorithm used to control the beam pattern. Then, in Chapter 4, a performance analysis is presented, including the studied test cases, a description of the evaluated parameters, and the results for an adequate WDCM. Next, in Chapter 5, a more realistic channel model is employed and more simulation scenarios are addressed, results for the gain coming from the use of Beamforming being presented.

2 The Universal Mobile Telecommunications System

2.1 Introduction

The great market expectations for third-generation mobile radio systems (IMT-2000) show an increasing demand for a wide range of services from voice to high and advanced data rate services in order to support mobile multimedia. The market for advanced wireless communications is the motivation for an international standardisation for IMT-2000, the European and Japan version being UMTS [ChMO99].

UMTS has been conceived to be a global system, comprising both national terrestrial and global satellite components [UMTS98a]. Figure 2.1 shows how UMTS universal coverage is conceived. It shows two goals to be achieved [UMTS98a], [HoTo00]:

- The first one tries to achieve the named personal communications, allowing roaming in private cordless or fixed network, into a pico / micro cellular public network, then into in a wide area macro cellular network and then to a mobile satellite network.
- The second one is to achieve this with a consistent delivery of the, "look and feel" of services via the so-called "virtual home environment" (VHE).

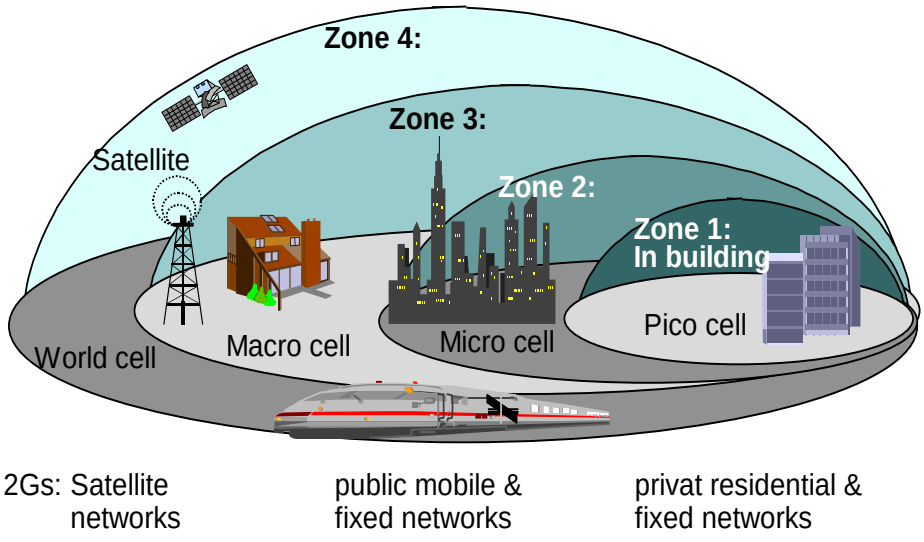

Figure 2.1. UMTS coverage is universal (extracted from [UMTS98a]).

UMTS will allow higher user bit rates [HoTo00] on circuit-switched connections up to 384 kbps and on packet-switched connections up to 2 Mbps. Although at the start of UMTS not all of the QoS functions will be implemented (like delay-critical applications, which will be carried on circuit-switched bearers), later it will be possible to support delay-critical services as packet data with QoS functions [HoTo00].

Guaranteeing QoS is a significant factor for the development of a telecommunications system. This is an important characteristic in UMTS, which must be carefully achieved, to cope with market expectations, thus ensuring the take off of UMTS. QoS has been defined by the UMTS Forum as the collective effect of service performance, which determines the degree of satisfaction of one user. Due to the multi-service nature of UMTS, different classes must be considered with different associated considerations for each one.

Availability of spectrum is a prerequisite for the economical success of a new radio system. It is important that all countries agree on a common spectrum for allocating third-generation systems, since different systems have to share a spectrum that is more saturated each day, with more radio systems, facilitating roaming within each third-generation system. Adequate access to spectrum is a key requirement for the development of UMTS [UMTS98b].

In Figure 2.2, the IMT-2000 spectrum situation is shown in some countries and regions. In Europe the identified bands for terrestrial UMTS in the Frequency Division Duplex (FDD) case are [1920, 1980] MHz in the Uplink (UL) and [2110, 2170] MHz in the Downlink (DL), and in the Time Division Duplex (TDD) case are [1900, 1920] MHz and [2015, 2025] MHz. This frequency distribution was agreed in the 1992 WARC Decision, but in WRC 2000 in Istanbul more bands were identified, depending of future market demand and on the decline of Global System for Mobile communications (GSM), so that different operators can use them in the next years [Fern00]. This chapter addresses both TDD and FDD bands.

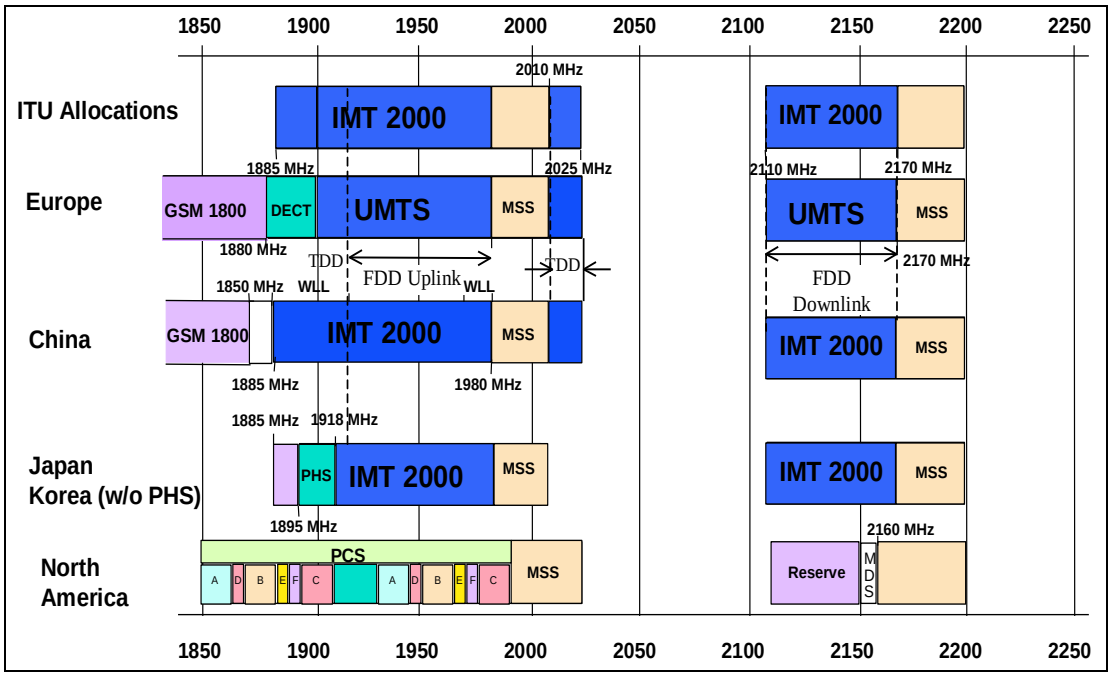

Figure 2.2. Frequency bands for IMT-2000 (extracted from [Fern00]).

2.2 WCDMA

2.2.1 General Concepts

WCDMA (Wideband Code Division Multiple Access) is a Direct-Sequence CDMA (DS-CDMA) system, which has been chosen as the basic radio access technology for UMTS Terrestrial Radio Access (UTRA). The user data bits are spread over a wide bandwidth by multiplying the user data with quasi-random bits (called chips) derived from CDMA spreading codes. The used chip rate 3.84 Mcps leads to a carrier bandwidth of approximately 5 MHz, supporting high user data rates, allowing certain benefits such as increased multipath diversity and making possible to a network operator to deploy multiple 5 MHz carriers to increase capacity in form of hierarchical cell layers. Each user is allocated frames of 10 ms duration, in which time the user data rate is kept constant, but this data rate can change from frame to frame [HoTo00].

WCDMA supports the operation of asynchronous Base Stations (BSs); hence, there is no need for a global time reference, such as Global Position System (GPS). The deployment of indoor and micro BSs is easier when no GPS signal needs to be received, which is an advantage for UMTS, being different from for example, IS-95, which requires a GPS reference [HoTo00].

WCDMA supports two basic modes of operation (see Figure 2.3) [HoTo00]:

- Frequency Division Duplex: Two separate 5 MHz carrier frequencies are used for the UL and DL respectively, hence requiring a pair of bands;
- Time Division Duplex: In the TDD mode only one 5 MHz carrier is time-shared between UL and DL, using a guard period between both ways, therefore being implemented in an unpaired band.

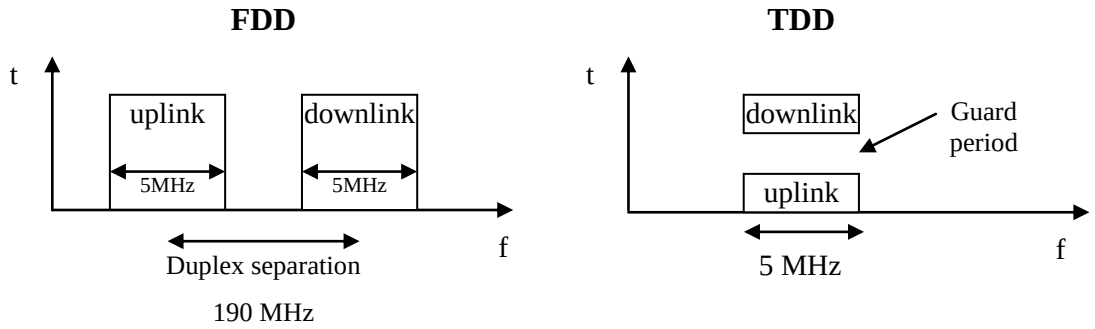

Figure 2.3. Principles of FDD and TDD operation (extracted from [HoTo00]).

WCDMA employs coherent detection in UL and DL, based on the use of pilot symbol or common pilot, and also introduces new features to get advanced CDMA receiver concepts, such as multi-user detection and Smart Antennas [HoTo00].

Table 2.1 summarises the main characteristics of WCDMA, which have been commented before.

Multiple access method	DS-CDMA
Duplexing method	FDD / TDD
Base station synchronisation	Asynchronous operation
Chip rate	3.84 Mcps
Frame length	10ms
Service multiplexing	Multiple services with different QoS requirements
Multirate concept	Variable spreading factor and multicode
Detection	Coherent using pilot symbols or common pilot
Multiuser detection, smart antennas	Supported by the standard, optional in the implementation

Table 2.1. Main WCDMA parameters (extracted from [HoTo00]).

UMTS will support inter-frequency handover for operation with hierarchical cell structures and handover to other systems, mainly GSM. The two systems will co-exist during many years, due to strong presence of second-generation systems today, which is not easily left behind [HoTo00].

2.2.2 The FDD Mode

In WCDMA data is modulated in Quadrature-Phase Shift Keying (QPSK), the spreading process being done by two sequences that are multiplied by the date rate to obtain the resulting chip rate. The process is shown in Figure 2.4:

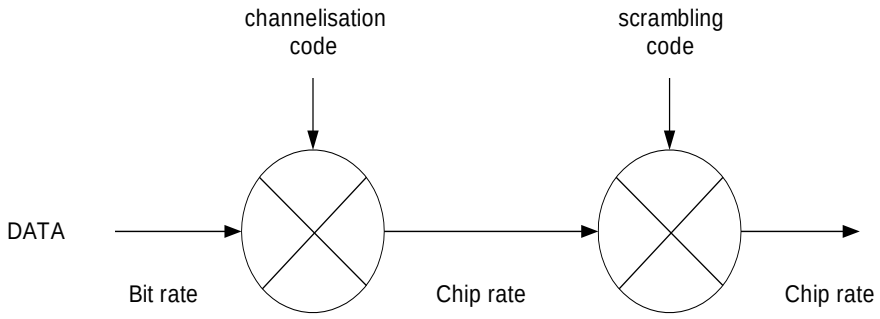

Figure 2.4. Relation between spreading and scrambling (extracted from [HoTo00]).

The spreading operation is the multiplication of each user data bit by a sequence of a defined length to achieve the final chip rate. Since in UMTS the bit rate is not fixed, the length of the channelisation codes can change according to [Ito00b], where the different lengths are defined for the established data rate. Scrambling is used on top of spreading, so it does not change the signal bandwidth but only makes the signals from different sources separable from each other.

The spreading/channelisation codes of UTRA are based on the Orthogonal Variable Spreading Factor (OVSF) technique [Ito00b], Figure 2.5. The use of OVSF codes allows the spreading factor to be changed and the orthogonality between different spreading codes to be kept.

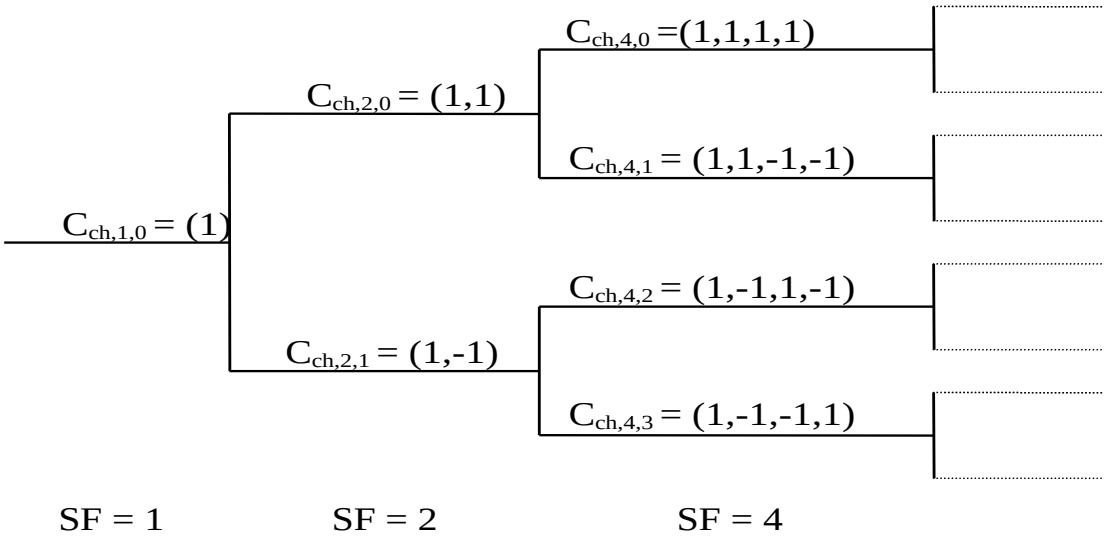

Figure 2.5. Channelisation code tree (extracted from [HoTo00]).

The functionality and characteristics of the scrambling and channelisation codes are summarised in Table 2.2.

	Channelisation code	Scrambling code
Usage	*Uplink*: Separation of physical data and control channels from same terminal *Downlink*: Separation of DL connections to different users within one cell	*Uplink*: Separation of terminal *Downlink*: Separation of sectors (cells)
Length	4-256 chips DL also 512 chips	*Uplink*: (1) 38400 chips (2) 256 chips Option (2) can be used with advanced BS Rx *Downlink*: 38400 chips
Number of codes	Number of codes under one scrambling code = spreading factor	*Uplink*: Several millions *Downlink*: 512
Code family	OVSF	Long 10 ms code: Gold code Short code: Extended S(2) code family
Spreading	Increase transmission bandwidth	No increase transmission bandwidth

Table 2.2. Functionality of the channelisation and scrambling codes (extracted from [HoTo00]).

Power Control is, perhaps, the most important characteristic in WCDMA, since without it one mobile could block a whole cell, in particular on the UL. WCDMA uses the closed-loop transmission power control, but the open-loop power control is also used to make the first estimation [HoTo00].

Open-loop power control: This mechanism consists in making a rough estimate of path loss by means of a DL beacon signal, which can induce errors because fast fading is uncorrelated between UL and DLs, (due to the frequency separation in the FDD mode). This mechanism is used only to make the first estimation of power of the Mobile Terminal (MT) at the beginning of a connection.

Fast closed-loop power control: In the UL, the BS performs frequent estimates of the received Signal-to-Interference Ratio (SIR) and compares it to a target SIR, after which the BS the BS will command the MT to lower or higher its power, Figure 2.6. In FDD mode, this measure command react cycle is executed at a rate of 1500 times per second (1.5kHz) for each MT, operating faster than the speed of fast Rayleigh fading for low to moderate mobile speeds.

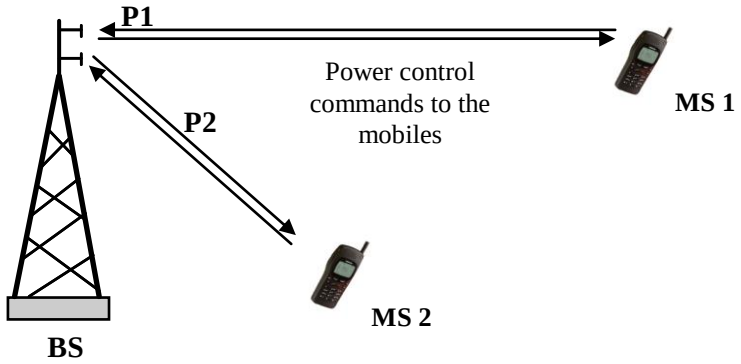

Figure 2.6. Closed-loop power control in CDMA (extracted from [HoTo00]).

Introducing power control in WCDMA leads to an additional gain, which is larger:

- for low mobile speeds than for high ones;
- in required E_b/N_o than in transmission power;
- for those cases where only a low multipath occurs.

where E_b is the energy per bit and N_0 is the spectral noise power density.

The main sources of errors in the received powers arise from inaccurate SIR estimation, signalling errors and delays in the power control loop. The compensation of fading causes peaks in the transmission power, which can be minimised by the use of diversity, leading to more stable transmitted power. Diversity can be implemented in several ways, like for example, receive antenna diversity, transmit antenna diversity or macro diversity.

In WCDMA fast power control operates on the basis of one command per slot, but multiples of that step size can be used and smaller step sizes can be emulated. The emulated step size means that the 1 dB step is used, for example only every second slot, thus emulating the 0.5 dB step size. Implementing true steps below 1 dB are difficult to achieve technologically. The other true step size specified is 2 dB [HoTo00].

In the DL, power control is used with another motivation. There is no near-far problem and the intention is to maintain the power level in order not to increase the interference with other cells.

Outer power control is associated to closed-loop power control. This property adjusts the target SIR setpoint in the BS according to the needs of the individual radio link and aims at a constant quality, usually defined as a certain target Bit Error Rate (BER) or Frame Error Rate (FER). The need for changing the target SIR setpoint appears from the nature of the system and its dependency with the mobile speed and the multipath profile. Due to the changing properties of the radio channel, it is not appropriate to configure the system for the worst case because it would be using many resources, therefore the best strategy is to let the target SIR setpoint float around the minimum value that fulfils the required target quality. In this way, the outer loop power control aims at providing the required quality, no more, no less. The outer loop is needed in both UL and DLs because there is fast power control in both [HoTo00].

Discontinuous Transmission (DTX) in WCDMA achieves its maximal value due to the limitations in CDMA, coming from intra-cell interference. It consists in detecting the absence of voice, and not to transmit in these periods. On average, one voice user only transmits in a 50 % of time, hence, using this characteristic one can reduced the interference in a cell as well as power consumption in the MT, which is very important in CDMA due to the limitation by interference [CFRR97]. The immediate effect for including DTX in the transmitter is an increasing of capacity due to the no transmission in an interval of time.

The handover mechanisms employed to transfer the call can be differentiated as follows: softer, soft and hard.

Softer handover: It is produced between adjacent sectors, within the same cell. The communications between MT and BS take place concurrently via two air interface channels, one for each sector separately. This requires the use of two separate codes in the DL direction, so that the MT can distinguish the signals. It must be possible generating the appropriate despreading operation.

In the UL a similar process takes place at the base station, the code channel of the mobile station is received in each sector. During softer handover only one power control loop per connection is active. The handover management is located in the Radio Network Controlled (RNC), Figure 2.7. Softer handover typically occurs in about 5-15% of connections [HoTo00].

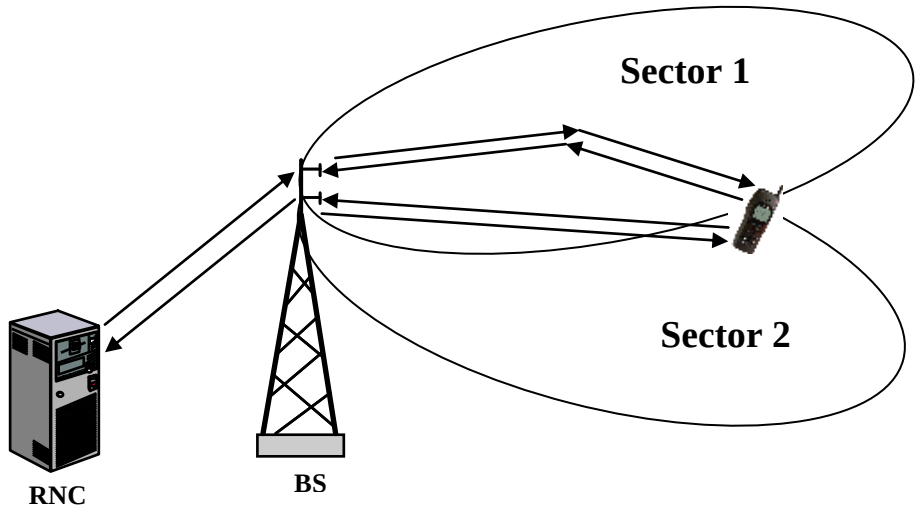

Figure 2.7. Softer handover (extracted from [HoTo00]).

Soft handover: During soft handover, a MT is in the overlapping cell coverage area of two sectors belonging to different BSs. As in softer handover, the communications between MT and BS is done via two channels from each BS separately, both channels being received at the MS by maximal ratio combining (Rake receiver). Seen from the MT there are very few differences between softer and soft handover. In the UL soft handover differs significantly from softer one: the code channel of the MT is received in both BSs, then it is selected the better frame between the two possible candidates by the same indicator used for outer loop power control. This selection takes place after each interleaving period. During soft handover

two power control loops per connection are active, one for each BS, Figure 2.8. Soft handover occurs in about 20-40% of connections.

The reasons for the need of these specific handover types, are similar to those of closed-loop power control, i.e., without soft/softer handover there would be near-far effects of a MT penetrating from one cell deeply into an adjacent one without being power-controlled [HoTo00].

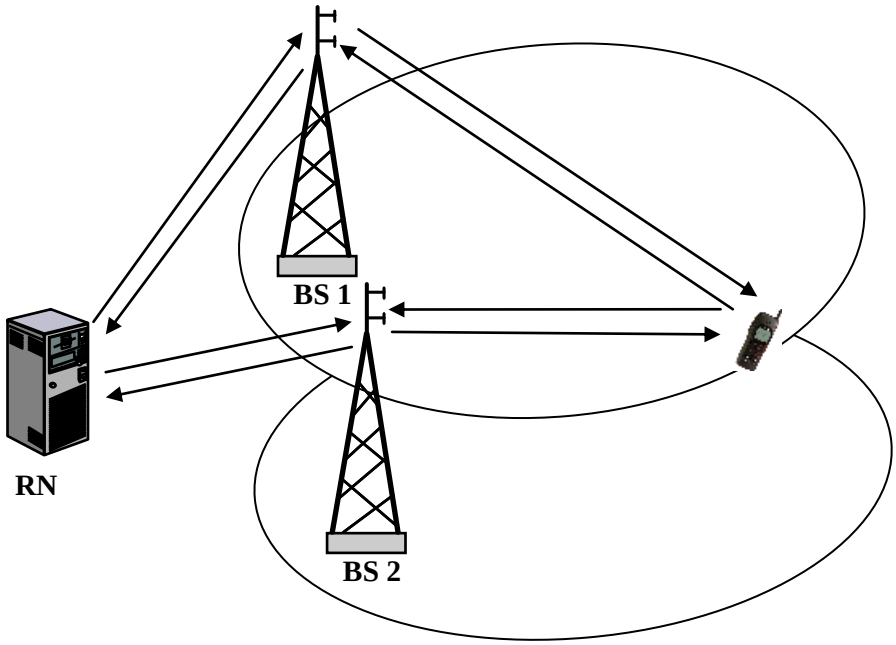

Figure 2.8. Soft handover (extracted from [HoTo00]).

WCDMA also provides hard handover types:

- Inter-frequency hard handovers that can be used to change the frequency carrier used by the MT. One application for this is high capacity BSs with several carriers.
- Inter-system hard handovers that take place between WCDMA FDD and another system, such as WCDMA TDD or GSM.

2.2.3 The TDD Mode

The TDD component is based on Time Division CDMA (TD-CDMA), which is a combination of Time Division Multiple Access (TDMA) and CDMA. Code, frequency and time slot define a physical channel, the different user signals being separated in both time and code domains. This mode uses the same frequency band in the DL and UL, but alternating the transmission in time.

Some characteristics defined in TDD are the following:

- Use of unpaired band: The FDD mode cannot be implemented on an unpaired band because it requires a pair of bands. TDD mode uses only one band because the DL and ULs are in the same band.
- Use of DTX: Use of the same band to transmit the UL and DLs, requires time for switching between both ways. To avoid corrupted transmission, the UL and DLs need a common means of agreeing on transmission ways and allowed time to transmit. To solve this problem a guard band is needed, which allows to account for the propagation delay.
- Interference between UL and DLs: Sharing the same frequency band can interfere the signal in both transmission ways. In UTRA TDD individual BSs are synchronised to each other at the frame level to avoid this interference.
- Asymmetric UL/DL capacity allocation: UL and DLs are divided in time domain, which makes possible to change the duplex switching point and move capacity from UL to DL, or vice versa, as a function of the requirements of each link.
- Reciprocal channel: In the TDD mode the same frequency is used in UL and DLs, therefore, the fast fading is the same in both links. Estimating the fast fading is possible with the aim of using it at the transceiver. It can be used in power control and in adaptive antenna techniques.

The data modulation scheme in TDD is QPSK as well. The modulated data symbols are spread with a specific channelisation code of length 1-16. The modulated and spread data is finally scrambled by a pseudorandom sequence of length 16.

The physical frame structure is similar to that of the FDD mode. The scheme is resumed in Figure 2.9. The frame length is 10 ms and it is divided into 15 timeslots, each of 2560 chips, i.e., the time slot duration is 666 μs.

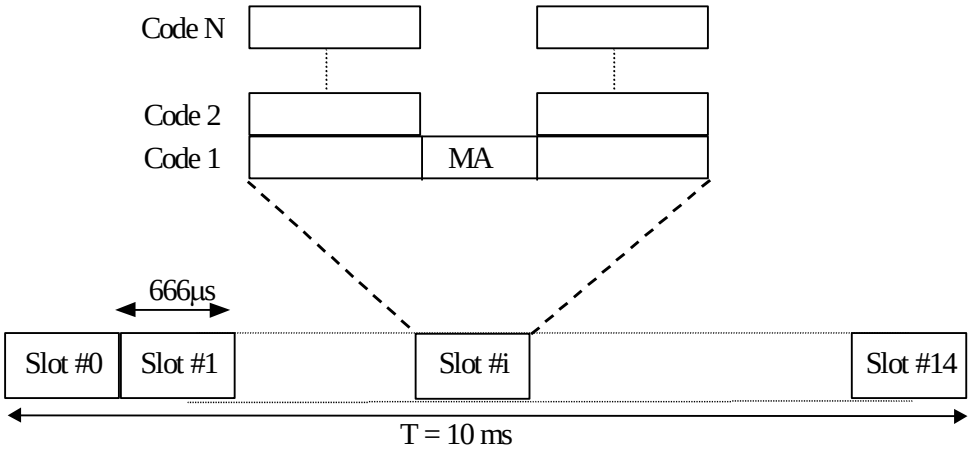

Figure 2.9. Frame structure of UTRA TDD (extracted from [HoTo00]).

The number of code channels that may be used within a single timeslot varies depending on the propagation conditions. Midamble is used to estimate the path loss, channel equalisation and coherent detection at the receiver.

Each of the 15 timeslots within a 10 ms frame is allocated to either UL or DL. Multiple switching points for different transmission directions per frame allow closed loop power control and a Physical Synchronisation CHannel (PSCH) in dedicated DL slots to speed cell search. With these characteristics it is allowed to cover dynamic asymmetric services due to the flexibility in slot allocation in the DL/ULs, thus, guaranteeing efficient use of the spectrum.

The maximum asymmetry slot allocation in DL is 14:1, where at least one timeslot has to be allocated to UL transmission for the random access channel, while in UL it is 2:13, where PSCH is mapped into two DL slots. Figure 2.10 shows how the timeslots are distributed in these cases.

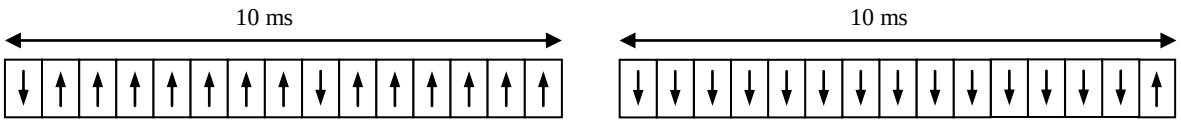

(a) Maximum UL asymmetry of 2:13 (b) Maximum DL asymmetry 14:1

Figure 2.10. UL/DL asymmetries in TDD (extracted from [HoTo00]).

2.3 Cell Structure

The UMTS Access Network will be designed with a hierarchical cell structure [Fern00], so that the cellular configuration in UMTS will support several cell sizes, such as pico-cells (radius < 100 m), micro-cells (100 m < radius < 1km), and macro-cells (radius > 1 km). This means that different types of cells can coexist in the network, making cell tiers, which will handle users with different traffic and mobility characteristics [DiTa00].

The maximum bit rate or service type offered that can be handled in UMTS depends on the cell structure that is being used [UMTS98b]. Cell type and mobility determine the maximum user bit possible that may be reached.

Table 2.3 shows the different data rates available as a function of cell type and mobility.

Cell type	Mobility class	Max. available user bit rate
Macro	High	384 kbps
Micro	High/Low	384 kbps / 2 Mbps
Pico	Low	2 Mbps/s

Table 2.3. Maximum available data rates (extracted from [UMTS98b]).

[UMTS98b] describes an optimal UMTS radio network, using a hierarchical cell structure, Figure 2.11, based on micro-, macro-, and pico-cells. The different components of UTRA (FDD or TDD) should be used in each scenario depending on its performance features, since the different traffic demands will require different layers.

The FDD macro-cell provides the wide area coverage and it is also used for high-speed mobiles, while micro-cells are used at street level for outdoor coverage to provide extra capacity where macro-cells can not cope with. The pico-cell will be used mainly for indoor environments, where the demand for high data rate services (such as laptops networking or multimedia conferencing) will occur.

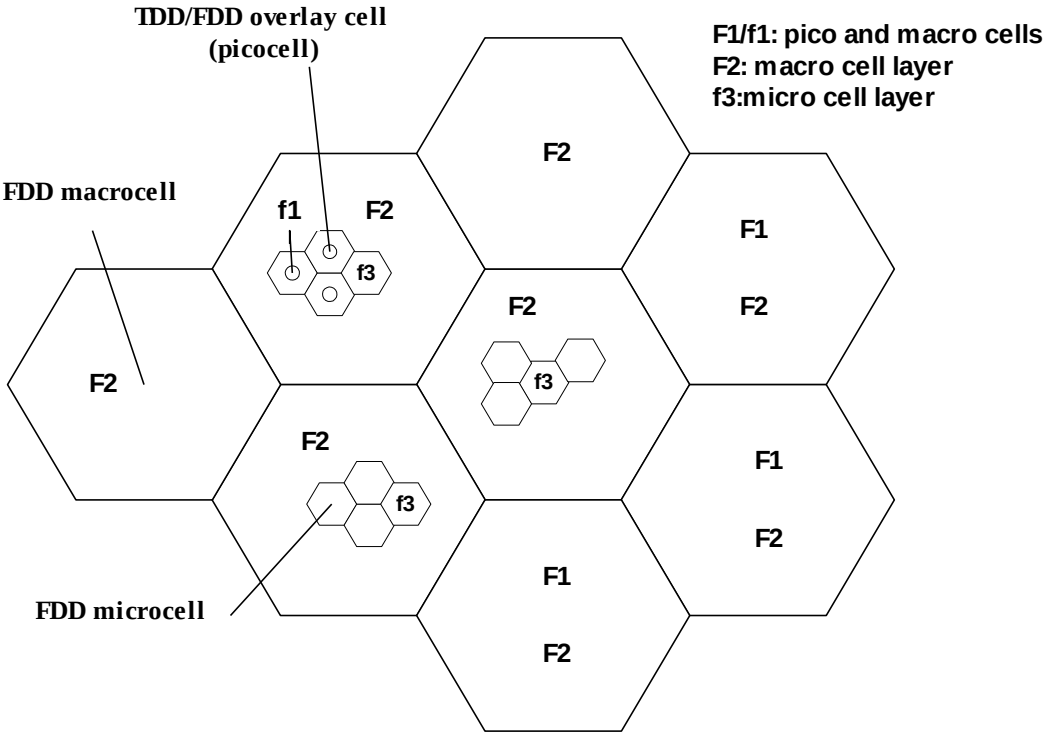

Figure 2.11. Example of UMTS layer network (extracted from [UMTS98b]).

TDD is better for a pico-cell environment [HoTo00]; the utilisation of discontinuous transmission and the reduction of average transmission power by a factor of 10log(*ts*/15), where *ts* is the number of active timeslots per slot, decrease the coverage. The consequence of this aspect is the need to use more BS sites than in UTRA FDD to get the same service. Due to these properties, TDD should be used in small cell environment, where power is not a limiting factor and data rates used for the coverage planning are higher.

3 Adaptive Beamforming

3.1 Introduction

In UMTS the use of SA has been considered from the start of system specification [ETSI98a] and work developed by the 3rd Generation Partnership Project (3GPP) Working Group 1. In the case of UMTS, the use of SA allows for intra- and inter-cell interference to be reduced, which directly implies an increase in system capacity.

Firstly, the exact idea of what is the concept of beamforming needs to be clarified. In [GiCo00] a beamformer is defined as the processor used with an array of sensors to apply some form of spatial filtering. By *spatial filtering*, from the receiver (Rx) point of view, is meant to separate signals that share the same frequency band, time-slot and possibly code, but originate from different spatial locations. From the transmitter (Tx) side, it implies that signals with the same frequency band, time-slot and/or code may be spatially separated and transmitted in certain differing directions.

SAs have been used in other preceding applications, such as sonar, radar, satellite systems, etc. Although in their first use the beamforming was analogue, the advance of techniques and processing capacity in Digital Signal Processing (DSP) and filtering techniques has allowed the development of digital techniques for beamforming. Digital Beamforming (DBF) is currently a technique very much used, and mature enough to make use of it in mobile communications. An application of it in UMTS to improve the Signal-to-Interference Ratio (SIR) is the main objective of this work.

The usual problem of adaptive non-blind beamforming is depicted in Figure 3.1, where the input signal, $\mathbf{x}(n)$, the output signal, $y(n)$, the reference signal, $d(n)$, and a block named **w** are shown. The latter are the weighs used to optimise the beamformer response with a prescribed criterion, defined in the adaptive processor, so that the output $y(n)$ contains minimal contribution from noise and interference. Some algorithms and criteria for the definition of the optimum weights will be presented in next sections.

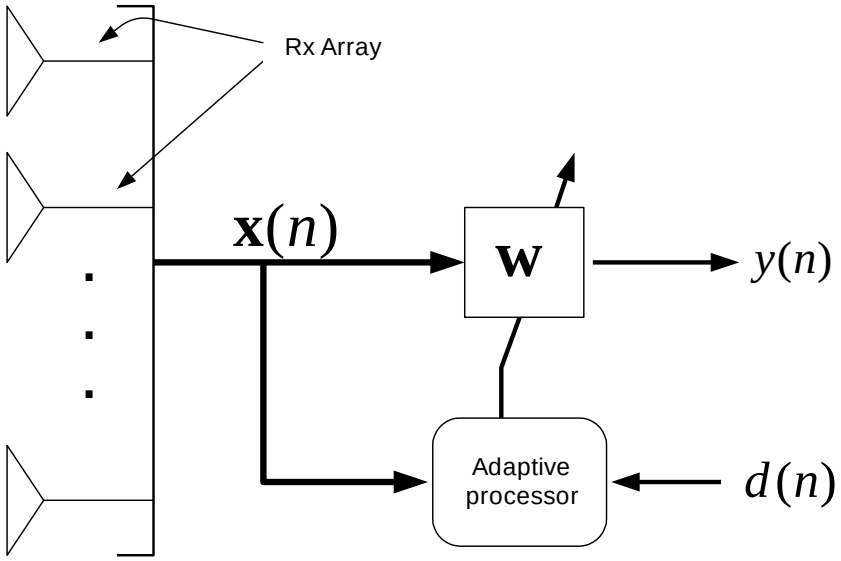

Figure 3.1. Generic adaptive beamforming scheme (extracted from [LiLo96]).

The beams and nulls are formed to provide maximum Signal-to-Interference plus Noise Ratio (SINR). The reference signal $d(n)$ can be obtained through different ways. It can be a spatial reference when information based on Direction-of-Arrival (DoA) is used, or a temporal reference, like a training sequence of an expected source identifying code.

The beamforming can use one or several main lobes towards the same Signal-of-Interest (SoI), directing zeros, adjusting lobe levels and lobe widths. All these objectives can be implemented using a cost function where an adaptive iterative algorithm takes part to minimise it through some means of interactive convergence [LiLo96].

In general terms, the DBF can be seen as a marriage between antenna and digital technology with the following advantages [LiLo96]:

- A large number of independently steered high-gain beams can be formed without any resulting degradation in Signal-to-Noise Ratio (SNR).
- All of the information arriving at the antenna array is accessible to the signal processor so that system performance can be optimised.
- Beams can be assigned to individual users, thereby assuring that all links operate with maximum gain.
- Adaptive beamforming can be easily implemented to improve the system capacity by suppressing cochannel interference.

- DBF systems are capable of carrying out antenna system real-time calibration in the digital domain, so that it cannot be so strict in terms of phase and amplitude between transceivers, because variation in these parameters can be corrected in real time.

Specifically for the case of mobile communications many features can be improved, some of them are [LiLo96]:

1. *Coverage*: Adaptive beamforming can increase the cell coverage range substantially, through antenna gain and interference rejection.
2. *Capacity*: It can be planned the reuse of frequency in a Frequency Division Multiple Access (FDMA) system or the code in a CDMA system. In general, adaptive beamforming can increase the number of available channels through directional communication links.
3. *Signal Quality*: The improvement of signal quality results from the interference rejection afforded against directional interferes, for interference-limited environments.
4. *Access Technology*: Beamforming adds dimension spatial gains to the techniques such as FDMA, TDMA, and CDMA. On the DL, energy can be focused at the mobile so that long delay multipath components can be reduced substantially. This allows the system to combat Inter-Symbol Interference (ISI) through discrimination of "interfering" signals on both UL and DLs.
5. *Power Control*: This key characteristic in CDMA can be improved with the use of adaptive antenna technology.
6. *Handover*: In many cases, adaptive antenna technology provides mobile location information that can be used by the system to substantially improve handovers in both the low and high tiers.
7. *Portable Terminal Transmit Power*: Implementing an adaptive antenna allows the reduction in transmission power levels, which results from the increase in antenna gain at the BS, and transmission only in advantageous directions relaxing the requirements on batteries. This is a key factor in UMTS, because with adaptive antennas at BSs, the transmit power levels from and to the MT can be kept minimum to provide the requested service.

3.2 Beamforming and Spatial Filtering

Fist of all, to define spatial filtering the notion of aperture, interval or domain, must be remembered. A temporal filter operates on a time aperture in the same way a frequency filter operates in a spectral aperture. The spatial filter implies a spatial aperture, where spatial sampling is discrete [GiCo00]. In Figure 3.2 an easy example of spatial filtering is shown.

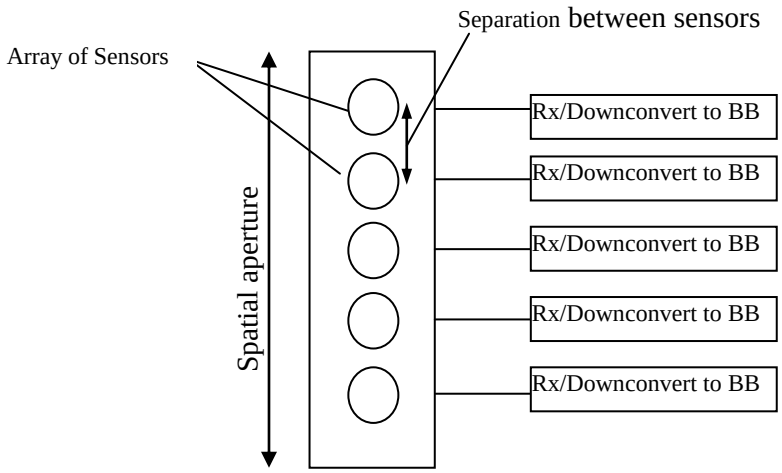

Figure 3.2. Spatial filtering elements.

The use of spatial discrete sampling brings two advantages [GiCo00]:

- On the one hand, spatial discrimination potential depends on the size of the spatial aperture, compared with the working wavelength (the larger the aperture, the better the discrimination).
- On the other, the filtering function may be changed in real time (such is not feasible with a continuous aperture antenna).

Aperture is an important factor in the array resolution capability, since the number of elements will determine the Degrees of Freedom (DoF) in the design of diverse patterns. Therefore, the spatial filtering will depend on spatial aperture characteristics such as number of elements and elements separation [GiCo00].

However, the characterisation of the samples in each sensor is not an easy task, due to the multiple parameters that must be taken into account. For example:

- In antenna/RF beamforming, the electromagnetic signal samples are characterised by more than one parameter (range, angle, polarisation and frequency), plus code in CDMA system and time, if the temporal variations are considered.
- Different signals, i.e., characterised by a different set of the referred parameters, can be correlated due to multipaths.
- Sampling in the spatial domain may not be uniformly distributed in space, i.e., non-uniform sampling is possible, besides being multidimensional.
- Sensor decalibration, as a spatial and responsive uncertainty factor, must often be considered (leading to the development of robust techniques to avoid the damage that this problem can cause).

As function of how the input signal is processed to get the output signal, two beamforming structures can be distinguished, narrow- and wideband. In Figure 3.3 both structures are presented, Figure 3.3 (a) corresponds to the narrowband (NB) general scheme, and Figure 3.3 (b) corresponds to the wideband (WB) general scheme [LiRa99], [GiCo00].

The difference between NB and WB can be seen in Figure 3.3. Meanwhile in NB scheme a unique beamforming processing is applied to the set of samples at instant n, in WB a beamforming processing is applied for each acquisition element, meaning in each sample obtained from the antenna. For NB scheme a set of M weights is used to update the output, $y(n)$ according to the number of antennas. Nevertheless, for WB scheme the number of weights can be different to the number of antennas, being independently calculated for each beaforming processing. Note that WB structure for each sample processing is similar to a Finite Impulse Response (FIR) filtering.

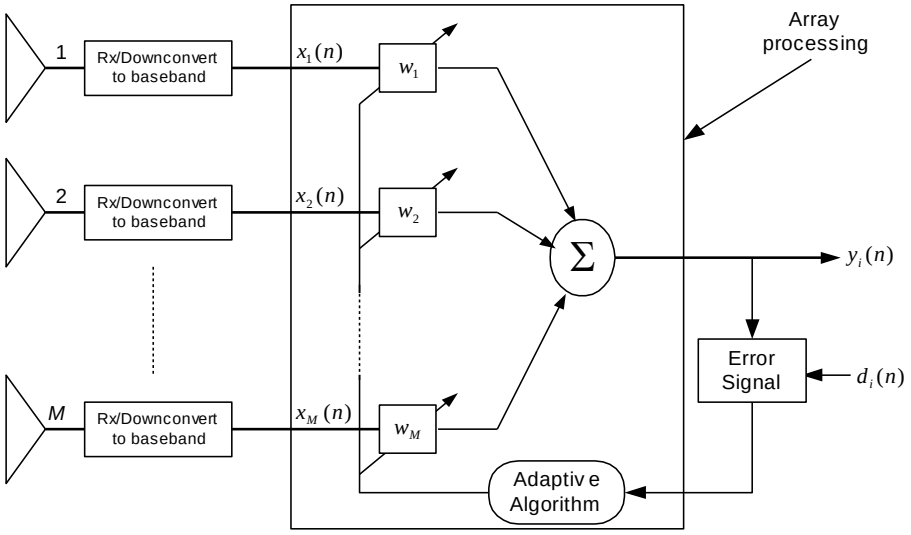

(a) NB general scheme

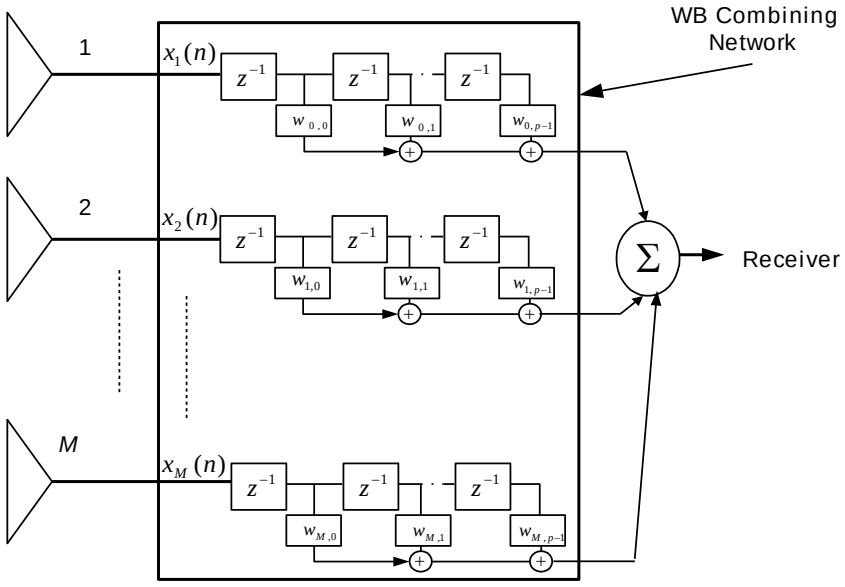

(b) WB counterpart

Figure 3.3. Representation of the NB and WB basic beamforming structures (extracted from [LiRa99]).

The minimisation of an error function is the objective of the majority of adaptive algorithms. The need for the use of a signal of reference characterises a non-blind algorithms. Speaking about a signal of reference is speaking of an estimation signal *a priori.* This reference can be divided into two categories: spatial and temporal reference. Spatial reference is mainly referred to the Angle-of-Arrival (AoA) information of a desired signal. Examples of temporal reference signal may be a pilot signal that is correlated with the desired signal, a

special sequence in a packet carried by the desired signal, or a known Pseudo-Noise (PN) code in a CDMA system [GiCo00], [LiLo96].

The optimisation problem is to minimise the mean squared error between beamformer output and reference, i.e.,

$$\min_{\mathbf{w}} \left\{ |\xi(n)|^2 \right\} = \min_{\mathbf{w}} \left\{ |y(n) - d(n)|^2 \right\} \tag{3.1}$$

where $y(n)$ is the output, given by $\mathbf{w}^{\mathrm{H}}\mathbf{x}$, with $d(n)$ being the reference desired output signal and $\mathbf{w}$ the weight vector, and $\xi(n)$ is the estimation error between $y(n)$ and $d(n)$. Considering that the inputs correlation matrix is $\mathbf{R}_x = \mathrm{E}[\mathbf{x}\mathbf{x}^{\mathbf{H}}]$, and that the cross-correlation between desired and main inputs is $\mathbf{r} = \mathrm{E}[\mathbf{x}d^*]$, the optimum solution to the problem, also known as Wiener solution [Hayk91] is given by $\mathbf{w}_{opt} = \mathbf{R}_x^{-1}\mathbf{r}$, if $\mathbf{R}_x^{-1}$ exists.

Adaptive beamforming can be divided into two classes [LiLo96]: fully adaptive and partially adaptive. In fully adaptive beamforming, every available DoF is used. That is, every element or beam is individually adaptively controlled to achieve maximum control of the beam pattern.

Fully adaptive beamforming can be preferred because of the following advantages:

- The full complements of the array´s DoF are available to the beamformer. Therefore, one is able to maintain the maximum control of the array's response.
- The maximum aperture gain can be retained, since all of the array elements are used.
- The maximum spatial resolution can be retained, since the entire array elements are used.

When the number of array elements becomes large, however, full adaptivity may be difficult to implement in practice. Exercising a large number of an array's DoF can result in a considerable level of computational complexity, as well as in a decrease in the convergence rate of the adaptive algorithm. It can be of interest to reduce the degrees of freedom, as a practical engineering procedure.

A number of strategies can be used to reduce the degrees of freedom that are presented to the adaptive algorithm, but in this work a fully adaptive solution will be considered due to the conditions that advise its implementation.

3.3 Recursive Least Squares Algorithm

As the name indicates, the RLS algorithm can be seen as an extension of the LS method in that recursion is included in the process – the new weight vector estimate, at iteration *n*, will result from a LS estimate obtained at iteration *n*-1, after the arrival of new data.

In [WaCr94] the application of RLS to a CDMA mobile environment is presented, evaluating BER performance in the case of existing intra- and inter-cell interferers.

To describe the algorithm, let *n* designate the iteration number, referring to the total iterations from the instant of initialisation. The RLS will base its calculations on the data arrived at instant *i*, before the iteration number *n*, i.e., $1 \leq i \leq n$. If with LS the cost function is the sum of error squares, for a certain time interval (due to the application of *data windowing*), in the RLS it accounts for the sum of weighed error squares until the instant *n*:

$$f(n) = \sum_{i=1}^{n} \beta_e(n,i) \left| \xi(i) \right|^2 \tag{3.2}$$

where $\beta_e(n,i)$ is the *i*th error square weight, for the *n*th iteration, and $\xi(i)$ is the estimation error. $\xi(i)$ is defined as the difference between the desired response, $d(i)$, and the transversal filter output, $y(i)$, at instant *i*:

$$\xi(i) = d(i) - y(i) \tag{3.3}$$

The output, $y(i)$, is equal to $\mathbf{w}^{\mathrm{H}}(n)\mathbf{x}(i)$. The *M*-by-1 input vector is $\mathbf{x}(i) = [x(i) \quad x(i+1) \quad \cdots \quad x(i+M-1)]^{\mathrm{T}}$, obtained at instant *i*, and the *M*-by-1 weight vector is $\mathbf{w}(n) = [w_1(n) \quad w_2(n) \quad \cdots \quad w_M(n)]^{\mathrm{T}}$, composed by the *M* tap weights calculated in the *n*th iteration. The process of calculation of the cost function requires that these tap weights used to calculate $f(n)$, in the *n*th iteration, do not change in time during the interval for which $f(n)$ is defined [Hayk91].

The *exponential weighting factor*, λ_{RLS}, is real, positive and lower but close to 1 (for all *n* and *i*), being related to $\beta_e(n,i)$ as indicated:

$$\beta_e(n,i) = \lambda_{RLS}^{n-i} \tag{3.4}$$

where λ_{RLS} is lower, but close to 1. In this way, for a given *n*, the cost function sum will have lower contributions from errors with large *n*-*i* and larger contributions for smaller *n*-*i*, i.e., the older errors are gradually *forgotten*. This is why the $\beta_e(n,i)$ is also called *forgetting factor*. By gradually considering less the farthest errors in time, the algorithm does afford to follow

statistical variations of a non-stationary channel. The quantity $\frac{1}{1-\lambda_{RLS}}$ is a measure of the *memory* of the process. In the case of the LS, where λ_{RLS}=1, the memory is *infinite*, meaning that the all squared errors have the same weights, being recalled equally, i.e., the LS is implemented.

In particular, notice how the signal correlation matrix, $\mathbf{R}_x$, and the cross-correlation between input and desired signals, **r**, are involved. In the RLS a similar group of equations is formed, leading to the calculation of a newly estimated value, $\hat{\mathbf{w}}(n)$, closer to the optimum:

$$\mathbf{\Phi}(n)\hat{\mathbf{w}}(n) = \mathbf{z}(n) \tag{3.5}$$

where $\mathbf{\Phi}(n)$ is the *M*-by-*M* correlation matrix and **z**(*n*) is the *M*-by-1 cross-correlation vector between inputs and desired response, defined below:

$$\mathbf{\Phi}(n) = \sum_{i=1}^{n} \lambda_{RLS}^{n-i} \mathbf{x}(i)\mathbf{x}^{\mathrm{H}}(i) \tag{3.6}$$

$$\mathbf{z}(n) = \sum_{i=1}^{n} \lambda_{RLS}^{n-i} \mathbf{x}(i)d^*(i) \tag{3.7}$$

The set of equations indicated within (3.5) are called *normal equations*. Notice how the forgetting factor also applies to the calculation of $\mathbf{\Phi}(n)$ and **z**(*n*), which are summations of past correlations and cross-correlations, respectively, the *older* of these being affected by smaller $\beta_e(n,i)$. Besides intuitively understanding that the $\mathbf{\Phi}(n)$ and **z**(*n*), resulting from the *n*th iteration, can be obtained from those of the *n*-1 iteration, it can easily be shown that such is so:

$$\mathbf{\Phi}(n) = \lambda_{RLS}\mathbf{\Phi}(n-1) + \mathbf{x}(n)\mathbf{x}^{\mathrm{H}}(n) \tag{3.8}$$

$$\mathbf{z}(n) = \lambda_{RLS}\mathbf{z}(n-1) + \mathbf{x}(n)d^*(n) \tag{3.9}$$

From (3.5) the tap weight vector estimate needs to be calculated. As in other algorithms, this can be done through the calculation of the inverse of matrix $\mathbf{\Phi}(n)$. But such *brute force method* means requiring too a large computational effort. Another means of calculating $\hat{\mathbf{w}}(n)$ is recursively, for *n*=1, 2, ..., minimising computational effort, building up the RLS algorithm [Hayk91].

The calculation of $\mathbf{\Phi}^{-1}(n)$ is possible by applying the *Matrix Inversion Lemma* to (3.8) , leading to the recursive equation for $\mathbf{\Phi}^{-1}(n)$ [Goda97], [Hayk91], [LiLo96]:

$$\mathbf{\Phi}^{-1}(n) = \lambda_{RLS}^{-1}\mathbf{\Phi}^{-1}(n-1) - \frac{\lambda_{RLS}^{-2}\mathbf{\Phi}^{-1}(n-1)\mathbf{x}(n)\mathbf{x}^{\mathrm{H}}(n)\mathbf{\Phi}^{-1}(n-1)}{1+\lambda_{RLS}^{-1}\mathbf{x}^{\mathrm{H}}(n)\mathbf{\Phi}^{-1}(n-1)\mathbf{x}(n)} \tag{3.10}$$

To be able to describe the algorithm itself, some definitions are put forward, in order to facilitate computation:

$$\mathbf{P}(n) = \mathbf{\Phi}^{-1}(n) \tag{3.11}$$

$$\mathbf{g}_{\mathrm{RLS}}(n) = \mathbf{\Phi}^{-1}(n)\mathbf{x}(n) \tag{3.12}$$

$\mathbf{P}(n)$ is the *inverse correlation matrix*, and $\mathbf{g}_{\mathrm{RLS}}(n)$ is called the *gain vector*. By dealing with (3.9) to (3.12), one arrives at the equations which constitute the RLS computation [Hayk91]:

$$\mathbf{g}_{\mathrm{RLS}}(n) = \frac{\lambda_{RLS}^{-1}\mathbf{P}(n-1)\mathbf{x}(n)}{1+\lambda_{RLS}^{-1}\mathbf{x}^{\mathrm{H}}(n)\mathbf{P}(n-1)\mathbf{x}(n)} \tag{3.13}$$

$$\xi(n) = d(n) - \hat{\mathbf{w}}^{\mathrm{H}}(n-1)\mathbf{x}(n) \tag{3.14}$$

$$\hat{\mathbf{w}}(n) = \hat{\mathbf{w}}(n-1) + \mathbf{g}_{\mathrm{RLS}}(n)\xi^{*}(n) \tag{3.15}$$

$$\mathbf{P}(n) = \lambda_{RLS}^{-1}\mathbf{P}(n-1) - \lambda_{RLS}^{-1}\mathbf{g}_{\mathrm{RLS}}(n)\mathbf{x}^{\mathrm{H}}(n)\mathbf{P}(n-1) \tag{3.16}$$

These are hereby presented in the order that these should be calculated, for each n=1, 2, ... The algorithm is initialised by setting $\mathbf{P}(0) = \delta_{\mathrm{RLS}}^{-1}\mathbf{I}$ where δ_{RLS} is a small positive constant compared to $0.01\sigma_x^2$ [Hayk91], σ_x^2 being the variance of the signal samples, $\mathbf{x}(n)$, and $\mathbf{I}$ is the $M \times M$ identity matrix and $\hat{\mathbf{w}}(0) = \mathbf{0}$.

Some comments on these follow:

- The *a priori estimation error*, $\xi(n)$, is so called since the estimate of the desired response. i.e., the $\hat{\mathbf{w}}^{\mathrm{H}}(n-1)\mathbf{x}(n)$ inner product, is based on the previous LS estimate.
- The calculation of the step-size parameter used in the Least Mean Squares (LMS) algorithm (see Appendix A), μ, is replaced by the calculation of the gain vector, $\mathbf{g}_{\mathrm{RLS}}(n)$, which is a simple scalar division involving a fast recursive calculation of $\mathbf{\Phi}^{-1}(n)$.
- (3.14) describes the filtering stage of the RLS.

- (3.15) describes the adaptive nature of the RLS. The estimation error is added to the old weight vector estimate, to correct it, being multiplied by a gain, dependent on n, i.e., the gain vector, $\mathbf{g}_{RLS}(n)$.
- (3.13) and (3.16) define the gain vector, $\mathbf{g}_{RLS}(n)$.

As far as the convergence of the RLS is concerned, its rate is usually one order of magnitude faster that of the simple LMS, in case the SNR is high, at the expense of larger computation complexity [Hayk91], [LiLo96]. It is also independent of the eigenvalue distribution of the correlation matrix [Goda97], [Hayk91].

Concerning initialisation, convergence and general performance, a detailed analysis is provided in [Hayk91], by means of some examples. The RLS is also viewed in the form of a state-space model, being compared with covariance Kalman filtering, though these are deterministic and stochastic approaches, respectively.

4 RLS Adaptive Beamforming Implementation

4.1 Algorithm Implementation

4.1.1 Assumptions

This chapter presents the study of an application of the RLS adaptive algorithm to beamforming at the BS, for the TDD case. The problem here presented is limited to the antenna array level, dealing with the formation of a lobe structure that results from the dynamic variation of an element-space processing weight vector. The beamforming is controlled by an adaptive non-blind algorithm, RLS, resulting in the increase of the SINR for each link due to the beamforming gain obtained. The reference acquisition method best suited for CDMA is used. For the algorithm convergence analysis, a non-specific WDCM cluster model is used, based on the Geometrically-Based Single Bounce (GBSB) models [LiRa99].

Figure 4.1 summarises the scheme under which this work is developed, the WDCM is defined, after that an adequate receiver structure must be specified. For this implementation a baseband model is used, obtaining the samples required for the beamforming application. Finally, the RLS algorithm is applied to calculate the weights in each iteration that are used to modify the beampattern diagram for each link, maximising the resulting SINR.

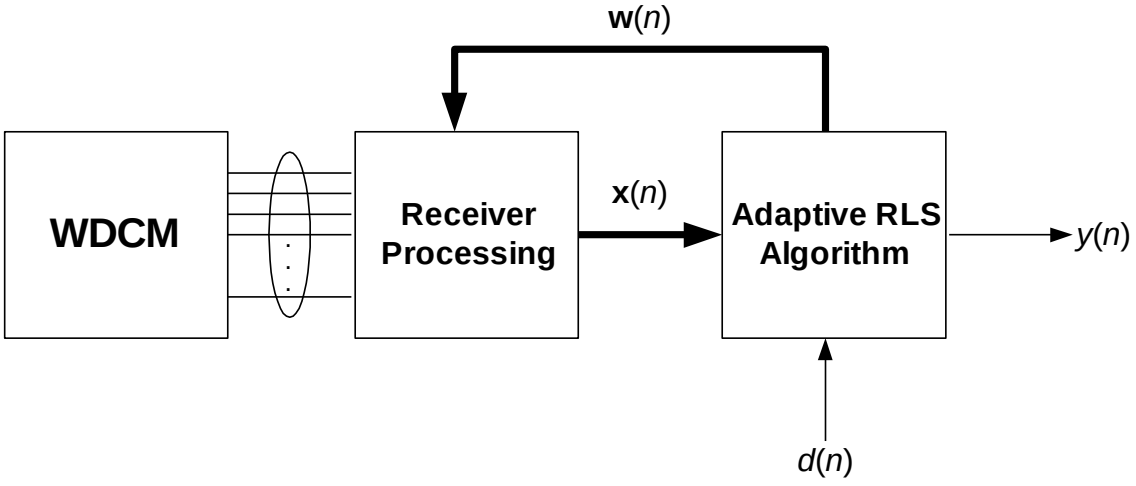

Figure 4.1. General Block Diagram of the Adaptive beamforming implementation.

Simulation results cover the number of iterations for algorithm convergence, error norms, SINR's, beamforming processing gains, BER's achieved and final resulting beampattern.

It will be necessary to achieve the largest SINR gain, for critical traffic areas and high data rate services provision. Some beamforming RLS implementations and recommendations are present in the literature, e.g. [WaCr94], [Hayk91], **[Goda97]**. RLS being very much used, for general adaptive filtering, it has been shown that it can converge sufficiently fast, depending on the correlation matrix and stationary conditions at stake. The algorithm's speed dependence on the correlation matrix eigenspread, transient response and final error can be pointed out to be the major factors that should be evaluated together with the application of a WDCM, within a *hostile* interference scenario.

In fact, for RLS, little or no explicit reference on the inherent introduction of noise and errors due to interference, nor dependence on propagation conditions have been found in the literature.

4.1.2 Wideband Directional Channel Model

The study of an adaptive algorithm within a beamforming solution needs to be verified together with a well-defined propagation channel. For UMTS, the channel additional characterisation of AoA is required, from the Rx perspective. The work develops on the WDCM based on the GBSB models (elliptical or circular) [LiRa99], [MaCo01], [ZoMa00], concluding on how the propagation channel characteristics affect the convergence.

For this study of the RLS application, the WDCM implemented is constituted by a set of N_c clusters, each composed by an equal number of I_s scatterers, placed within the horizontal plane. Cluster angular positions are randomly generated, with an azimuth, ϕ_{n_c}, following a uniform distribution within [-π/2, π/2], in respect to the linear array normal. The scatterers are gaussian distributed around each cluster azimuthal position, with a standard deviation of π/50. An incoming signal with AoA ϕ_{i_s,n_c}, from the i_sth scatterer, in the n_cth cluster, is characterised by a reflection coefficient, Γ_{i_s,n_c}, whose modulus and phase are uniformly distributed within [0, 1] and [0, 2π[, respectively. An overall equivalent attenuation has been introduced, α_{n_c}, controlling the n_cth cluster contribution for each of the simulations.

All incoming signals from each cluster are seen as arriving at the same instant, τ_{n_c}, only allowing for relative delays between clusters. In this way, the channel baseband response,

function of the continuous time variable, τ, related to each lth link, independent among links, can be represented by (4.1):

$$h_l(\tau,\phi)=\sum_{n_c=1}^{N_C}\alpha_{n_c,l}\left(\phi_{n_c,l}\right)\delta\left(\tau-\tau_{n_c,l}\left(\phi_{n_c,l}\right)\right)\sum_{i_s=1}^{I_s}\Gamma_{i_s,n_c,l}\left(\phi_{i_s,n_c,l}\right) \qquad (4.1)$$

where the coefficients mentioned and the Time-of-Arrival (ToA) are explicitly shown to vary with the AoA, and the l index has been added. Note that a *link* is hereby defined as an active MT-BS pair, code-, spatial and temporally independent of any other active MT-BS pairs.

Relative delays are introduced as integer multiples of the chip duration, 0.26 μs, for a chip rate of 3.84 Mchip/s [Fern99]. This relative delay corresponds to a whole path, from the MT to the BS, relative length difference of near 78 m. In a micro-cell scenario, where Line-of-Sight (LoS) exists, with most reflections happening near the MT-BS line [LiRa99], [MaCo01], [ZoMa00], LoS will be the first incoming signal, establishing the temporal reference for ToA. Therefore, all incoming single-bounce-reflected signals imposed by the channel, arriving during the first chip can be seen as resulting from reflections happening inside an elliptical region, with the MT-BS line as major axis. All other considered delayed signals will correspond to other larger elliptical regions, defined by a chip multiple duration, with the same major axis. Since the sampling rate hereby considered is equal to the chip rate, only the ellipses contribute with reflecting clusters. In [MaCo01], [ZoMa00], where a WDCM based on the GBSB elliptical model [LiRa99] is presented, clusters are uniformly distributed inside an elliptical region, with sampling rates larger than the chip rate, in order to characterise the channel.

Dropping τ due to sampling, the signal matrix $\mathbf{U}(n)$ is the $N_s \times M$ signal matrix obtained from a block of N_s baseband signal samples, taken at chip-rate, at instant n, from each of the M array elements, including thermal Additive White-Gaussian Noise (AWGN). Resulting from the baseband model described before, for each mth array element and instant τ_n, each element of $\mathbf{U}(n)$, $u(n,m)$, is given by:

$$u_{n,m}=\sum_{l=1}^{L}u^{(l)}_{(n,m)l}=$$

$$\sum_{l=1}^{L}\sum_{n_c=1}^{N_c}\alpha_{n_c,l}\left(\phi_{n_c,l}\right)\cdot c_l\left(n-\tau_{n_c,l}\left(\phi_{n_c,l}\right)\right)\sum_{i_s=1}^{I_s}\Gamma_{i_s,n_c,l}\left(\phi_{i_s,n_c,l}\right)\cdot a_{i_s,n_c,l}\left(m\right)+\overline{n_{n,m}} \qquad (4.2)$$

where $a_{i_s,n_c,l}(m) = e^{j\frac{2\pi}{\lambda}d_{el}(m-1)\sin(\phi_{i_s,n_c,l})}$ is the corresponding steering vector element (d_{el} is the element spacing and λ is the wavelength), independent of the sampling instant n, and $c_c^{(l)}(n)$ is the transmitted signal (codes for this case). As mentioned, each $u(n,m)$ is the sum of all L contributions with a $\overline{n_{n,m}}$ complex noise component. Among links, propagation channels and consequent steering vectors are independent.

Stationarity is assumed during each time-slot, the sampled data generating a unique and stable signal matrix. Doppler shift and slow fading have not been considered.

Since one is interested, at present, in applying this work to the TDD mode, the propagation channel symmetry allows for using the same beamforming weights for either UL and DL. Tx or Rx diversity are not considered directly in this work. Anyhow, in a system's approach, the considered beamforming stage does not eliminate several diversity schemes.

4.1.3 Application to UTRA TDD

In the case of UMTS, CDMA is especially favourable for providing a signal reference closely correlated to the SoI, but very weakly correlated to the interfering sources – a code. It is known that such a referential source existing, it should be used to its maximum extent, providing best convergence and final error performance [LiLo96].

According to [Tosk00], for separating different MTs, the following code families are defined:

- For FDD, Gold codes with 10 ms period, or alternatively S(2) codes 256 chip period.
- For TDD, codes with period of 16 chips and midamble sequences of different length depending on the environment.

Separating different cells is also important, besides identifying MTs, because neighbour cells may have one MT each, in low traffic-demanding conditions, with the same MT identifying channelisation code. To separate different cells the following solutions are supported:

- For FDD, Gold codes with 10 ms period (38 400 chips at 3.84 Mcps) are used.
- For TDD mode, scrambling codes with length 16 are used.

Consequently, for the TDD mode, a combination of channelisation and scrambling codes is required, resulting in a spreading factor of 16 [Ito00a]. It is assumed that, for each link, the desired code is known at the BS, having been determined by the RNC. The signal

sample data can be obtained at the beginning of the first data block, within each time-slot, so that the formation of beams is completed before the midamble.

Another possibility would be to use the midamble to identify the MT, as mentioned. Among the three types of bursts, burst 1 supports the largest number of training sequences, which can be used to estimate the different channels for different MTs in UL and, in case of beamforming, also in DL. When DL beamforming is used, at least that user to which beamforming is applied, and which has a dedicated channel, shall get one individual midamble [Hira00].

The channelisation and scrambling codes, or their combination, have been chosen as the most adequate reference sources for the following reasons:

- They can be used for either TDD and FDD, with a simple change in the code used.
- Midambles exist within the TDD time-slot, after the first data symbols, requiring that the reference acquisition be made at that block only, whereas the channelisation and scrambling codes are present during all time-slot.
- The use of channelisation and scrambling codes allows for easier integration of the suggested beamformer with a RAKE Rx structure.

4.1.4 RLS Problem Description

The RLS algorithm was described in Chapter 3. The RLS algorithm is used to update the weights after each input vector **x**(*n*) at the instant *n* used to modify the beampattern. It minimises (3.2), where in each iteration (3.14) is being taken into account to achieve the steady-state that takes place when the algorithm converges and (3.2) is minimum. According to (3.14),

$$\xi_l(n) = d_l(n) - \hat{\mathbf{w}}_l^{\mathrm{H}}(n-1)\mathbf{x}(n) = c_d^{(l)}(n) - \hat{c}_d^{(l)}\left(n \middle| X_n\right) \qquad (4.3)$$

where $c_d^{(l)}(n)$ is the code symbol corresponding to the desired signal at instant *n*, from link *l* and $\hat{c}_d^{(l)}\left(n \middle| X_n\right)$ is the beamformer output estimate corresponding to **x**(*n*), from link *l*. The cost function (3.2) will tend to the minimum when the algorithm is working, in its LS condition [Hayk91] that minimises it. According to [Ito00a] the codes are orthogonal, therefore, the SoI weight vector will be closely orthogonal to those of the interfering signals, ideally placing a null of the beam pattern in this position.

For a user *l*, RLS is implicitly solving the problem:

$$\mathbf{w}_l = \left(\mathbf{U}^{\mathrm{H}}\mathbf{U}\right)^{-1}\mathbf{U}^{\mathrm{H}}\mathbf{c}_d^{(l)} \tag{4.4}$$

The RLS then estimates $\mathbf{R}^{-1}$ ($M\times M$) by a sample-by-sample recursive process, through the calculations of the matrix **P**. RLS does not require knowing all matrix **U**, at each instant, because the weight vector updating is made sample-by-sample, meaning that to achieve the steady-state the algorithm needs the same number of samples than the number of iterations.

The physical interpretation for the RLS algorithm can be understood together with the interpretation of the LS in its geometrically meaning. There are many interpretations for LS, but one very useful and easy to understand is the projection operation to find the direction of the desired signal, in this case, the code. Using (4.4) the whole estimated code vector will be:

$$\hat{\mathbf{c}}_d^{(l)} = \mathbf{U}\hat{\mathbf{w}}_l = \mathbf{U}\left(\mathbf{U}^{\mathrm{H}}\mathbf{U}\right)^{-1}\mathbf{U}^{\mathrm{H}}\mathbf{c}_d^{(l)} \tag{4.5}$$

According to [Hayk91], the multiple matrix products $\mathbf{U}\left(\mathbf{U}^{\mathrm{H}}\mathbf{U}\right)^{-1}\mathbf{U}^{\mathrm{H}}$ can be seen as a *projection operator* onto the linear space spanned by the columns of the data matrix **U.** The matrix difference $\mathbf{I}-\mathbf{U}\left(\mathbf{U}^{\mathrm{H}}\mathbf{U}\right)^{-1}\mathbf{U}^{\mathrm{H}}$ is the *orthogonal complement projector* and it is equal to the minimum residual error $\mathbf{res}_{\mathrm{opt}} = \hat{\mathbf{c}}_d^{(l)} - \mathbf{c}_d^{(l)}$. Note that both the projection operator and its complement are uniquely determined by the signal matrix **U**. Vectors $\mathbf{res}_{\mathrm{opt}}$ and $\hat{\mathbf{c}}_d^{(l)}$ will be orthogonal, being $\mathbf{res}_{\mathrm{opt}}$ ideally equal to **0.**

The norm of vector $\mathbf{res}_{\mathrm{opt}}$ is the minimised *"cost function"*, it being the minimum subspace contribution in the *"direction"* of each of the considered desired signal, minimising the difference between them. This aspect must be well understood because of the importance of the loss of the orthogonality between signals (or worst, the presence of a correlated signal) which can worsen the properties of convergence and lead to an inadequate final solution. Also, as mentioned before, when the number of codes is higher than the number weights/antennas, the loss of orthogonality will be more severe since the dimension of the codes, subspace L_T, being L_T the number of arriving orthogonal codes, is higher than that of the subspace of weights, M. This results in the loss of orthogonality between the solution/weights and interfering codes, driving to a final higher error.

The existence or not of more solutions or local minima is explained by the own LS problem at stake. The LS estimate $\hat{\mathbf{w}}_l$ is unique if, and only if, the nullity of the data matrix **U** equals zero [Hayk91]. The presence of AWGN in the data matrix assures that the matrix **U**

will have full rank, therefore, the solution will be unique since it has no linearly dependent columns.

4.2 RLS Performance

4.2.1 Description of Evaluated Quantities

Several error norms have been used to evaluate the algorithm' performance. The error norm whose results are presented in this document is the residual error norm, defined as $\|\mathbf{res}_l\| = \left\|\mathbf{U}\mathbf{w}_l - \mathbf{c}_d^{(l)}\right\|$ (or its square), calculated at each iteration [Shew94], [GoLo96].

The weight estimation error norm, $\|\mathbf{e}_l\| = \|\mathbf{w}_l - \mathbf{w}_{opt,l}\|$, calculated at each iteration [Hayk91], where the optimum *Wiener* solution vector, $\mathbf{w}_{opt,l}$, has been obtained by directly calculating the correlation matrix inverse, has been useful for evaluation purposes only.

The *a priori estimation error*, given by [Hayk91] can also be useful for the evaluation of its results. The *a priori estimation error* along iterations is also known as *learning curve* [Hayk91], and is defined as $|\xi_l(n)|^2 = \left|c_d^{(l)}(n) - \hat{\mathbf{w}}_l^{\mathrm{H}}(n-1)\mathbf{x}(n)\right|^2$ calculated at each iteration. Note that, for the RLS, the weights obtained at iteration *n*-1 are used to update the *a priori estimation error* at iteration *n*.

The definition of number of iterations needed for convergence will be extracted from the residual error norm that will not exhibit variations greater than 1% of its initial value, thus, provide a reference for the number of iterations to be registered.

The calculation of the SINR, after CDMA despreading, follows (4.6) [LiRa99]:

$$SINR = \frac{P_{DesS}}{\frac{1}{G_p}\sum_{l=1}^{L_T} P_{NDesI} + N} \tag{4.6}$$

where G_p is the spread spectrum processing gain, equal to 12 dB for a SF of 16, P_{DesS} and P_{NDesI} are the DesS and NDesI powers, respectively, and N is the total noise power.

The beamforming processing gain, G_{bf}, is hereby defined as the gain in SINR resulting from the use of the presented beamforming solutions, compared to that of a single omnidirectional antenna at the BS:

$$G_{bf\,[\mathrm{dB}]} = SINR\big|_{\mathrm{beamformer}\,[\mathrm{dB}]} - SINR\big|_{\mathrm{single}\,[\mathrm{dB}]} \tag{4.7}$$

The calculation of the BER for QPSK, is calculated using the known relationship (4.8), resorting to the *Q*-function [Carl86]:

$$BER = Q\left(\sqrt{\frac{2E_b}{N_0}}\right) \tag{4.8}$$

where E_b is the energy per bit, and N_0 is the total noise power density. Considering that the noise equivalent bandwidth is close to $1/T_b$, where T_b is the bit duration, and applying the *Gaussian Approximation* to consider the NDesI signal contribution as a Gaussian random variable, it is easily shown that $SINR = E_b / N_0$ [LiRa99]. Therefore, the BER is calculated using:

$$BER = Q(\sqrt{2SINR}) \tag{4.9}$$

As far as processing speed is concerned, the number of flops are roughly calculated using MATLAB®, accounting for the calculations involved in each algorithm iteration, only. The number of flops involved in the initialisation process is not counted. Since MATLAB® can provide only a rough estimate for the number of flops required, these results are mostly to make only complexity estimation.

4.2.2 Initialisation and Transient Phase Analysis

The initialisation of RLS must be understood and compared to see with what kind of values the algorithm is initialised in the correct way. In [Mous97] a deep study of the transient and initial phase for the RLS is done, where it is demonstrated, that when the algorithm is working in a low SNR environment, the initial matrix values are less dependent than in a high SNR one. Besides, in [Hayk91] it is advised that, for the initialisation $\mathbf{P}(0) = \delta_{RLS}^{-1}\mathbf{I}$ must be used, where δ_{RLS} is a small positive constant compared to $0.01\sigma_x^2$ [Hayk91]. To verify all these criteria several simulations were done, varying δ_{RLS}, for the same number of antennas, 12, and where three codes were taken into account, i.e., one code per user, from a set of 3 codes. The results extracted from these simulations are shown in Figure 4.2, for the square error evolution. Since the *a priori estimation error* is used to update the weights in the following iteration, a good behaviour of the initialisation is observed for lower δ_{RLS}. To make the square error as small as possible, the values of δ_{RLS} must be at least of the order 10^{-5}. However,

values too small will produce a very high weight estimation error due to the initialisation with large value of the matrix [Hayk91].

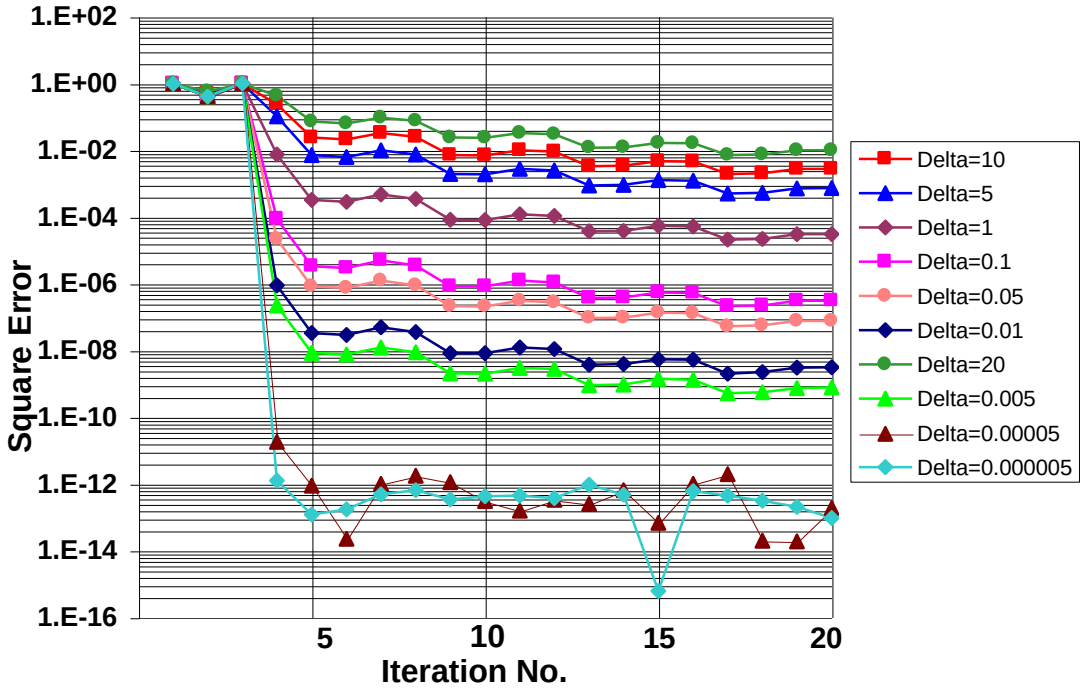

Figure 4.2. Square error representation vs. number of iterations for several δ_{RLS}.

Table 4.1 shows the weights calculated after 5 and 20 iterations for the δ_{RLS} selected for the simulations. The table provides an important information: when δ_{RLS} decreases its value, the convergence is achieved with much less iterations than with larger ones. But after a such a small value for δ_{RLS}, the weights may already converge to their final value.

A value of δ_{RLS}=0.05 is enough to assure the convergence in a favourable environment. However, it is expected that the behaviour in a critical environment requires a smaller value, within the limitations expressed before. Therefore, for all simulations, a value of $\delta_{\mathrm{RLS}} = 0.001$ will be used but always keeping in mind that in a real application this constant may need to be adjusted dynamically. λ_{RLS} will be set to 1 as in [WaCr94] a and $\hat{\mathbf{w}}(0) = \mathbf{0}$.

δ_{RLS}	$\mathbf{w}_{RLS}$(it=5)	$\mathbf{w}_{RLS}$(it=20)	$\mathbf{w}_{RLS}$(opt)
1	0.0730- 0.0024j	0.0734- 0.0025j	0.0571 - 0.0152j
	-0.0779- 0.0295j	-0.0792- 0.0297j	-0.0351 + 0.0170j
	0.0593+ 0.0586j	0.0602+ 0.0594j	0.0405 - 0.0278j
	-0.0281- 0.0884j	-0.0288- 0.0901j	-0.0238 + 0.0923j
	-0.0190+ 0.0797j	-0.0198+ 0.0808j	-0.0452 - 0.0858j
	0.0396- 0.0669j	0.0399- 0.0676j	0.0300 + 0.0473j
	-0.0632+ 0.0448j	-0.0641+ 0.0454j	-0.0715 - 0.0862j
	0.0781- 0.0257j	0.0789- 0.0264j	0.1254 + 0.0218j
	-0.0902- 0.0209j	-0.0921- 0.0212j	-0.1092 + 0.0501j
	0.0635+ 0.0540j	0.0642+ 0.0551j	0.0888 - 0.0202j
	-0.0356-0.0754j	-0.0361- 0.0765j	-0.0595 + 0.0834j
	0.0038+ 0.0727j	0.0036+ 0.0734j	0.0024 - 0.0767j
0.05	0.0737+ 0.0025j	0.0737+ 0.0025j	0.0718 + 0.0080j
	-0.0795+ 0.0297j	-0.0796+ 0.0298j	-0.0386 - 0.0100j
	0.0604- 0.0596j	0.0605- 0.0597j	0.0445 - 0.0891j
	-0.0289+ 0.0904j	-0.0289+ 0.0905j	-0.0119 + 0.1051j
	-0.0199- 0.0811j	-0.0200- 0.0811j	-0.0330 - 0.0632j
	0.0401+ 0.0678j	0.0401+ 0.0678j	0.0540 + 0.0650j
	-0.0643- 0.0455j	-0.0643- 0.0455j	-0.0715 - 0.0334j
	0.0792+ 0.0266j	0.0792+ 0.0266j	0.0715 + 0.0065j
	-0.0924+ 0.0213j	-0.0925+ 0.0213j	-0.1251 + 0.0393j
	0.0644- 0.0553j	0.0645- 0.0553j	0.0996 - 0.0315j
	-0.0362+ 0.0768j	-0.0362+ 0.0769j	-0.0802 + 0.0703j
	0.0036- 0.0736j	0.0036- 0.0736j	0.0191 - 0.0672j

Table 4.1. Representation of the weight values at iteration 5, 20 and the optimal weight.

4.2.3 Test Cases

Several simulations have been held, varying the number of antennas, *M*, of clusters, N_c, of active links, *L*, and of the total number of arriving signals including delayed versions, L_T. For all cases, the number of scatterers per cluster, I_s, has been set to 10. $\tau_{n_c,l}$ is the delay of signal coming from cluster n_c and link *l*. $\alpha_{n_c,l}$ is the attenuation of the path for a given n_c and *l*. Note that, $\alpha_{n_c,l}$ is a relative value. In Table 4.2, the parameters for some cases (Cs) are

indicated. A set of 100 independent simulations has been used to extract average results on how the algorithms perform. In this way, each simulation corresponds to a totally new and uncorrelated concretisation of the WDCM, where the cluster and scatterer positions, as well as the scatterer coefficients, are totally renewed. For each simulation, the evolution along iterations of the residual error, SINR and processing gain are stored, to be finally averaged between all the uncorrelated concretisations corresponding to the same Cs. These average results are used to provide information about the algorithms' tendency overall behaviour, not corresponding to any succession of correlated WDCM concretisations within a non-stationary scenario.

Cs #1 is a non-restrictive case, with no considered delays, implying best convergence, since the number of antennas, 6, is larger than the number of arriving orthogonal codes, 3, equal to the number of active links.

For Cs #2-4, the number of antennas is equal to the number of arriving orthogonal codes. Cs #4 is a case where much higher NDesI power is introduced, relative to link 1, so as to also evaluate how the algorithm behaves.

Cs #	M	N_c	L	$\alpha_{n_c,l}$	$\tau_{n_c,l}$	L_T
1	6	4	3	$\alpha_{n_c,l}=1$, for all n_c, l	$\tau_{n_c,l}=0$, for all n_c, l	3
2	6	4	3	$\alpha_{n_c,l}$=1, for all n_c, l	$\boldsymbol{\tau}_{1..N_c,l}=\begin{bmatrix}0 & 1 & 0 & 0\end{bmatrix}^T$, for all l	6
3	12	4	3	$\alpha_{n_c,l}$=1, for all n_c, l	$\boldsymbol{\tau}_{1..N_c,l}=\begin{bmatrix}0 & 1 & 2 & 3\end{bmatrix}^T$, for all l	12
4	12	4	3	$\boldsymbol{\alpha}_{n_c,1..L}=\begin{bmatrix}1 & 2 & 2\end{bmatrix}$, for all n_c	$\boldsymbol{\tau}_{1..N_c,l}=\begin{bmatrix}0 & 1 & 2 & 3\end{bmatrix}^T$, for all l	12
5	3	1	4	$\alpha_{n_c,l}$=1, for all n_c, l	$\tau_{n_c,l}$=0, for all n_c, l	4
6	3	10	4	$\alpha_{n_c,l}$=1, for all n_c, l	$\boldsymbol{\tau}_{1..N_c,l}=n_c-1$, for all l	40

Table 4.2. Parameters for the simulations.

Cases #5-6 are all beyond such limit. Cs #5 presents no cluster delays, but more active links than the number of antennas. Cs #6 is the worse case, with the largest number of strongly delayed clusters, 40 orthogonal codes present and an antenna array of only three elements. The behaviour of the algorithms to such a large L_T number of orthogonal codes may also give some prediction of their behaviour in a very highly densed MT area, but with little cluster delay contributions.

4.2.4 RLS Performance Results on Average WDCM

The average residual error norms obtained with the RLS are shown in Figure 4.3, a), b) and c), averaging the results from a 100 independent WDCM concretisations. Cs #1 is the best case among all, the error norm being highly reduced, and nearing zero along iterations. Also, such evolution monotonically decreases as the algorithm converges.

There are six codes arriving for Cs #2 for the same number of antennas resulting that the convergence is achieved after several iterations respecting Cs #1, stabilising the error in intermediate phase between iteration 4 and 8, with the respecting increase of the residual norm, compared to Cs #1. Cs #1 and Cs #2 present the best convergence properties since the number of signal / codes considered is small compared to the number of antennas.

Cs #3 and #4 are interesting from the point of view of the same number of codes than antennas are considered. The difference between both cases is the different values of the interfering power, achieving the convergence at the same number of iterations with a residual error evolution with the same behaviour.

Cs #5 and #6 are the worst cases since the number of codes is higher than the number of antennas. In both cases the final residual error achieves values relatively far from. Cs #6 is the case that presents worst properties of convergence; the error norm evolution presents little final effective reduction (relative to the initial values), exhibiting a relatively large transient peak after two iterations. This behaviour could seem strange, but in [Mous97], where the behaviour of the transient phase is discussed, one can see that when RLS is working in a low SINR environment the initial transient error increases until the algorithm begins to convergence, being dependent on the initial values. For this application one can see that the RLS will be working in low SINR environment when the number of codes are close to or higher to the number of antennas.

Note that the Cs #6 is a case that is taking into account 40 codes for 3 antennas, which means that the algorithm has to calculate the weights for many different AoA's accounting 40 arriving codes contributing for the signal matrix. For this situation the behaviour of the sample-by-sample RLS exhibits large oscillations that will be more important for the selection of the number of iterations needed to convergence.

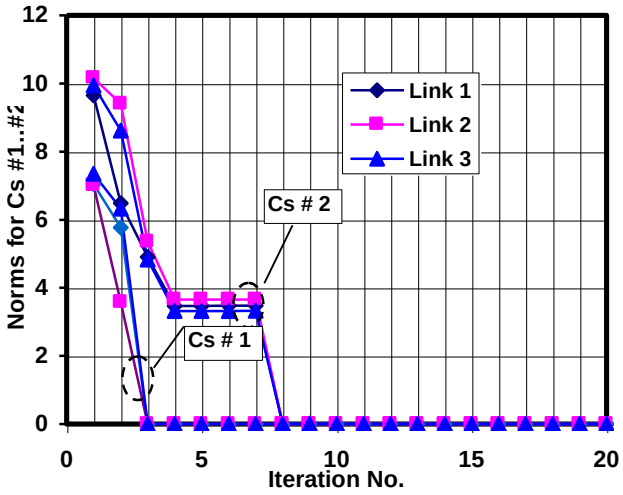

(a) Cs #1 and #2

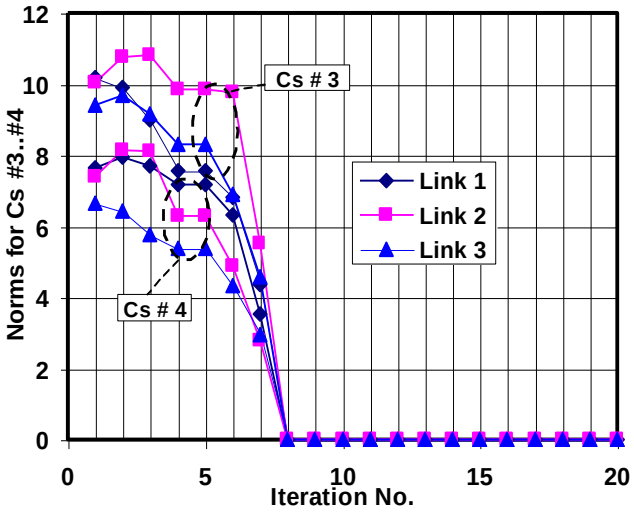

(b) Cs #3 and #4.

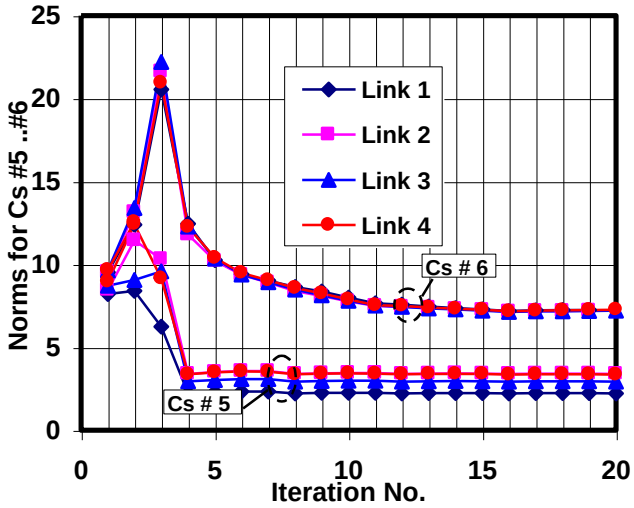

(c) Cs #5 and #6.

Figure 4.3. Plot of the residual error norms vs. the number of RLS iterations for all active links.

The number of RLS iterations required to achieve the defined steady-state, minimising the cost function and stabilising the residual norm within a variation no greater than 1% of its initial value, are provided in Table 4.3. This criterion could seem restrictive for RLS, but it can be used jointly with another kind of implementation, as Conjugate Gradient block-by-block [GiMC01]. It will be also referred what happened if the criterion is more relaxed.

Cs #	1	2	3	4	5	6
No. of Iterations	3	8	8	8	8	16

Table 4.3. Number of iterations for RLS convergence.

These values have been obtained from average error results after 100 WDCM concretisations, for each case and each link.

When the number of arriving signals is equal to the number the antennas, the number of iterations to converge is 8 independently of the delays of the arriving signal. That happens for Cs #2, #3 and #4. For Cs #5, where one code more than number of the antennas is being considered, the algorithm needs the same number of iterations than the cases referred to before.

Cs #6 is the worst case needing 16 iterations to convergence, for the criterion of the 1%, showing the bad convergence properties and the need for more iterations to reduce the final residual. It is seen in Figure 4.3 b) that the residue is decreasing after 10 iterations toward levels comparable to the final residual achieved. Nevertheless, the criterion is not satisfied until the iteration 16.

On the other hand, if the criterion would be more flexible, meaning that variation would be accepted to be greater than 1% of its initial value, for example 5%, it affects considerably the number of iterations in the worst cases due to the oscillations, concluding that the number of iterations would be close to 10.

Figure 4.4 presents the average SINR results from the RLS implementation for link MT1-BS. The other links are also presented in Appendix B.

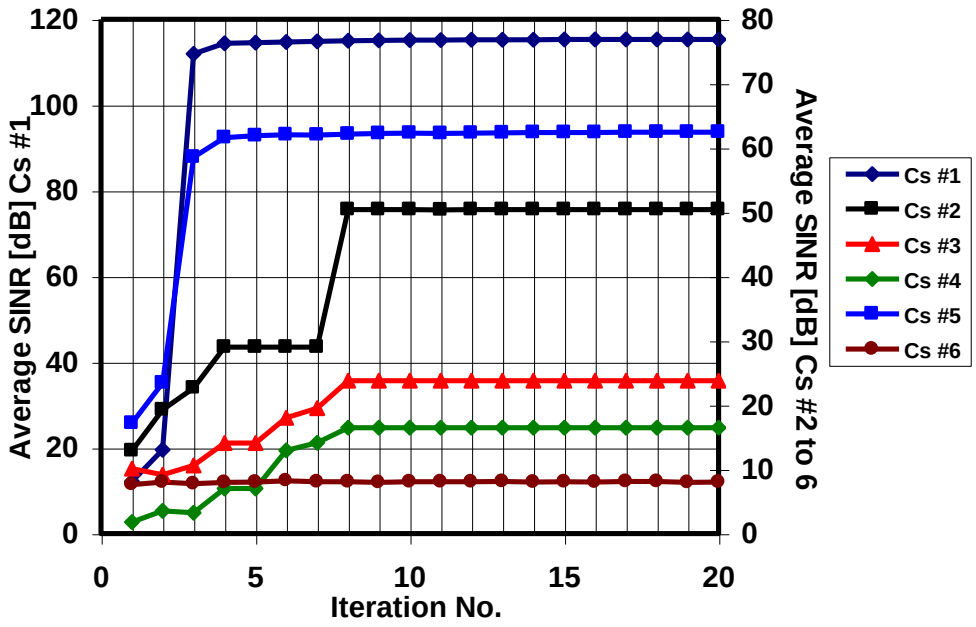

Figure 4.4. Average SINR vs. the number of RLS iterations, for link MT1-BS.

For Cs #1, the SINR obtained is higher than 100 dB due to the non-restrictive case already described.

An interesting result is that Cs #5, for which $L_T > M$, but with no relative cluster delays contributing to L_T, exhibits relatively very good SINR, even surpassing that of Cs #2, but with a number of cluster delay contributions. Therefore, the presence of a certain number of orthogonal delayed codes results in worse SINR levels than the case of the same number of excess non-delayed link codes being present. The other links are shown in Appendix B and this last conclusion is verified.

Cs #4 achieves lower SINR levels, compared to Cs #3, due to the presence of much higher interfering power.

Table 4.4 summarises the average beamforming processing gains, G_{bf}, after final convergence, for each case and link.

Average Beamforming Gain, G_{bf} [dB]				
Cs #	Link 1	Link 2	Link 3	Link 4
1	111	111	109	-
2	45	47	43	-
3	23	24	33	-
4	31	25	27	-
5	54	53	51	55
6	24	33	39	25

Table 4.4. Final beamforming average gain for the RLS.

For all links, beamforming achieves positive processing gains, showing the advantages of its use in this application. Cs #3 and Cs# 4 present the lowest gains, as foreseen due to strong presence of delay version of the SoI . Cs #5 achieves the second best results as with the SINR results. It is also interesting to notice that Cs #4, with higher interfering power than Cs #3 exhibits higher gains than those of Cs #3. Despite the use of 100 WDCM concretisations, the average beamforming gains presents great variation between links, which is specially critical in Cs #6 as expected due to the greater variance in the WDCM with a high number of the arriving signals.

Figure 4.5 shows the average BER for Cs #6 versus the number of RLS iterations, for all active links. Note that the behaviour is similar to the SINR result due to the own definition used.

The other cases' results exhibit lower BER, and the less restrictive the case is the more all link results are near to each other. As seen, for Cs #6 BERs differ among links, depending on the propagation conditions, because the WDCM variations affect differently each link. Also, such worst case implies relatively large final BER oscillations, with convergence in the mean. The discrepancies in the results among links, specially in Cs #6, have been shown to result from the variation of many WDCM parameters, leading to great variances in the final results.

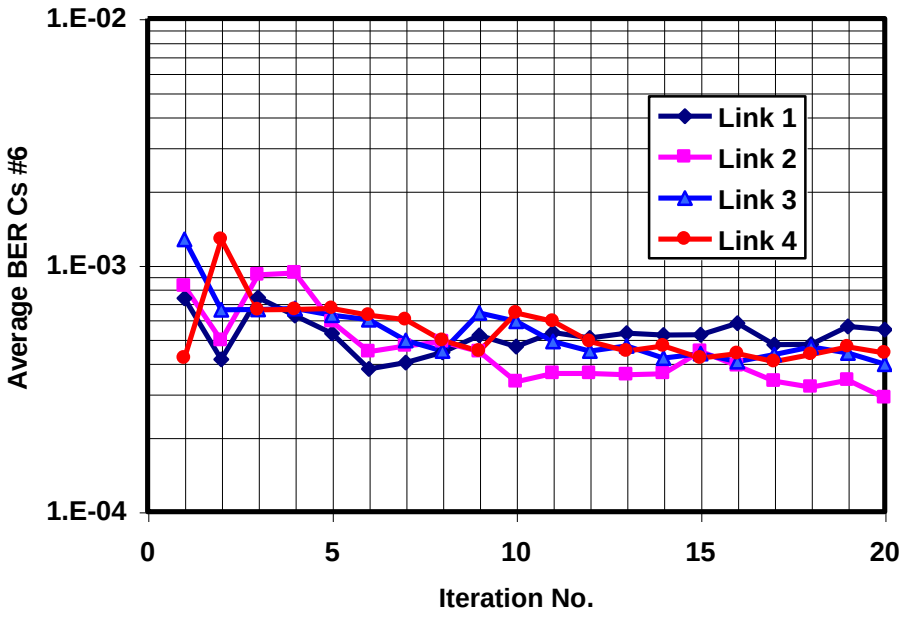

Figure 4.5. Average BER vs. the number of RLS iterations for all active links, Cs #6.

Another characteristic that is verified, as it was the case for the SINR levels, is that for Cs #6 the variation of the BER, in the mean, is very little, compared to its initial value. In other words, before any iteration takes place, the initial BER (as the SINR) is close to its final mean after many iterations.

4.2.5 RLS Performance Results on one WDCM Concretisation

The analysis of the last section algorithm's performance has resorted to the averaging of the results obtained from a 100 totally independent WDCM concretisations, as mentioned several times. Such was found of importance in order to analyse how the algorithm generally performs, in absolute terms. It is also important to evaluate how the RLS behaves toward exactly in a concrete WDCM channel, establishing exactly the same scatterer characteristics and cluster positions. Also, in order to present the results in the clearest way, numerical tables of some parameters are presented, including weight vector elements evolution.

In Figure 4.6, plots of the residual norm evolution along iterations for Cs #5 and #6 are presented, showing the RLS performance towards a WDCM concretisation, for all cases. The other cases are included in Appendix B.

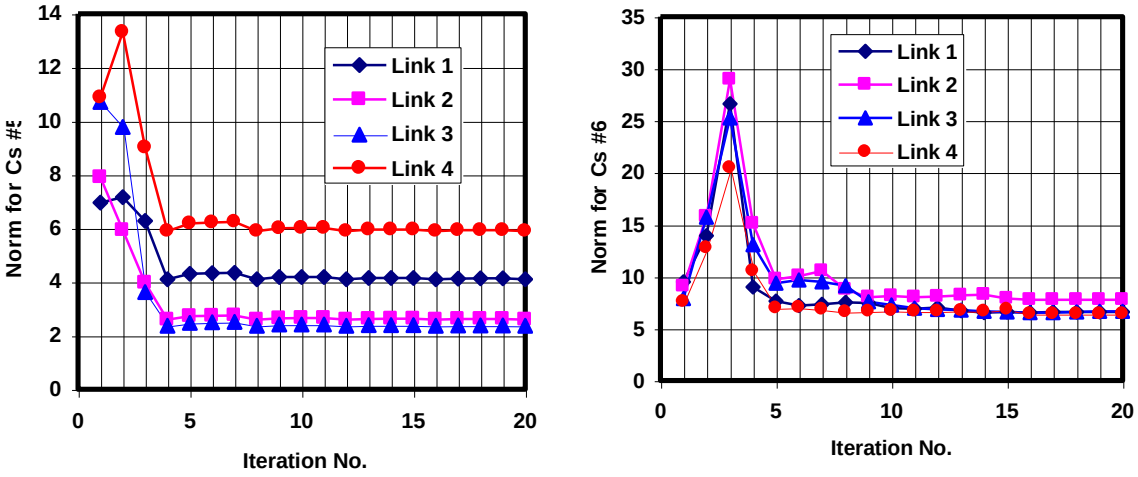

(a) Cs #5. (b) Cs #6.

Figure 4.6. Residual norm vs. number of RLS iterations for all links, cases #5 and #6.

The first conclusion is that the final residual between links is different with respect to the average values obtained in the preceding section. From here one can extract the important conclusion that the channel will be a key factor in the resulting final error that will be required for the algorithm.

The final residual for the RLS is higher for Cs #5 and #6, being highest in the latter case. For this, the effective residual reduction is lower for these two cases, which is predictable results since these are the cases for which the number of arriving orthogonal codes is higher than the number of antennas. For Cs #1 to #4, the residual reaches values very close to zero, compared to the initial values, suggesting that the final SINR values should be better than those of Cs #5 and #6.

A brief analysis of the autocorrelation matrix was also done to verify any relation between eigenvalues and bad convergence properties for Cs # 6. Oscillations of the RLS convergence depend on the minimum eigenvalue [Hayk91]. It was not possible to find any conclusion about this issue, because with smaller eigenvalues for other cases best convergence is also achieved.

The responses among links are different, for each case. Such is also a natural result, thinking that each cost function corresponding to each of the links is independent of each other, with independent WDCM characteristics among links. Nevertheless, the evolution of the residuals of the existing active links has many common tendency segments, among links, meaning that, along the same set of iterations, altogether the links' residuals may decrease or maintain their value, for each case. Cs #5 and #6 present a transitory peak after the second and third RLS iteration, not as severe as in the cases where the L_T=M.

According to the criterion previously presented, the number of iterations has also been found, for all cases and all links.

Unlike the average results, it has been found that this number depends on the link. Such is an expectable result, though, where such differences are seen to arise from the different angular placement and characteristics of the several corresponding clusters.

	Number of Iterations			
Cs #	Link 1	Link 2	Link 3	Link 4
1	3	3	3	-
2	9	9	9	-
3	11	11	11	-
4	11	11	11	-
5	12	8	8	12
6	14	14	14	14

Table 4.5. Number of RLS iterations after which the 1% variation criterion is met.

The discrepancies in the number of iterations, among links (for these WDCM concretisations) are clear. Cs #5 is the case that presents the largest discrepancies. In this case one can see what is the importance to define a criteria to extract the number of iterations required. If the criteria were more relaxed the number of iterations would not be the same, being nearest to the same number of iterations for all links. Being the number of codes the major limiting factor to determine the number of iterations.

The plots of the SINR evolution for Cs #3 and #6 are presented in Figure 4.7, the other cases are presented in Appendix B.

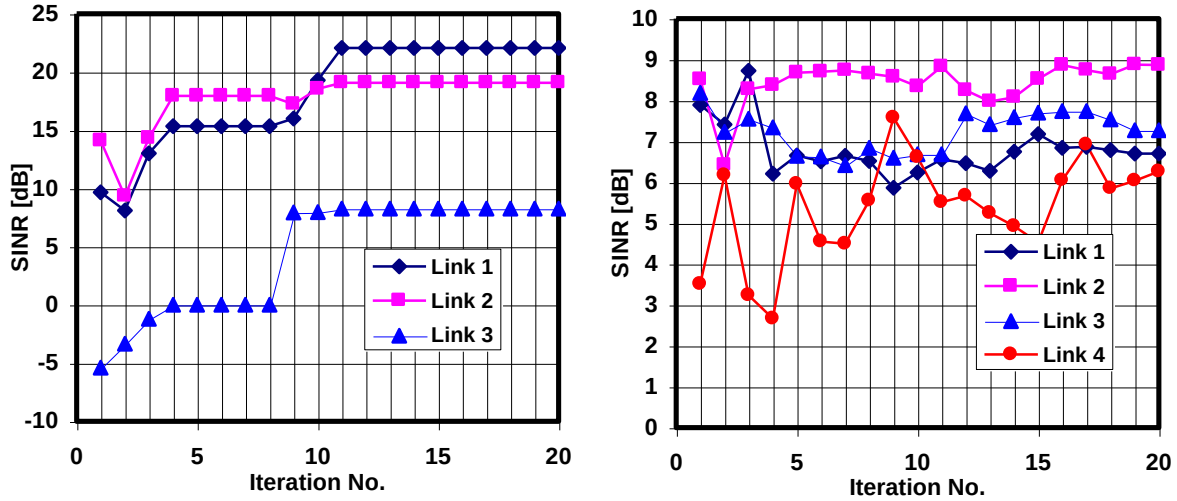

(a) Cs #3. (b) Cs #6.

Figure 4.7. SINR vs. the number of iterations for all links, cases #3 and #6.

The final SINR is lower for Cs #6, as predicted. For Cs #1 and #2, the SINR reaches values above 30 dB. For Cs #3 and #4 the SINR varies between 7 dB and 25 dB, depending on the link (other cases see Appendix B). Cs #5, for which the final residual error is the second worst, suggesting that the final SINR values would also be the second lowest, achieves SINR values between 8 dB and 22 dB, thus exhibiting overall better results than those of Cs #3 and #4, as it was concluded in the previously described RLS average analysis.

The SINR among links are different, for each case, as it happens with the residual norm. Also, the evolution of the SINR presenting many common tendency segments, among links. It becomes clear that the SINR evolution does not reflect the evolution of the residual norm. This becomes more clear in Cs #5 and #6 RLS cases, which present residual error peaks, not reflected in the SINR plots. Cs #3 and Cs #4 present very large discrepancies among links' SINR final results; this fact may be related to the cluster angular positioning. For

Cs #6, the RLS SINR evolution presents many points where its evolution is not very stable, as the residuals.

The beamformer processing gain results that have been obtained are qualitatively very similar to the SINR ones, in terms of evolution along iterations. Expectedly, the gain profiles follow those of the SINR very closely, meaning that, higher or lower SINR involves higher or lower processing gain, respectively, along iterations of each link.

Also, it has been found that the results among links generally respect the same relations as with the corresponding SINRs. Nevertheless, one exception has been found, for the specific Cs #4 WDCM concretisation. For this reason, other Cs #4 concretisations were tested, verifying that the exception is due to the specific channel case, also being possible to happen for the other WDCM study cases.

In Figure 4.8 the BER results for Cs #6 are presented. As in the SINR analysis, it is clear how the BER for the RLS presents difficult stabilisation.

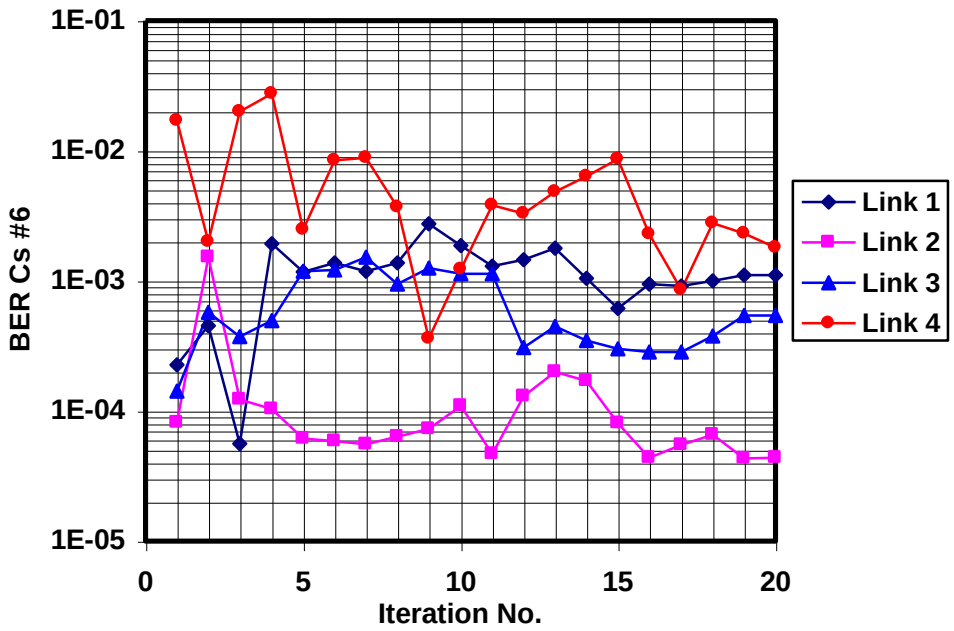

Figure 4.8. BER vs. the number of iterations for all links, Cs #6.

The other study cases achieve very low BER levels, according to the assumed approximations. The comments put forward for the SINR are similar to those for the BER results, and the most critical evaluation is best suited to the cases which present the lowest SINR levels.

The results of the RLS present oscillations, as referred to before. Such stability differences are more clear in Cs #6, where the RLS results are much more unstable than those of Cs #4.

In Table 4.6 the BER values for Cs# 4 and Cs #6, along iterations, for RLS, link number 1 are shown. For Cs #4, the RLS results stabilise (to the second decimal) at 2.53×10^{-4}. at the 11th iteration, but this is not the case for Cs #6. It results impossible for Cs #6 (by using the BER plot), to identify the iteration at which the convergence is achieved.

Between Cs #4 and Cs #6, as mentioned before, the former achieves BER final values that are lower than those of the latter case.

Iteration number	**Cs #4**	**Cs #6**
1	1.01E-01	2.26E-04
2	1.40E-01	4.50E-04
3	3.99E-32	5.62E-05
4	1.66E-06	1.93E-03
5	1.66E-06	1.18E-03
6	1.66E-06	1.37E-03
7	1.66E-06	1.19E-03
8	1.66E-06	1.37E-03
9	7.73E-03	2.75E-03
10	4.35E-04	1.87E-03
11	2.53E-04	1.31E-03
12	2.53E-04	1.46E-03
13	2.53E-04	1.78E-03
14	2.53E-04	1.05E-03
15	2.53E-04	6.17E-04
16	2.53E-04	9.43E-04
17	2.53E-04	9.13E-04
18	2.53E-04	1.00E-03
19	2.53E-04	1.11E-03
20	2.53E-04	1.11E-03

Table 4.6. The BER values for Cs# 4 and Cs #6, along iterations, for link number 1.

As it has been mentioned before, the number of *Flops* has been calculated, using MATLAB®, accounting solely for the number of calculations involved in each iteration. The

result is plotted as a function of the number of antennas. Note that the number of antennas used is higher than a real situation, but the idea is to see the whole evolution of the *Flops*. Figure 4.9 shows the evolution of the flops versus number of the antennas. The utility of this study is to find a relation between number of antennas and *Flops*. For this result MATLAB® was useful using the command POLYFIT which finds the coefficients of a polynomial of degree *N* in a least-squares sense. For degree 2 the following expression was obtained for the *Flops* in function of the number of antennas per iteration for one user:

$$Flops \approx 24M^2 + 30M + 1 \tag{4.10}$$

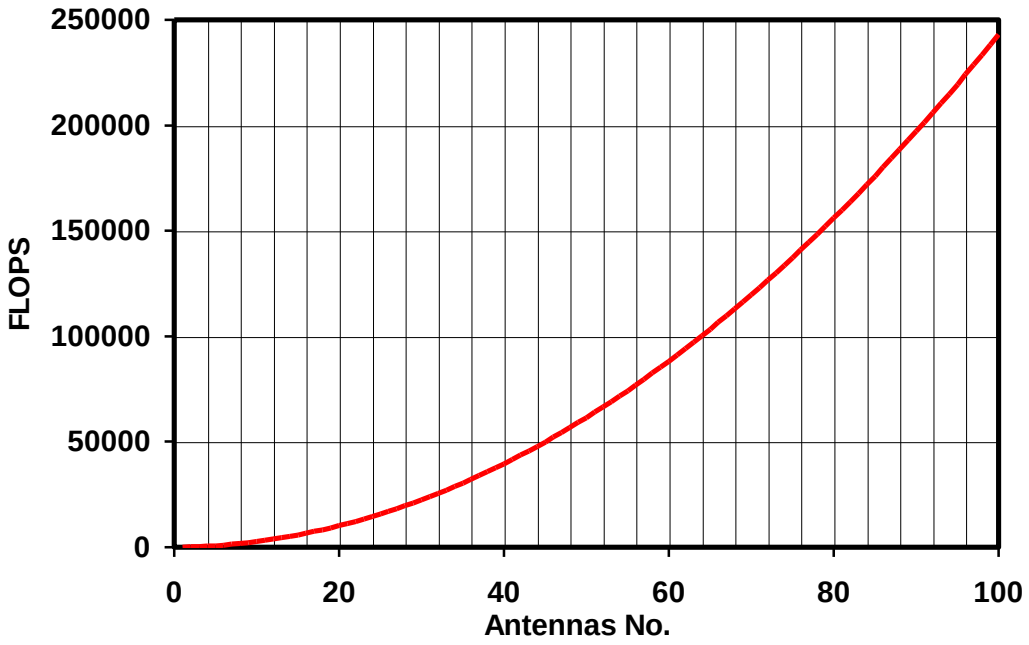

Figure 4.9. Number of RLS flops per iteration vs. the number of antenna elements.

The proximity between (4.10) and the number of flops obtained in the simulations was analysed, being found that it is very close to these calculations. It also results interesting to find what is the impact by adding a new user in the required *Flops*. For that, some simulations were done, varying the number of users to find a relation between *Flops* and a new user. Figure 4.10 summarises the evolution of the number of *Flops* with the increase of the number of users. It can be seen that the increase of the number of links implies a proportional increase in the number of operations. This increase is small since only a small change in the source code is necessary, in order to include an additional user.

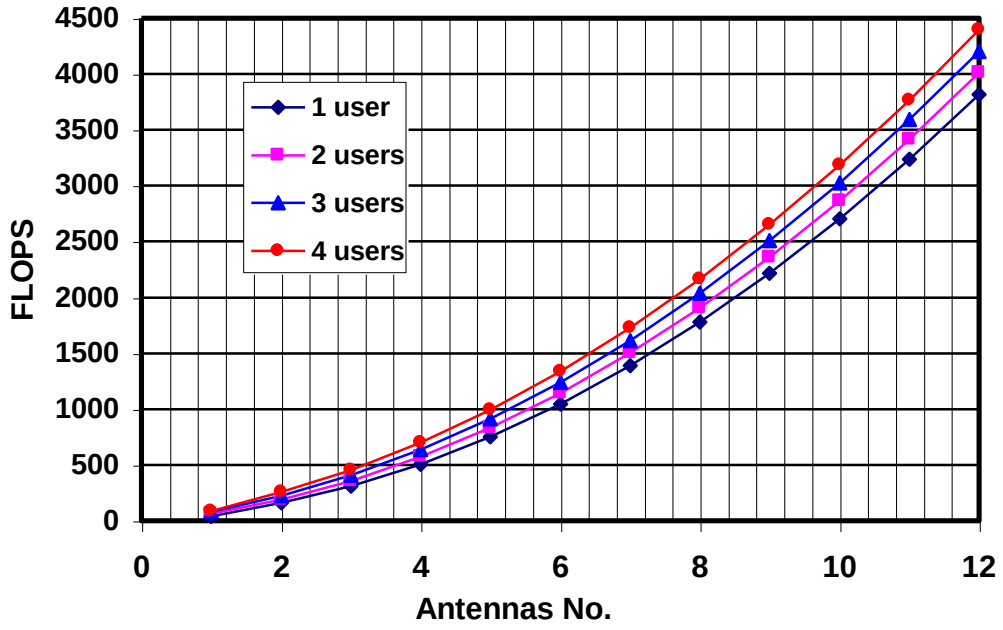

Figure 4.10. Number of RLS flops per iteration vs. the number of antenna elements, function of the number of users.

To include a new user in those calculations, the number of additional *Flops* required can be seen as an offset between added each user. Each user supposes an increase in the number of *Flops* required, and that number is fixed for each number of antennas. After a careful study of the number of flops, it was conlcuded that the increase is 16*M Flops* for each user. Therefore, including this small increase needed for each new user in (4.10), a good approximation to estimate the number of *Flops* per iteration as function of the number of antennas and users is:

$$Flops \approx 24M^2 + (30 + 16(L-1))M + 1 \qquad (4.11)$$

where M is the number of antennas and L the number of links/users. From (4.11) one can judge the complexity by the number of *Flops*: the processing complexity of adding a new user is very small.

In order to better view the involved weight vectors, Table 4.7 presents the values that have been obtained, for Cs #1 link 1, and Table 4.8 the values for Cs #6, link 1.

Pointing out that the high residual error and consequent low SINR tendency, which characterise Cs #6, result from discrepancies at weight element decimals lower than the fourth decimal, one confirms that a *weight estimation error* does not clearly translate such. This is due to the nature of the signal matrix, **U**, that in Cs #6 includes information from many

orthogonal sources, compared to the number of antennas, making the residual error and SINR much more sensitive to smaller changes in weights. As expected, due to the overpassing of this number, the algorithms' sensitivity to smaller weight variations is much more critical.

Iter. No.	w_1	w_2	w_3	w_4	w_5	w_6
1	0.0389-0.0678j	-0.0292+0.0541j	0.1235+0.0261j	0.0021+0.0471j	0.0021+0.0471j	-0.0441-0.0685j
2	0.0094-0.0961j	-0.0178+0.0549j	0.1237+0.0083j	0.0897-0.1206j	0.0897-0.1206j	-0.0413-0.0823j
3	0.0970-0.1573j	-0.1258+0.1059j	0.1855+0.0297j	0.0705-0.1495j	0.0705-0.1495j	0.0501-0.0415j
4	0.0970-0.1573j	-0.1258+0.1059j	0.1855+0.0297j	0.0705-0.1495j	0.0705-0.1495j	0.0501-0.0415j
5	0.0970-0.1573j	-0.1258+0.1059j	0.1855+0.0297j	0.0705-0.1495j	0.0705-0.1495j	0.0501-0.0415j
6	0.0970-0.1573j	-0.1258+0.1059j	0.1855+0.0297j	0.0705-0.1495j	0.0705-0.1495j	0.0501-0.0415j
7	0.0970-0.1573j	-0.1258+0.1059j	0.1855+0.0297j	0.0705-0.1495j	0.0705-0.1495j	0.0501-0.0415j
8	0.0970-0.1573j	-0.1258+0.1059j	0.1855+0.0297j	0.0705-0.1495j	0.0705-0.1495j	0.0501-0.0415j
Opt w_i	**0.1193-0.1525j**	**-0.1316+0.1082j**	**0.1893+0.0360j**	**0.0649-0.1325j**	**0.0649-0.1325j**	**0.0275-0.0799j**

Table 4.7. The weight vectors calculated, along iterations, for link 1, Cs #1.

The oscillatory behaviour of the RLS can be again seen in Table 4.8 for Cs # 6, not achieving in any moment a fixed value, although stabilising in values close to the optimum solutions.

Iteration No.	w_1	w_2	w_3
1	-0.0039-0.0316j	-0.0332+0.1081j	0.0204+0.0140j
2	-0.2283-0.3146j	-0.0703-0.0015j	0.0855-0.0224j
3	-0.1314-0.4003j	-0.1197+0.0644j	-0.1349-0.4949j
4	-0.2313+0.1777j	-0.1446+0.0993j	-0.0056+0.0399j
5	-0.1074+0.2257j	-0.1391+0.1138j	0.1501+0.0413j
6	-0.1130+0.1727j	-0.1484+0.0795j	0.1194+0.0430j
7	-0.1184+0.1872j	-0.1526+0.0636j	0.1430+0.0376j
8	-0.1121+0.1883j	-0.1554+0.0733j	0.1461+0.0192j
9	-0.1616+0.1518j	-0.1818+0.0674j	0.1098+0.0192j
10	-0.1617+0.1359j	-0.1656+0.0498j	0.0993+0.0565j
11	-0.1359+0.1243j	-0.1524+0.0374j	0.1361+0.0513j
12	-0.1351+0.1235j	-0.1585+0.0395j	0.1391+0.0398j
13	-0.1587+0.1109j	-0.1450+0.0205j	0.1047+0.0523j
14	-0.1280+0.0969j	-0.1098+0.0041j	0.0921+0.0652j
15	-0.0993+0.0810j	-0.0912-0.0133j	0.1001+0.0741j
16	0.0993+0.0810j	-0.1112-0.0193j	0.0840+0.0808j
17	-0.1259+0.0848j	-0.1009+0.0159j	0.1019+0.0775j
18	-0.1347+0.0761j	-0.1101+0.0107j	0.1020+0.0825j
19	-0.1292+0.0994j	-0.1144+0.0133j	0.0916+0.0656j
20	-0.1364+0.1068j	-0.1154+0.0113j	0.0892+0.0668j
Optima w_i	**-0.1304+0.0723j**	**-0.1112-0.0193j**	**0.0840+0.0808j**

Table 4.8. The weight vectors calculated, along iterations, for link 1, Cs #6.

Also with the objective of clearer describing the results, some antenna patterns are shown in Figure 4.11. These refer for all links, Cs #1 and Cs #6. The plots also indicate the direction at which the clusters are angularly placed, referring to the corresponding link.

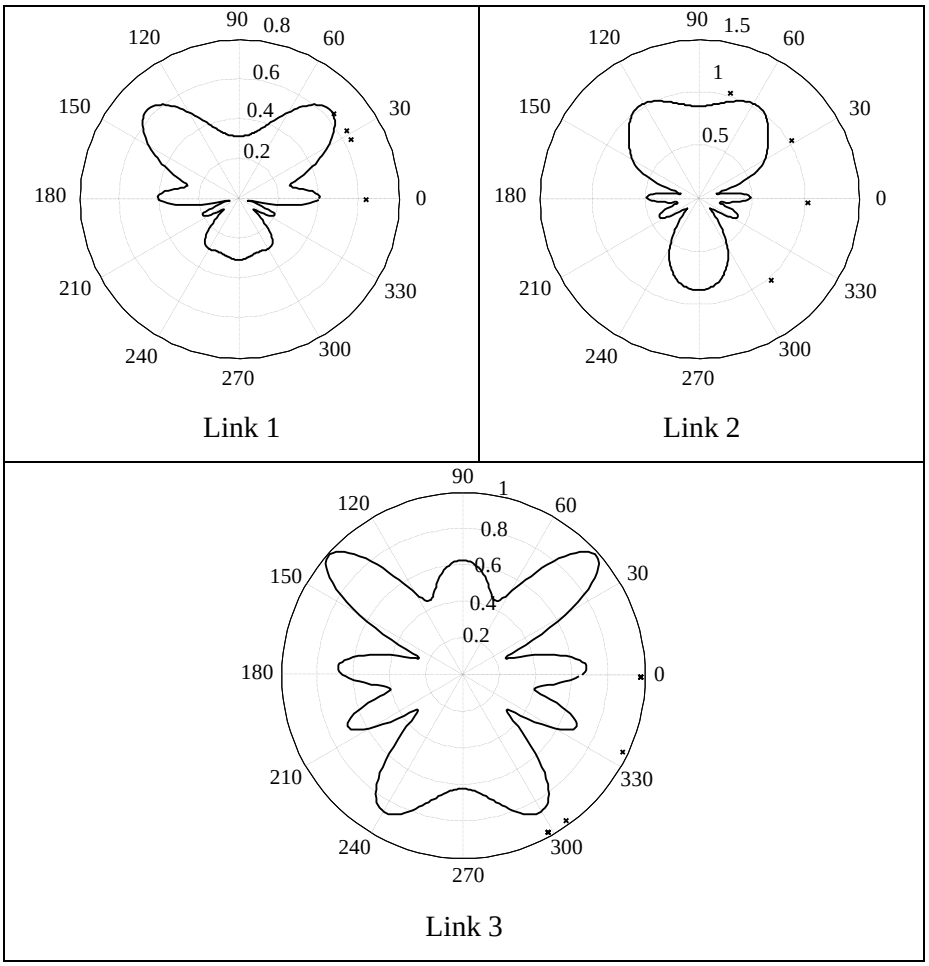

Figure 4.11. The final antenna patterns, for all links, Cs #1, with the indication of the angular position of clusters.

One must note that the diagrams are not shaped with obvious pointing main lobes mainly due to the characteristics of the incoming signals, from clusters of scatterers whose reflection coefficients are randomly generated in modulus and phase.

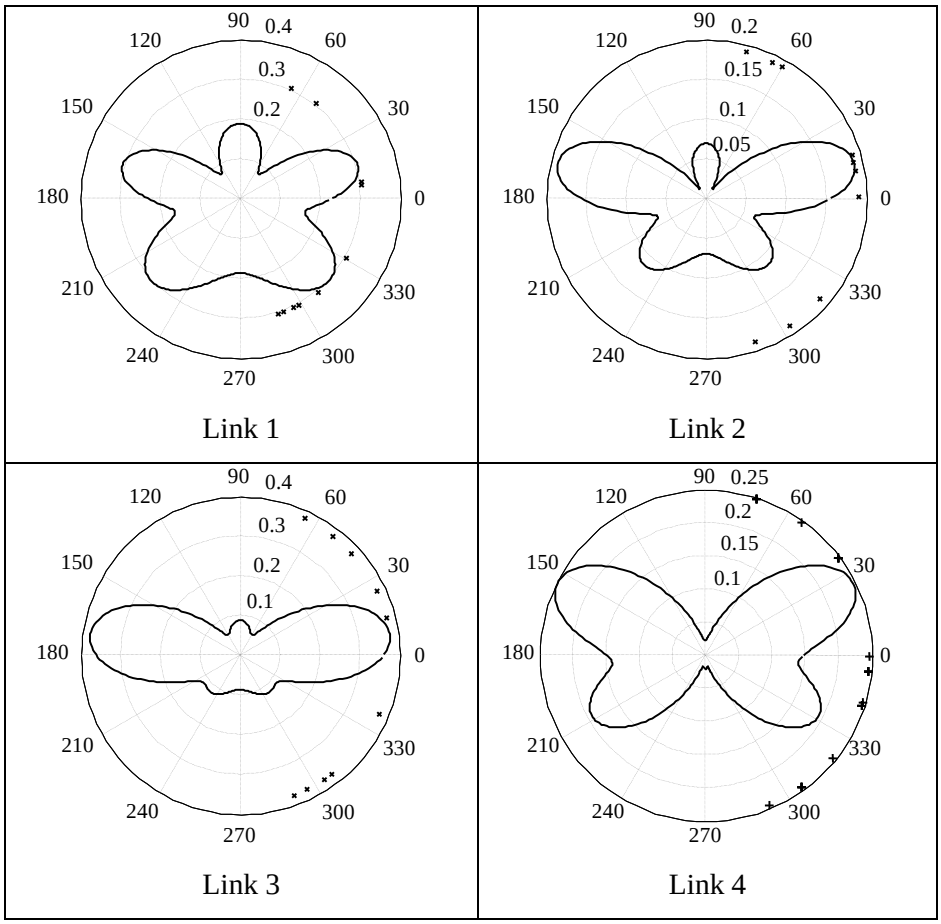

Figure 4.12. The final antenna patterns all links, Cs #6, with the indication of the angular position of clusters.

Even for Cs #1, where the absolute optimum is reached, the diagrams reveal such characteristics. For example, for the applied WDCM, a cluster may exist but with negligible power and even such may happen with all existing clusters (a definite step in the application of the RLS is to refine the WDCM reflecting a specific propagation scenario, thus defining LoS and general cluster definitions accordingly, being developed in next chapter). In this way, the directivity of the arrays would undoubtedly improve if no multipath nor several AoA would be considered. On the other hand, the implementations inherently make use of all possible incoming DesS, in the sense of minimum squared error.

5 Application of the RLS Algorithm to Specific Scenarios

5.1 Scenarios Description

In Chapter 4 some simulations were held using a general scenario, which is not very realistic, in the perspective of understanding and analysing the convergence of the RLS algorithm in a WDCM environment. Once this is done, a more realistic scenario is used in this chapter with the purpose of applying the algorithm to a case study. The WDCM used for UTRA-TDD was the one implemented in [Marq01]. This model is proposed for a micro-cell environment, in which it is assumed that the BS is below rooftop level, and a particular environment is chosen, the LoS street operational environment, which considers both BS and MT positioned along the same street.

This model considers a group of scatterers distributed along a planar region according to a predefined Probability Density Function (PDF). This PDF is restricted to a delimited region, and the shape of this region depends on the environment where the model is to be applied. This model assumes that only a single specular reflection in one scatterer occurs, as proposed by the GBSB [LiRa99], [Marq01].

[Marq01] proposes as scattering region an ellipse whose foci are the BS and the MT. The ellipse size is confined to the street width. Clusters are distributed uniformly within the street, and scatterers have a Gaussian distribution within a cluster.

Figure 5.1 depicts an example of the operational environment and the resulting scatterers positioning. The elliptical scattering region for a particular MT position is also represented. Some exemplifying signal paths are also represented in the picture.

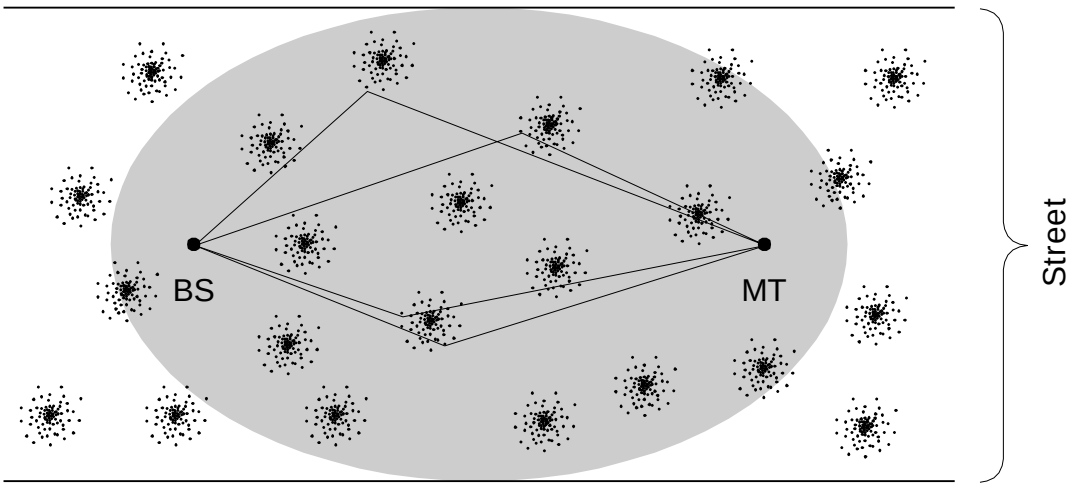

Figure 5.1. Spatial distribution of scatterers within a street (extracted from [Marq01]).

It is assumed that the MT moves along the street axis, parallel to it.

The WDCM for micro-cell environments used in this work has a strong dependency on the geometry of the scenario [Marq01]: for an increasing BS-MT distance, it can be seen that the number of delay chips present in the signal decreases; the Directional Channel Impulse Response (DCIR) is shown for two positions (see Figure 5.2). The number of depicted rings corresponds to the number of delay chips where incoming signal exists; the angle analysis is referenced with respect to LoS, which is assumed to exist for an AoA of 0º. The angle resolution is 3º, the colour scale representing the linear amplitude of SoI in linear, and the ToA being separated in chips.

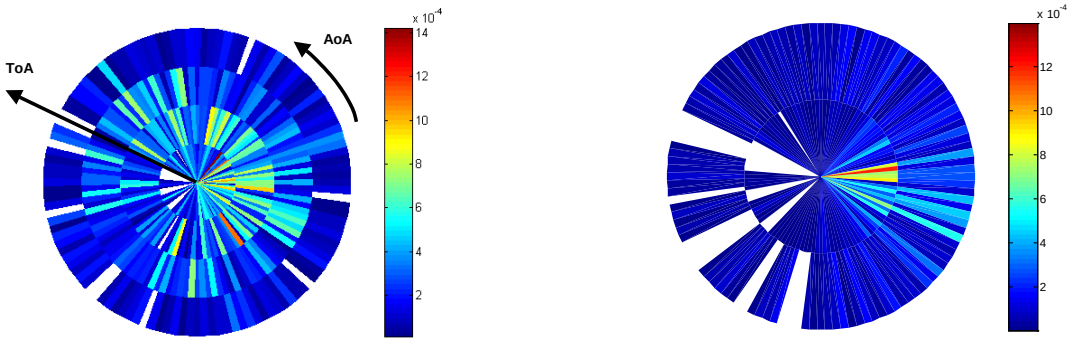

Figure 5.2. DCIR results for 50 m and 500m.

From these DCIRs one can conclude that for shorter distances, the angular discrimination is lower; therefore, the represented signal does not show a very intense variation in the same ring. This discrimination is larger for longer distances, corresponding to a concentration of the signal around the LoS AoA [Marq01].

When more than one delay ring exists, a phenomenon similar to a pair of lobes can be observed at peripheral rings: for these rings the signal is weaker in the LoS direction, while it is stronger in two groups of directions close to the LoS, and symmetrical with respect to it [Marq01].

These last DCIR results can be helpful to enable the analysis of the resulting beampattern after the calculation of the weights that minimise the cost function; hence, one can check the formation of the lobes as a function of the AoA and of the amplitude of the SoI.

The final beampattern takes the different contributions into account as a function of the distance.

In order to test the RLS together with the WDCM previously described, several scenarios were defined. The environment where the simulations were developed is based on the DCIR obtained for distances equally spaced from 50 to 1000 m along a street with a width of 40 m [Marq01], Figure 5.3.

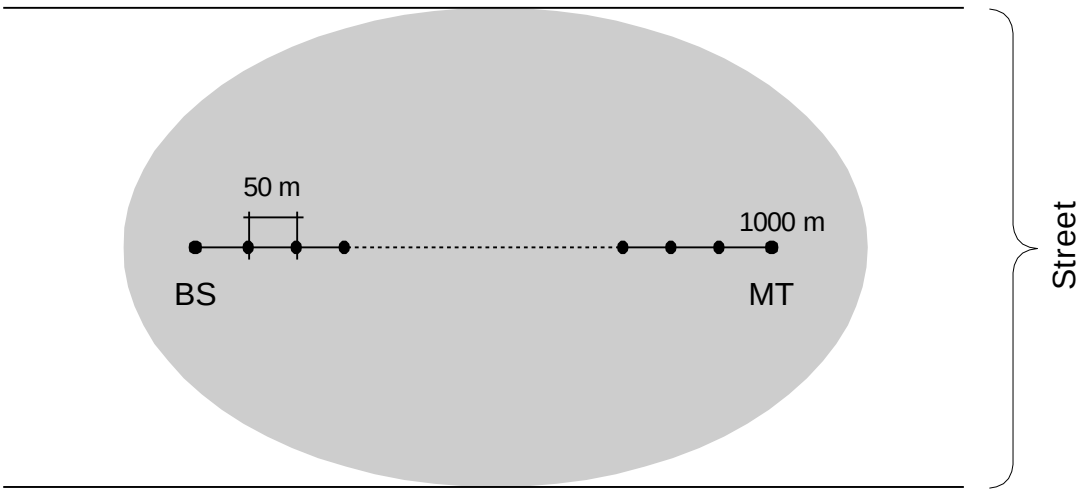

Figure 5.3. Environment for simulation.

Many simulations were held, varying the BS-MT distance, $d_{\text{BS-MT}}$, the number of antennas, M, and the number of links, L. The cases of interest that are considered in this chapter are:

- For the same number of antennas (12 in this case), the position of the MTs was varied along the street for three different $d_{\text{BS-MT}}$, 50, 500 and 1000 m. For each $d_{\text{BS-MT}}$, all the MTs are located at the "same distance". The simulations cover 4, 8 and 16 active links for the specified $d_{\text{BS-MT}}$. The reason for this selection is that they are the worst cases (concerning the number of users) for the same length of the channelisation code in TDD.
- For the same number of active links, L=16, the number of antennas, M, is varied to check the effect that this change has on the parameters to evaluate.
- MTs equally spaced distributed along the street, i.e., $d_{\text{BS-MT}}$ is not the same for all MTs, for L=16 and M=12.

As it was referred before, there are users located at the “same distance”. Obviously, this is not exact. To simulate MTs close to each other, an approximation is done: the same DCIR is assumed in signal distribution for the MTs that are considered at the “same distance”, but with different phases. The phase of the DCIR is varied uniformly in the interval $[0,2\pi[$. There is a physical reason for this approximation: the wavelength in the UMTS band is of the order of a few centimetres, a separation between MTs of one metre producing a large phase variation; consequently the MTs will have a different phase profile, but the amplitude can be considered approximately the same. The reason for this approximation is the time cost that it would take to perform the simulation of more DCIRs for a given $d_{\text{BS-MT}}$. The reason to do this approximation in order to obtain different DCIRs is because taking the same DCIR for all MTs implies that the algorithm does not converge, due to the inexistence of the inverse of the autocorrelation matrix.

The results cover the SINRm, Gbfm and BERm. Their mean values for each link, in the sense of covering all MTs at the same distance, in one concretisation is considered. The dependency on the number of users of the final SINR and the resulting beampatterns after weight calculations for different $d_{\text{BS-MT}}$ with respect to a given DCIR are presented.

5.2 Analysis of Results

Note that the obtained results are limited, since only one concretisation is considered. Both SINRm and Gbfm are expected to increase with distance for this kind of scenario, as one can see from the mean of all links that has been calculated for this case. The variance is high when the number of orthogonal codes and active links is very high, being necessary to perform more simulations in order to estimate the real tendency of SINRm and Gbfm. Due to the lack of time it was possible to perform simulations for one case only.

Tables 5.1, 5.2 and 5.3 summarise the results extracted from the simulations for one concretisation. For the simulations, the number of users has been varied as a function of the channelisation code used. L_{T} is the number of arriving orthogonal codes at the BS for a given $d_{\text{BS-MT}}$. For all scenarios, the number of antennas is M=12.

$d_{BS\text{-}MT}$	$SINR_m$[dB]	G_{bfm}[dB]	BER_m	L_T
50 m	8.8	6.8	$4.9 \cdot 10^{-5}$	16
500 m	17.1	11.4	$<10^{-18}$	8
1000 m	63.1	56.5	$<10^{-18}$	4

Table 5.1. Simulation results for L=4.

$d_{BS\text{-}MT}$	$SINR_m$[dB]	G_{bfm}[dB]	BER_m	L_T
50 m	6.6	6.9	$1.2 \cdot 10^{-3}$	32
500 m	10.3	10.4	$1.8 \cdot 10^{-6}$	16
1000 m	57.0	53.0	$<10^{-18}$	8

Table 5.2. Simulation results for L=8.

$d_{BS\text{-}MT}$	$SINR_m$[dB]	G_{bfm}[dB]	BER_m	L_T
50 m	7.7	10.1	$3.0 \cdot 10^{-4}$	64
500 m	5.7	7.4	$3.2 \cdot 10^{-3}$	32
1000 m	17.8	17.6	$<10^{-18}$	16

Table 5.3. Simulation results for L=16.

The worst case corresponds to the MTs located at $d_{BS\text{-}MT}$=50 m, as expected due to the high dispersion angular, as shown in Figure 5.2. When the number of actives links rises, for the same $d_{BS\text{-}MT}$, the corresponding $SINR_m$ and G_{bfm} must decrease, since a higher number of arriving orthogonal codes are accounted for, therefore, the interfering signal present at the BS produced by the other MTs is higher. That happens, as the tables show, in all the cases but less in Table 5.3, in this case, for L=16 and M=12, when the MTs are located at 500 m, the resulting $SINR_m$ and G_{bfm} are smaller than the for $d_{BS\text{-}MT}$=50 m.

To check that this result is due to the high variance of the WDCM in one concretisation, average results are presented in Table 5.4. As it can be seen, the results are expected. When the $d_{BS\text{-}MT}$ increases, both $SINR_m$ and G_{bfm} are higher. However, G_{bfm} is not very far from the results obtained in one concretisation, specially for $d_{BS\text{-}MT}$=1000 m.

$d_{BS\text{-}MT}$	$SINR_m$[dB]	G_{bfm}[dB]	BER_m	L_T
50 m	3.0	7.3	$2.3 \cdot 10^{-2}$	64
500 m	7.2	8.9	$7.4 \cdot 10^{-4}$	32
1000 m	17.8	18.0	$<10^{-18}$	16

Table 5.4. Simulations average results for 100 WDCM concretisations, for L=16.

The case where $d_{BS\text{-}MT}$=50 m for all links, and L=16, is shown in Table 5.5. The number of antennas, M, has been modified, to evaluate its influence in both $SINR_m$ and G_{bfm}.

M	$SINR_m$[dB]	G_{bfm}[dB]	BER_m	L_T
3	1.6	7.3	$4.3 \cdot 10^{-2}$	64
4	1.4	7.0	$4.8 \cdot 10^{-2}$	64
6	2.0	7.5	$3.7 \cdot 10^{-2}$	64
12	7.7	10.1	$3.0 \cdot 10^{-4}$	64

Table 5.5. Simulation results for L=16 and $d_{BS\text{-}MT}$=50 m.

As the number of antennas increases, $SINR_m$ and G_{bfm} increase as expected; nevertheless, for M=4, the result is as expected, for the reasons mentioned before. When M is only 3, an effective Beamforming processing gain of 7.3 dB has been found. However, the SINRm shows a slow increase until M=6, this change is very high from M=6 to 12. Note that this is a critical case, the worst one, since the maximal number of users was used for TDD. Anyway, a positive G_{bfm} has been confirmed for all cases.

In Table 5.6, a simulation varying the position of the MTs for one WDCM concretisation is presented. The expected result, if average results were analysed, is that SINR and G_{bf} must decrease as $d_{BS\text{-}MT}$ increases, since no power control is being considered due to the simplification of the problem. However, for one concretisation, as the variance is high, a solution not according very well to this expectation is obtained, confirming a great variance between links. Anyway, a tendency to decrease both SINR and G_{bf} levels as MTs are moving away from the BTs can be seen without extracting a definitive result, which comes from the

fact that interfering signal contribution is greater for MTs far away from the BS, since attenuation is higher with distance. For all cases, a positive G_{bfm} exists, revealing the improvement by the use of Adaptive Beamforming.

$d_{\text{BS-MT[m]}}$	100	200	300	400	500	600	700	800
SINR_m[dB]	13.4	3.8	10.5	8.9	-2.0	8.4	5.0	-1.1
G_{bfm}[dB]	7.7	2.8	9.7	10.0	0.2	13.6	9.0	5.3
BER_m	$2.2\cdot10^{-12}$	$1.4\cdot10^{-2}$	$1.1\cdot10^{-6}$	$4.1\cdot10^{-5}$	$1.3\cdot10^{-1}$	$1.0\cdot10^{-5}$	$6.0\cdot10^{-3}$	$1.0\cdot10^{-1}$
L_T	18	18	18	18	18	18	18	18

Table 5.6. Simulation results for L=8 and M=12.

In Figure 5.4 and Figure 5.5, the DCIRs for $d_{\text{BS-MT}}$= 500 and 1000 m are compared to the resulting beampatterns after the calculation of the weights by the RLS algorithm. Note that it is calculated taking only the signal contribution of the semi-plane that contains the LoS into account. It is easy to see that the lobes formation is done according to the signal distribution, obtaining maxima of the beampattern at the direction of higher signal contributions. On the other hand, interfering signals have been taken into account in the weights calculation: since the interferences are orthogonals to the SoI, the cost function minimises their contribution for their AoA, maximising it for the AoA of the SoI, resulting in the maximisation of the SINR. This can result in a not very common beampattern, but being effective in the maximation of the SINR.

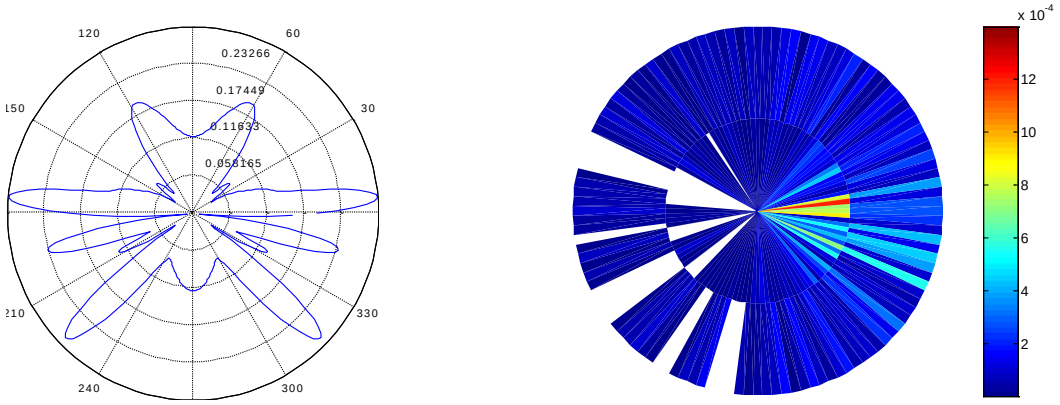

Figure 5.4. Beampattern vs the DCIR for $d_{BS\text{-}MT}$= 500 m.

For $d_{BS\text{-}MT}$= 1000 m a maximum for AoA=45º and 90º has been found. That happens because only a source has been analysed, but many beams are formed in the AoAs of the strongest signal around the LoS.

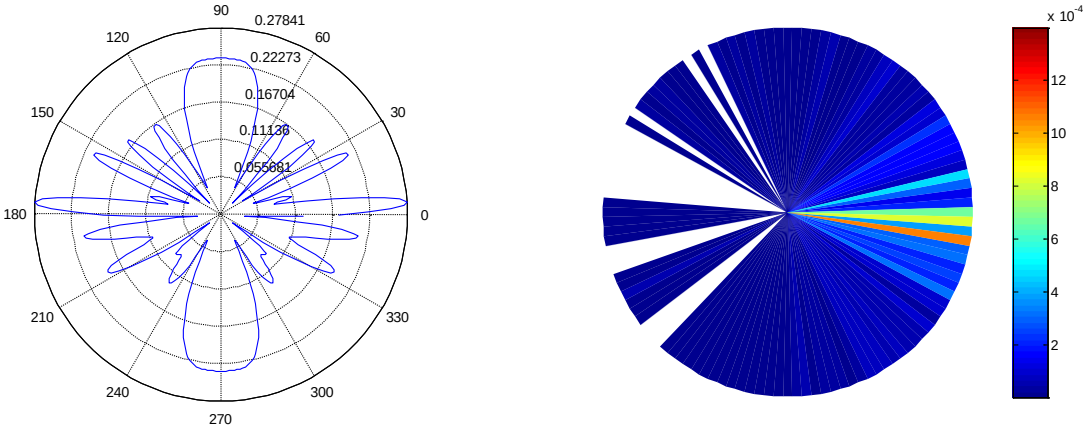

Figure 5.5. Beampattern vs. the DCIR for $d_{BS\text{-}MT}$= 1000 m.

One concretisation for all active links at 50 m is shown in Figure 5.6 and Figure 5.7. The first figure shows the SINR evolution for L=4 and the second one for L=8. The idea is to present the influence in the final stabilisation when the number of links increases.

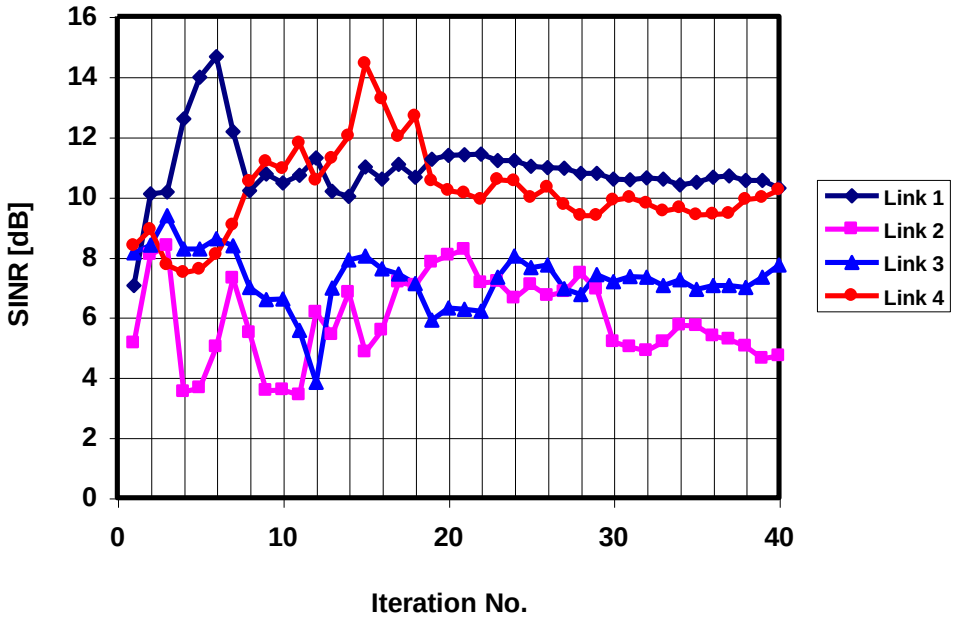

Figure 5.6. SINR vs. the number of iterations, for *L*=4 at 50 m.

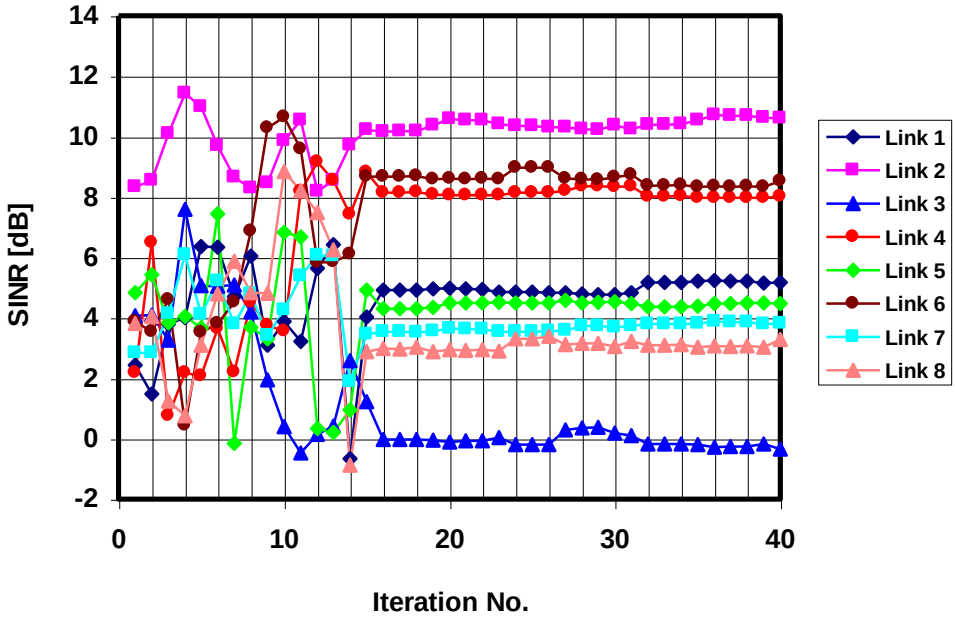

Figure 5.7. SINR vs. the number of iterations, for *L*=8 at 50 m.

The SINR presents a very different behaviour between the two cases. Regarding Figure 5.7, there are 10 dB difference between the solution for links 3 and link 2, showing high variance between links as happened in Chapter 4. This shows the critical importance that the WDCM has, involved within a *hostile* scenario, when the number of orthogonal codes is much higher than the number of antennas. One should remember that the difference between both links is solely the phase that has been changed randomly in the interval between [0, 2π[,

resulting in a 10 dB difference between both links. The number of iterations is also different for both cases, requiring for the first one a number difficult to determinate but always than the second case that is fixed to 16 with absolute clarity. If the number of users were 16, it would require the same number of iterations as it is shown in Appendix C. Also, it must be pointed out that the stability of the final solution is better than in the case of 8 links, with SINR smaller as expected. Finding an explanation to this result is not easy. Two possible ones could be:

- One can find a certain relation between the length of the channelisation codes and the convergence properties. This requires a deeper study of the orthogonality between codes, a fact being that the cross product between codes and their delayed versions is not the same. That was tested during the generalisation of codes. Nevertheless, the real length is the sum between the channelisation and the scrambling codes, its length being 16 for all cases, enssuring the orthogonality between them.
- The other possible motive can be found through the "distance" between codes, i.e., the number of bits that differentiate them. In fact, for the case of 4 links the length of the channelisation code is 4. On the other hand, for the case of 8 links, the length of the channelisation code is 8. From here, the "distance" between codes will be higher for the second case than for the first one, therefore, the difference between them will be higher.

Anyway, no strong relation was found but it is of interest to emphasise this difference.

6 Conclusions

The great problem for the development of this work was the scarce information about implementations like this in a WDCM scenario found in the literature. The more similar work found is described in [WaCr94], but it addressed a macro-cell environment taking only LoS into account. A comparison with that paper was the start of this work. Nevertheless, along this work a deep study of the application of the RLS Beamforming Algorithm in a WDCM scenario in a UTRA-TDD perspective has been described and implemented. The effective gain of the beamforming utilisation has been demonstrated and proven. The RLS algorithm was implemented in MATLAB® and an adequate WDCM was used.

For the first WDCM scenario developed in Chapter 4, a set of average results has been extracted from applying the RLS algorithm to several WDCM concretisations. The general tendency is to increase the average SINR, while the cost function does not exhibit local minima. The relation between the number of arriving orthogonal signals and the number of existing antennas is the most important overall performance parameter. For this, several propagation cases have helped to analyse its influence in the final SINR results, either along iterations or in final values.

A general conclusion that arises from the average simulations phase is that the variability of the WDCM characteristics is much more severe in the cases where the number of orthogonal signals is larger, compared to the number of antennas. Also, great variations in the final SINR results among links has been observed for a number of antennas comparable to the number of codes. Variations of up to 20 dB between links have been found. Hence, as the averaging number of channel concretisations rises, such variation is compensated, and the SINR levels, Gbf and BER tend to similar levels. The major part of these results were obtained in Chapter 5.

The RLS is also known for the heavy calculations that it needs compared to the classical LMS; nevertheless, it is one of the algorithms that requires less iterations to convergence, always from the point of view of an implementation on the basis of sample-by-sample. That was the motivation to select it being confirmed than it requires a number relatively small of iterations and Flops. The complexity cost to add a new user to the RLS Adaptive Beamforming structure is low, and an approximated equation to estimate the number of Flops involved in that structure was presensted.

Concerning the beamformer processing gain, it has been seen that the cases considered in Chapter 4 imply a minimum of 23 dB effective gain. For the worst propagation conditions cases, the increasing evolution of the SINR and processing gain has been found to be smaller which was confirmed in Chapter 5 a positive gain being found in all studied cases.

A conclusion derived from Chapter 5 is that the length of the channelisation codes affects the convergence properties, the response with more users (varying the length of the channelisation code) being more stable; nevertheless, more iterations are needed, and the final Gbf and SINR are smaller, as expected. It was also confirmed that the SINR and Gbf depend on the number of antennas.

For all cases, and for all simulations, a positive beamforming gain has been found always larger than 7 dB. Although this work involves TDD, the same result may be expected for FDD. This is a theoretical study at baseband level, and many technical concepts that can influence its implementation were not considered, e.g. weight calibrations, analysis of the channel stationarity, influence of the modulation / demodulation process over the baseband level, the influence of synchronisation, etc. There are many areas to extend the study of Adaptive Antennas, mainly technological ones, that need to be clarified.

Appendix A Criteria and Algorithms for Adaptive Beamforming

A.1 Criteria

A.1.1 Method of Least Squares

The *Method of Least Squares* has been one of the most used in linear filtering. To describe the problem, considerer a physical phenomenon that is characterised by two sets of variables, $\{d(i)\}$ and $\{x(i)\}$. The variable *d(i)* is observed at time *i* in response to the subset of variables *x*(*i*), *x*(*i*+1), ...,*x*(*i*+*M*-1) applied as *inputs*.

To solve the LS problem a multiple linear regression model is used, being described as:

$$d(i) = \sum_{k=0}^{M-1} w_k^* x(i+k) + e_0(i) \tag{A.1}$$

where $e_0(i)$ is known as measurement error, being an unobservable random variable that is introduced into the model to account for its inaccuracy. It is customary to assume that the measurement error process $\{e_0(i)\}$ is white with zero mean and variance σ_e^2.

The implication of this assumption is that (A.1) can be written as:

$$E[d(i)] = \sum_{k=0}^{M-1} w_k^* x(i+k) \tag{A.2}$$

where the values of *x*(*i*), *x*(*i*+1), ..., *x*(*i*+*M*-1) are known. The mean of the response *d*(*i*), in theory, is uniquely determined by the model.

The problem to solve is to *estimate* the unknown parameters of the multiple linear regression model, the w_k, given the two *observable* sets of variables: $\{d(i)\}$ and $\{x(i)\}$, *i*=1,2...,*N*.

By forming inner products of *x*(*i*), *x*(*i*+1), ..., *x*(*i*+*M*-1) and w_1, w_2, ..., w_M, respectively and by using *d*(*i*) as the *desired response*, the *estimation error* $\xi(i)$ as the difference between the desired response *d*(*i*) and the output, *y*(*i*), as shown by:

$$\xi(i) = d(i) - y(i) \tag{A.3}$$

where

$$y(i) = \sum_{k=1}^{M} w_k^* u(i+k-1) \tag{A.4}$$

That is,

$$e(i) = d(i) - \sum_{k=1}^{M} w_k^* u(i+k-1) \tag{A.5}$$

In the method of LS the weights are chosen in the way to minimise a cost function that consists of the sum of error squares:

$$\xi(w_1, ..., w_M) = \sum_{i=i_1}^{i_2} |e(i)|^2 \tag{A.6}$$

where i_1 and i_2 define the index limits at which minimisation occurs. Depending on the type of windowing employed.

Basically, the problem has to solve, substituting (A.4) into (A.5) and then minimise (A.6) with respect to the weights.

A.1.2 Method of Steepest Descent

The *Method of Steepest Descent* (SD) is the basis for gradient-based algorithms. It is a *recursive* method due to calculate a new weight vector, going through the error surface minimising the squared error function, starting with a specific initialisation vector [GiCo00].

Just as in the Wiener filter, the SD is based on minimising the ensemble average of estimation error:

$$\xi(n) = d(n) - y(n) = d(n) - \mathbf{w}^{\mathrm{H}}\mathbf{x}(n) \tag{A.7}$$

where $\mathbf{w}^{\mathrm{H}}\mathbf{x}(n)$ is an estimate of the output signal $y(n)$.

Since the problem applies to a non-stationary channel, the weights vector will vary with n, and the estimation error will be function of $|n|$. The function to minimise in this method will be:

$$\xi^2(n) = E\left[\xi(n)\xi^*(n)\right] = R_d - \mathbf{w}^{\mathrm{H}}(n)\mathbf{r} - \mathbf{r}^{\mathrm{H}}\mathbf{w}(n) + \mathbf{w}^{\mathrm{H}}(n)\mathbf{R}_x\mathbf{w}(n) \tag{A.8}$$

where $\mathbf{r}$ is the cross-correlation $r = E\left[x(n)d^*(n)\right]$. R_d and $\mathbf{R}_x$ are the autocorrelation of d(n) and $\mathbf{x}(n)$ respectively.

The MSE is given by setting the gradient vector of (3.17) and equalling it to zero, and achieving the solution [Hayk91]:

$$\mathbf{w}_{\mathrm{opt}} = \mathbf{R}_{\mathrm{x}}^{-1}\mathbf{r} \tag{A.9}$$

The equation is also known as the Wiener-Hoptf or the optimum Wiener solution [Hayk91].

The SD Algorithm uses the error surface function, moving in such surface along the direction opposite to the higher MMSE increase, i.e., along the maximum gradient at such point [GiCo00]. If $\nabla\{\xi^2(n)\}$ is the gradient vector at instant *n*, the new weight vector estimate, at time *n*+1 is calculated by *:*

$$\mathbf{w}(n+1) = \mathbf{w}(n) + \frac{1}{2}|\mu|\left[-\nabla\{\xi^2(\mathrm{n})\}\right] \tag{A.10}$$

where μ is a positive real-valued constant that determines the convergence step.

Calculating the gradient vector from (A.8):

$$\nabla\{\xi^2(n)\} = -2\mathbf{r} + 2\mathbf{R}_x\mathbf{w}(n) \tag{A.11}$$

If $\mathbf{R}_x$ and $\mathbf{r}$ are known then, the gradient can be used and the new weights can be calculated as:

$$\mathbf{w}(n+1) = \mathbf{w}(n) + \mu\left[\mathbf{r} - \mathbf{R}_x\mathbf{w}(n)\right] \tag{A.12}$$

A.2 Adaptive Algorithms

At this point some adaptive algorithms will be presented. The choice of an adaptive algorithm is an important factor since its selection will determine both the speed of convergence and hardware complexity required to implement the algorithm [Hayk91], [LiLo96].

There are many algorithms that can be used to implement this kind of applications, being described some of them, mainly the most known, but existing much more. Some of these algorithms used in adaptive beamforming are the Least Mean Square (LMS), RLS (RLS), Constant Modulus Algorithm (CMA), Sample Matrix Inversion (SMI), Conjugate Gradient algorithm (CG), Neural Networks (NN) being impossible to talk of everyone.

Many adaptive algorithms derive from statistically optimum beamforming. For example, the SD, LMS and RLS algorithm derive from the Wiener filter or minimum mean squared error (MMSE) algorithms [GiCo00]. RLS was described in Chapter 4.

A.2.1 Least Mean Square Algorithm

The LMS is the most common adaptive algorithm for continuous adaptation, widely used due to its simplicity and low computational requirements. It is based on the SD method [Hayk91], [GiCo00]. It does not require the calculation of correlation matrices or matrix inversions. As the SD, it develops on the error-performance curve, according to a gradient vector. In SD both $\mathbf{R}_x$ and $\mathbf{r}$ are known, meanwhile in LMS both are estimated.

With LMS the convergence speed is directly dependent on the eigenvalues of $\mathbf{R}$ – smaller time constant corresponds to larger eigenvalue. Since the maximum and the minimum eigenvalues normally correspond to the strongest and the weakest sources, respectively, the LMS will imply that a strongest source will be cancelled before a weaker one [Hayk91].

The correlation matrix $\mathbf{R}$ is estimated by the input samples. There is an input vector, $\mathbf{x}(n)$, and the weight vector used to obtain the beamformer response, $\mathbf{w}^{\mathrm{H}}\mathbf{x}(n)$. The weights are estimated in each iteration and applied to the inputs.

$$\hat{\mathbf{R}}(n) = \mathbf{x}(n)\mathbf{x}^{\mathrm{H}}(n) \tag{A.13}$$

Then, afterwards an iteration the filter output will be:

$$\mathbf{y}(n) = \hat{\mathbf{w}}^{\mathrm{H}}(n)\mathbf{x}(n) \tag{A.14}$$

where $\hat{\mathbf{w}}(n)$ is the estimated weight vector; $\hat{\mathbf{w}}(n) = \begin{bmatrix} \hat{w}_1(n) & \hat{w}_2(n) & \dots & \hat{w}_M(n) \end{bmatrix}^{\mathrm{T}}$ and $\mathbf{x}(n)$ the input vector , $\mathbf{x}(n) = \begin{bmatrix} x(n) & x(n+1) & \dots & x(n+M-1) \end{bmatrix}^{\mathrm{T}}$.

Assuming that the desired signal, $d(n)$, is known, the second stage follows – calculation of the estimation error, $\xi(n)$:

$$\xi(n) = d(n) - y(n) \tag{A.15}$$

The weights can then updated as:

$$\hat{\mathbf{w}}(n+1) = \hat{\mathbf{w}}(n) + \mu\mathbf{x}(n)\xi^*(n) = \hat{\mathbf{w}}(n) + \mu\mathbf{x}(n)[d^*(n) - \mathbf{x}^{\mathbf{H}}(n)\hat{\mathbf{w}}(n)] \tag{A.16}$$

The gain constant μ, controls convergence characteristics of the random vector sequence $\mathbf{w}(n)$. Note that this is a continuously adaptive approach, where the weights are updated as the data are sampled such that the resulting weight vector sequence converges to the optimum solution. Continuous adaptation works well when statistics related to the signal environment are stationary. LMS is a very simple algorithm, used in many applications,

however its convergence characteristics depend on the eigenstructure of $\hat{\mathbf{R}}$ [Hayk91], [GiCo00].

In SD, the calculation of the weights vector involves the deterministic evolution through the error-performance surface, leading to the Wiener optimum solution. The LMS algorithm works in other way, not reaching the Wiener optimum, though converging toward it.

The μ factor controls both the speed convergence and the gradient noise, so μ must be found to maximise performance. To guarantee the convergence, i.e., the tendency for the transient response to reach zero, the following condition must be respected [GiCo00]:

$$0 < \mu < \frac{2}{\lambda_{\max}} \tag{A.17}$$

where $\lambda_{\max}$ is the maximum eigenvalue of $\mathbf{R}_x$. The problem of this criterion is that the matrix calculation does not make part of the LMS, so that a conservative estimate of $\lambda_{\max}$ is given by the trace of $\mathbf{R}_x$, tr[**R**].

$$0 < \mu < \frac{2}{\mathrm{tr}[\mathbf{R}]} \Leftrightarrow 0 < \mu < \frac{2}{\sum_{m=0}^{M-1} \mathrm{E}\left[\left|x(n-m)\right|^2\right]} \tag{A.18}$$

In fact, the definition of μ involves two conflictive behaviours: on one hand, larger steps imply reaching the vicinity of the solution faster, while on the other hand, smaller μ will mean lower convergence error, but slower convergence. A solution to the conflicting results of a large/small step size is to use a variable step size, along the iterations [GiCo00], [Hayk91].

A.2.2 Direct Sample Covariance Matrix Inversion

The Wiener solution, given by (A.9), can be approximated by using an estimate of the inverse of matrix $\mathbf{R}_x$. Remembering that the channel suffers frequent changes, the estimated weights can be calculated using block adaptation, as mentioned before. Therefore, the estimates of $\mathbf{R}_x$ and **r** can result from a simple arithmetic averaging calculation, an array data block which forms a total of N_b data vectors **[Goda97]**, [LiLo96].

$$\hat{\mathbf{R}}_x = \frac{1}{N_b} \sum_{i=0}^{N_b-1} \mathbf{x}(i)\mathbf{x}^{\mathbf{H}}(i) \tag{A.19}$$

$$\hat{\mathbf{r}} = \frac{1}{N_b} \sum_{i=0}^{N_b-1} d^*(i)\mathbf{x}(i) \qquad \text{(A.20)}$$

where upper and lower window limits refer to the array *snapshot* **[Goda97]**. $\hat{\mathbf{R}}_x$ is called the sample covariance matrix. According to [ReMB74], such is a maximum likelihood estimate of $\mathbf{R}_x$. As a consequence, the estimate of the weight vector can be calculated, similarly to the Wiener-Hopf equations, (A.9):

$$\hat{\mathbf{w}} = \hat{\mathbf{R}}_x^{-1}\hat{\mathbf{r}} \qquad \text{(A.21)}$$

As it is understood, as the size of the block or snapshot is raised, the correlation estimates approach their true value, nevertheless requiring more computational effort. The expected average loss in SNR compared to the optimum, due to using N_b data samples, is approximately less than 3dB if the number of samples is near 2*M*, recalling that *M* is the number of antenna elements. Such power loss reveals to be the trade-off between performance and the number of samples used in the SMI [ReMB74].

It can be said that the SMI is not a truly adaptive algorithm, in the sense that it is an open loop system. On the whole, though, it is adaptive since it is set to produce a weight vector for each new scenario. Accordingly, it is very important to balance the need for enough N_b data samples, for each correlation matrix estimate, on one hand, and to apply the resulting calculations in time before the environment changes, on the other.

Along with the input data being acquired periodically, the correlation estimated must be recomputed, depending on the rate of channel changes (referred to as *fading-rate* in mobile communications). In order to keep up with the required fast convergence, the calculation of the $\mathbf{R}_x^{-1}$ may follow the matrix inversion lemma introduced with the RLS algorithm (3.10), leading to a faster matrix calculation. The calculation can be made using a fast recursive algorithm just as with the RLS case ((3.13) to (3.16)) **[Goda97]**.

A major advantage of the algorithm is that, in case the eigenvalue spread of the *sample covariance matrix* being large, the performance is almost independent of it. This can result in several orders of magnitude faster convergence than the LMS, [LiLo96], [ReMB74]. The convergence rate will be dependent on the number of weights, being independent of the noise and interferences.

According to [Vaug88], the SMI is an algorithm with a great probability of being used for beamforming in mobile communications. It relies on its simple conception, its fast weight calculation capabilities and its independence of eigenvalue spread, as long as the number of

correlation samples is enough. Nevertheless, as far as number of complex products is concerned, using 2*M* data samples to calculate the matrix estimate will require a number of operations of O(M^3), which is much larger than other algorithms [ReMB74], [Vaug88]. Besides requiring more processing steps, the SMI also requires high digital signal processing accuracy.

A.2.3 Conjugate Gradient Algorithm

The CG Algorithm is an alternative to the widely used LMS, RLS, not requiring matrix inversions and avoiding in stability problems [GiCo00].

This method is used to solve the $\mathbf{Xw}=\mathbf{d}$ system in order to obtain **w**. For array processing, the weight vector, **w**, needs to be calculated, **d** can be a vector composed by N_s consecutive desired responses, **x** can be a matrix whose *M* columns refer to each of the *M* array elements, and each lines correspond to each sampling period, out of the total N_s sampling periods.

The cost function that is involved with such linear equation system solving is given by *f*(**w**), called *quadratic form* [GiCo00]:

$$f(\mathbf{w})=\frac{1}{2}\mathbf{w}^{\mathrm{T}}\mathbf{Xw}-\mathbf{w}^{\mathrm{T}}\mathbf{d} \qquad \text{(A.22)}$$

and the minimum of such quadratic form is the solution to the system.

In this way, the cost function is also said to be the sum of the squared error given by $\mathbf{res}^{\mathrm{H}}(n)\mathbf{res}(n)$, where $\mathbf{res}(n)=\mathbf{d}-\mathbf{Xw}$, or by $\|\mathbf{Xw}-\mathbf{d}\|^2$

The approach used in CG is a search of orthogonal directions and to choose one of these in order to minimise the error along one search direction, for very iteration.

During the iteration process, residual and direction vectors, **res**(n) and **dir**(n), respectively, are updated in order to calculate the successive weight vector. The recursive equation of this vector is similar to the used in the LMS, in (A.16).

$$\mathbf{w}(n)=\mathbf{w}(n-1)+\mu(n)\mathbf{dir}(n) \qquad \text{(A.23)}$$

In this case the step-size parameter $\mu(n)$ is calculated for each repetition of the algorithm minimising the cost function in the **dir**(n) direction of the steepest descent

A.2.4 Constant Modulus Algorithm

The Constant Modulus Algorithm (CMA), also called Godard algorithm [GiCo00], is a particular case of the Bussgang algorithms [Hayk91], [LiLo96]. These are blind adaptive techniques, in the sense that these develop independently from training sequences, by trying to restore a known property of the received signal. Though these adaptive beamforming algorithms have been developed for equalisation, its use is possible adaptive beamforming [GiCo00].

However, the CMA is found not to be adequate for CDMA systems [GiCo00], in particular, the power control process, inherent to preventing the near-far effect in CDMA mobile case, will affect the variation of envelopes, either per physical channel (code) or between each chip (in UMTS), influencing above the CMA, eliminating the envelope fluctuations in which the algorithm is based [GiCo00].

A.2.5 Other Algorithms

Other algorithms are present at the literature as Neural Networks which are an ideal tool for use in adaptive signal processing. The application of NN can result in very attractive solutions to complex problems, due to the intrinsic interconnected structure, processing efficiency and fast convergence. A Neural Network may consist of a layered or multilayered nonlinear network that tries to reproduce human intellectual capabilities through a “learning” and “adapting” process. NN can be an ideal tool for use in adaptive signal processing, where a signal-processing problem is represented in terms of optimisation with a cost function matches the energy function of a particular neural network by minimising its energy function. Recurrent networks are usually suitable for this type of processing, in which the output of a neuron is fed back as inputs to other neurons and/or to itself.

Also the MUSIC algorithm is present in the literature as Beamforming implementation in [Goda97] where a study about this possibility is addressed.

Appendix B Plots of the Cases Under Study of Chapter 4

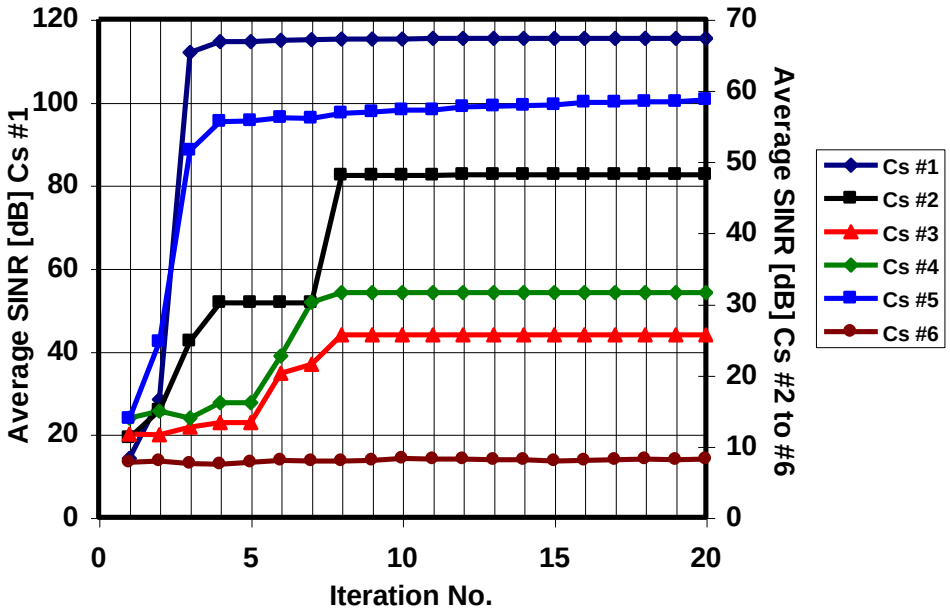

Figure B.1. Average SINR vs. the number of iterations, for link MT2-BS.

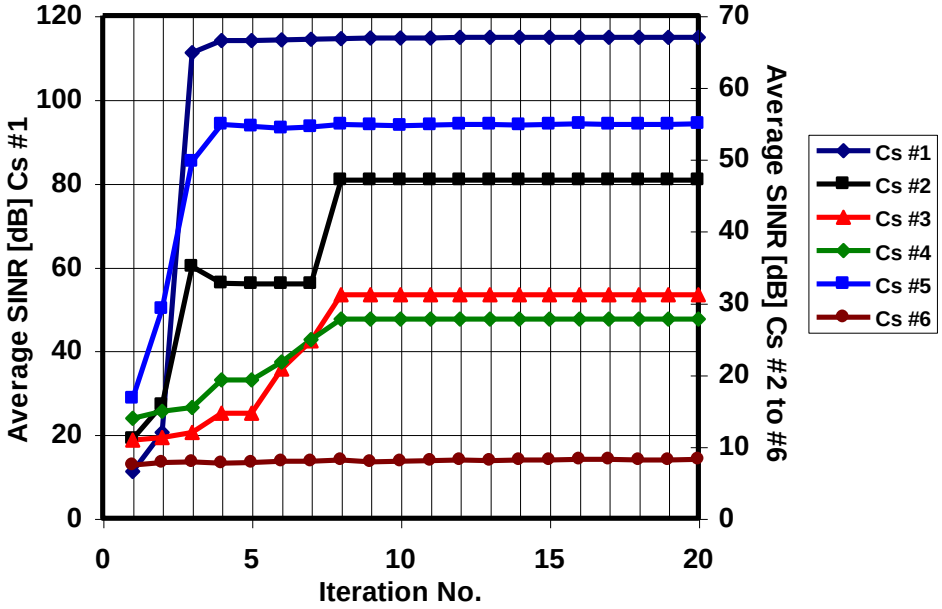

Figure B.2. Average SINR vs. the number of iterations, for link MT3-BS.

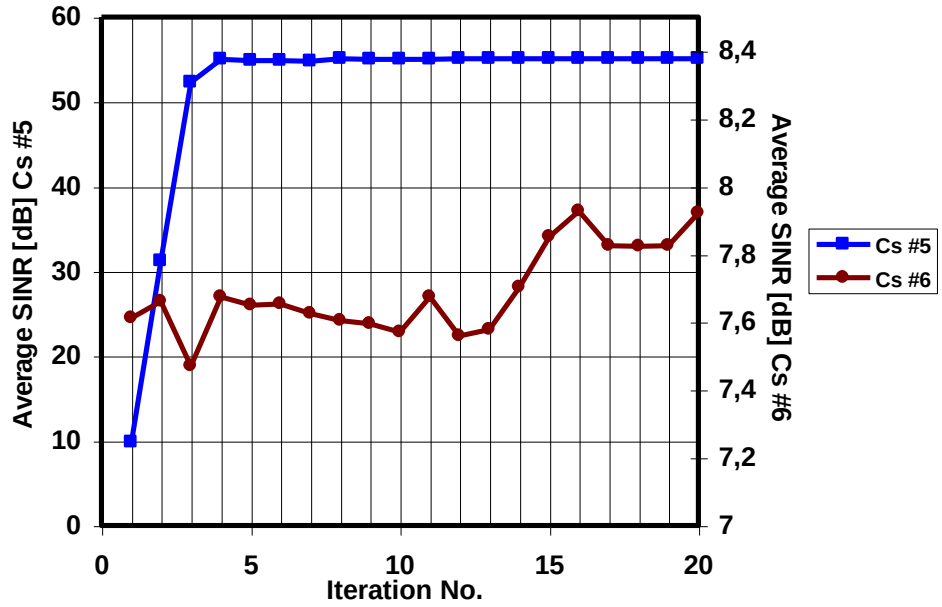

Figure B.3. Average SINR vs. the number of iterations, for link MT4-BS.

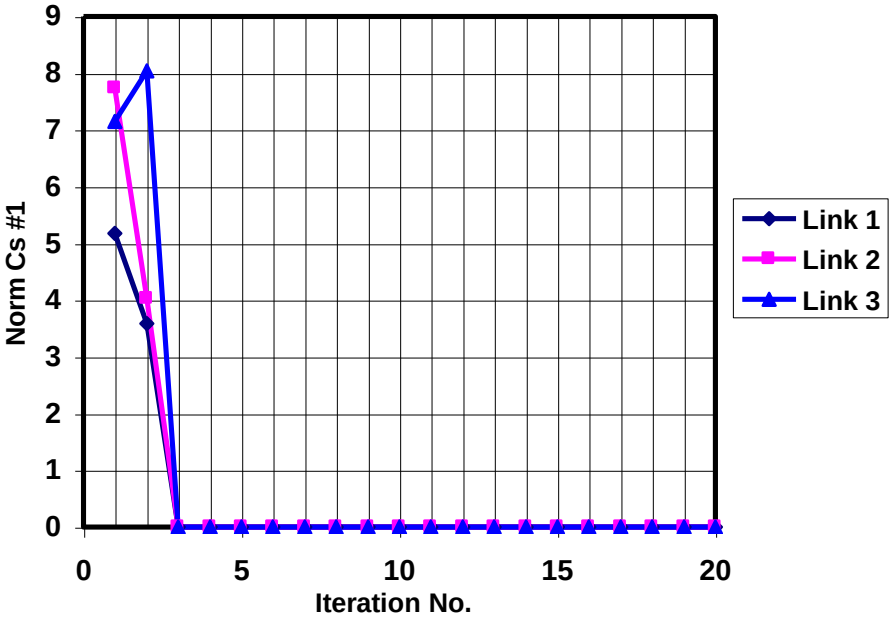

Figure B.4. Residual Norm for Cs #1.

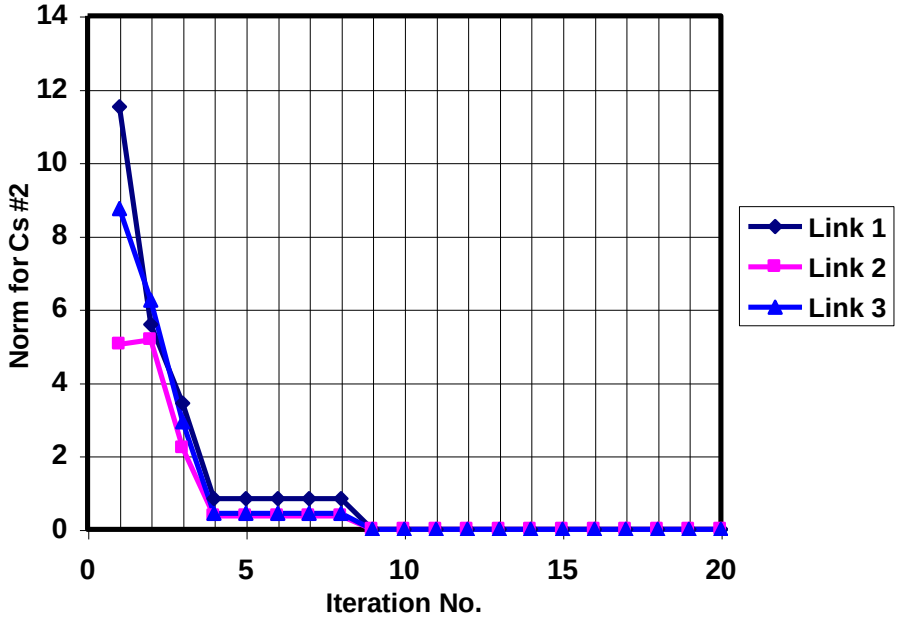

Figure B.5. Residual Norm for Cs #2.

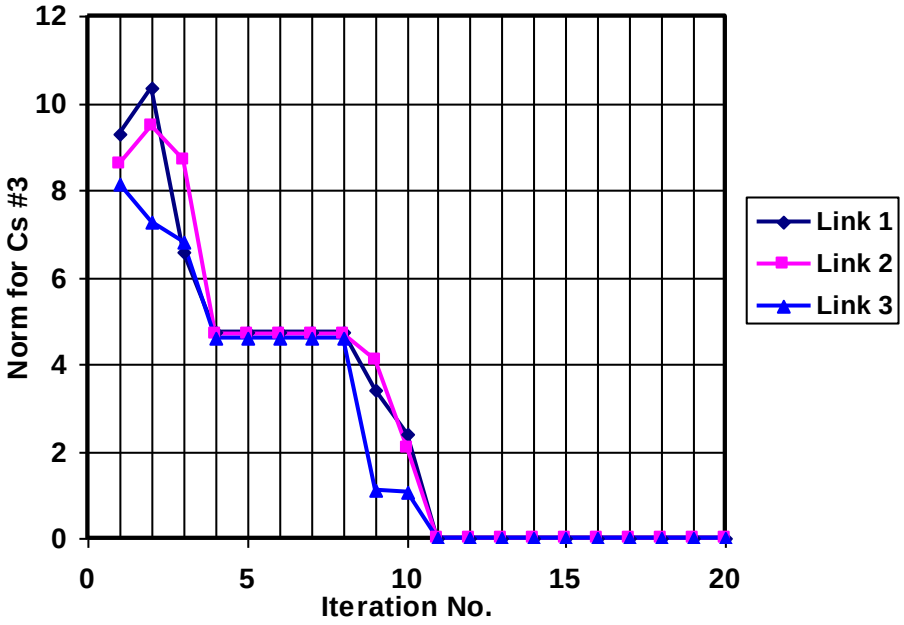

Figure B.6. Residual Norm for Cs #3.

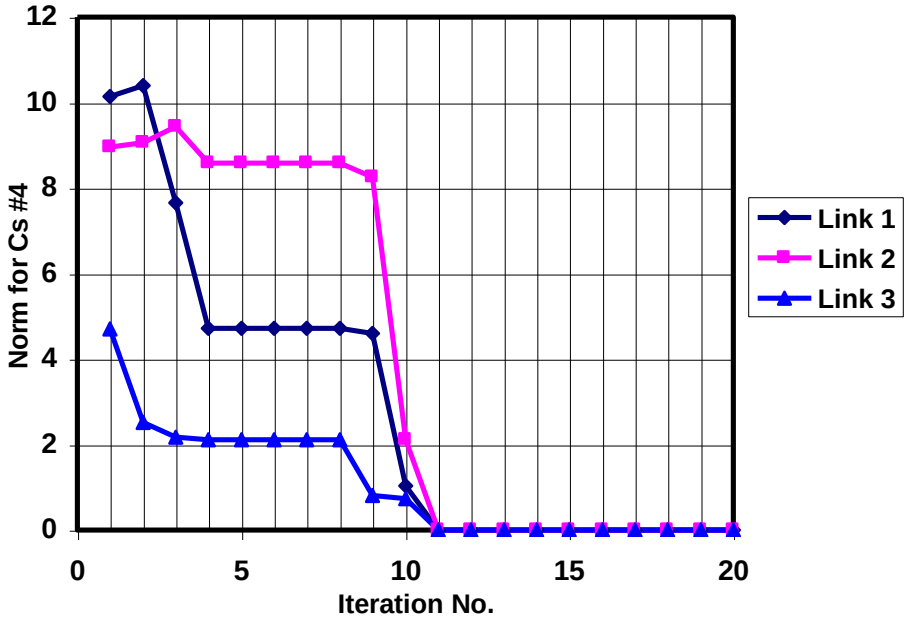

Figure B.7. Residual Norm for Cs #4.

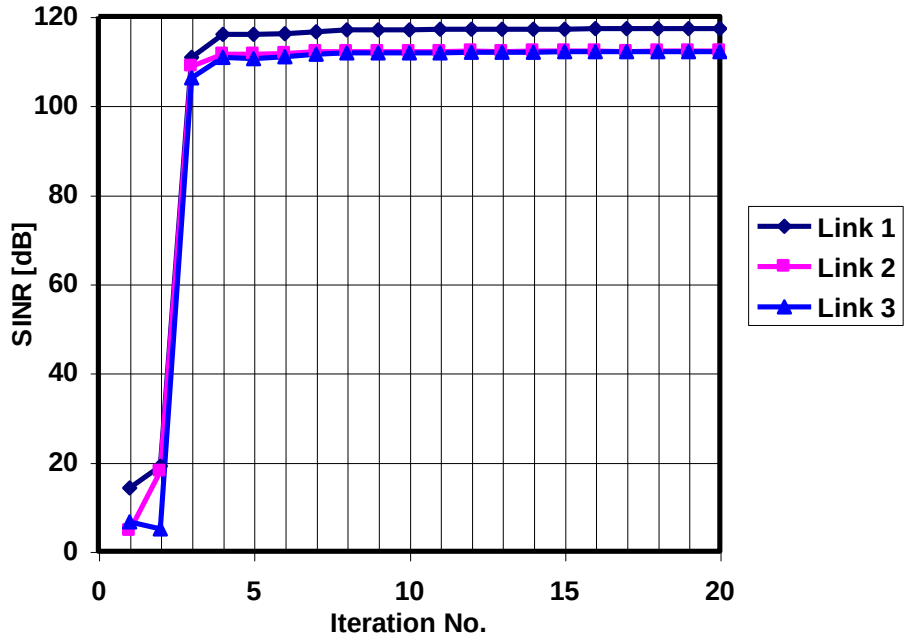

Figure B.8. SINR for Cs #1.

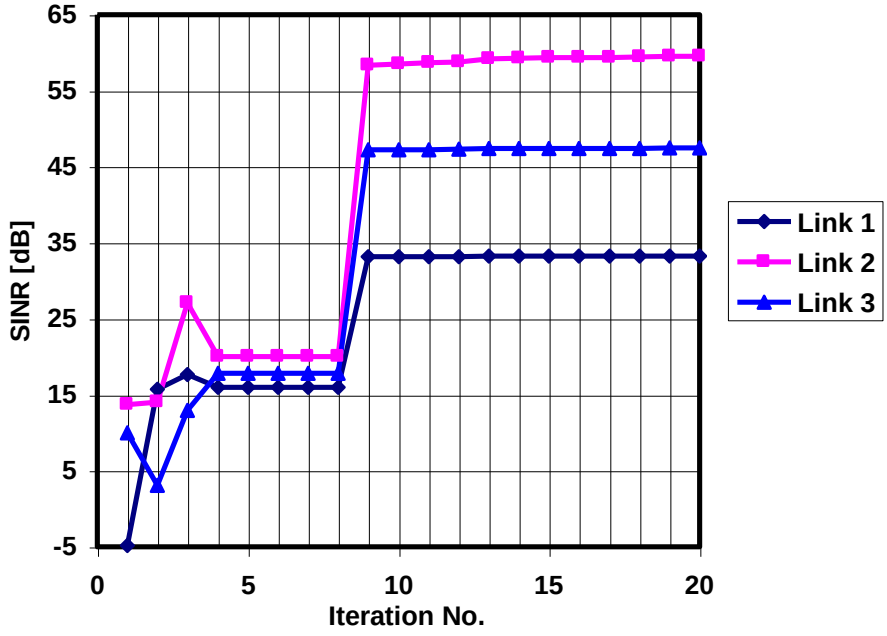

Figure B.9. SINR for Cs #2.

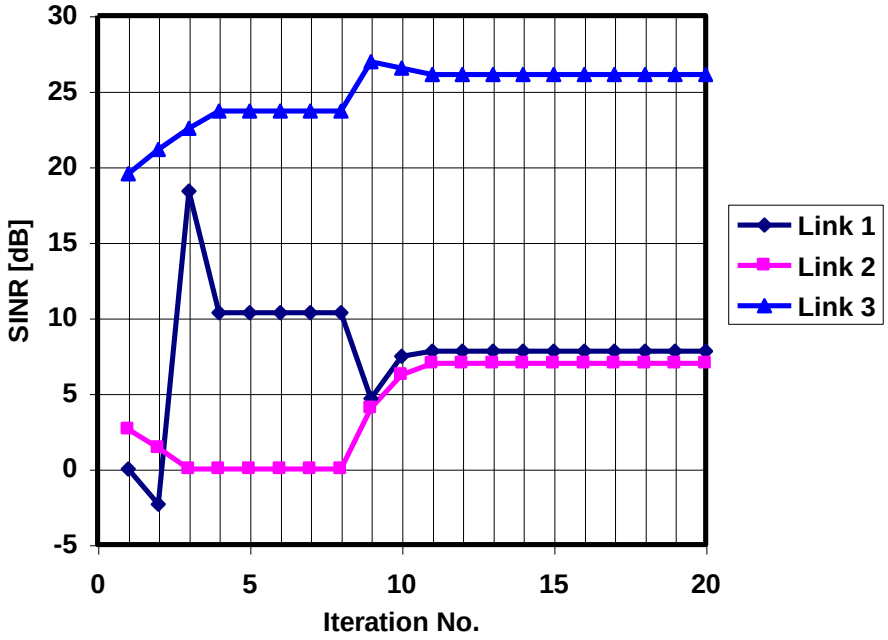

Figure B.10. SINR for Cs #4.

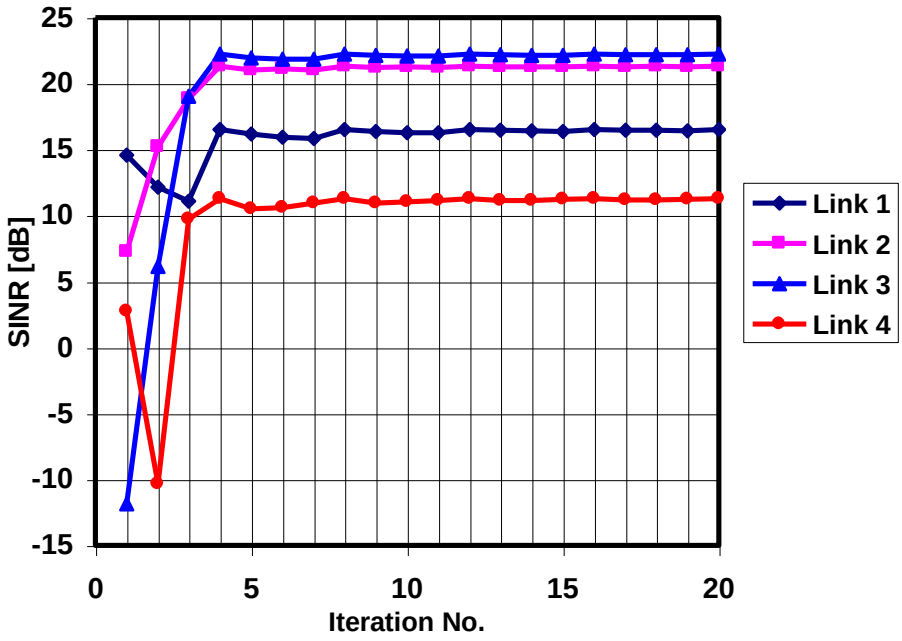

Figure B.11. SINR for Cs #5.

Appendix C Plots of other Scenarios of Simulation

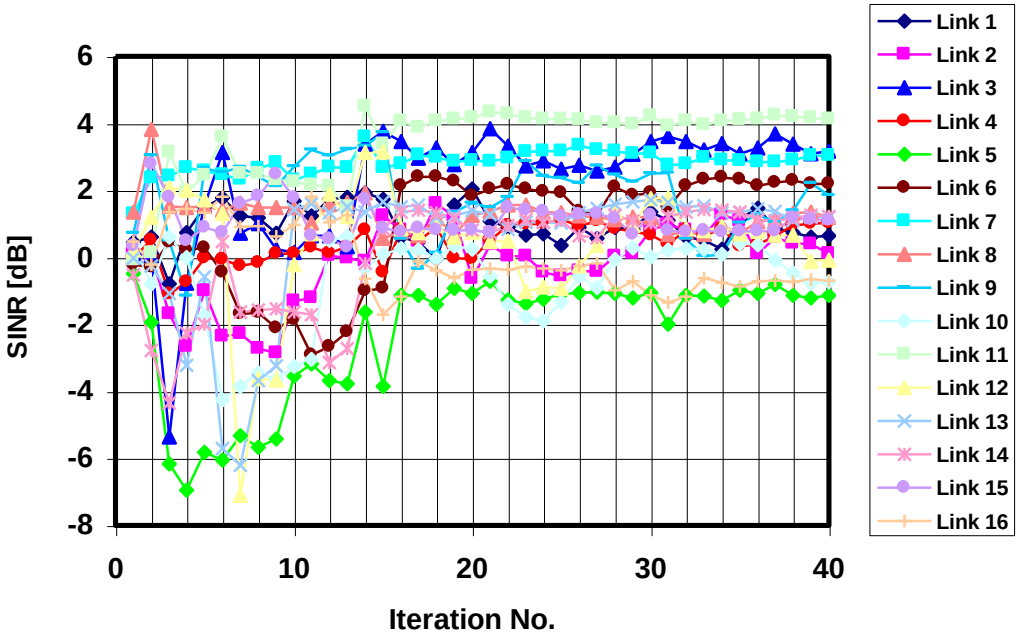

Figure C.1. SINR vs. the number of RLS iterations for 16 links and *M*=4.

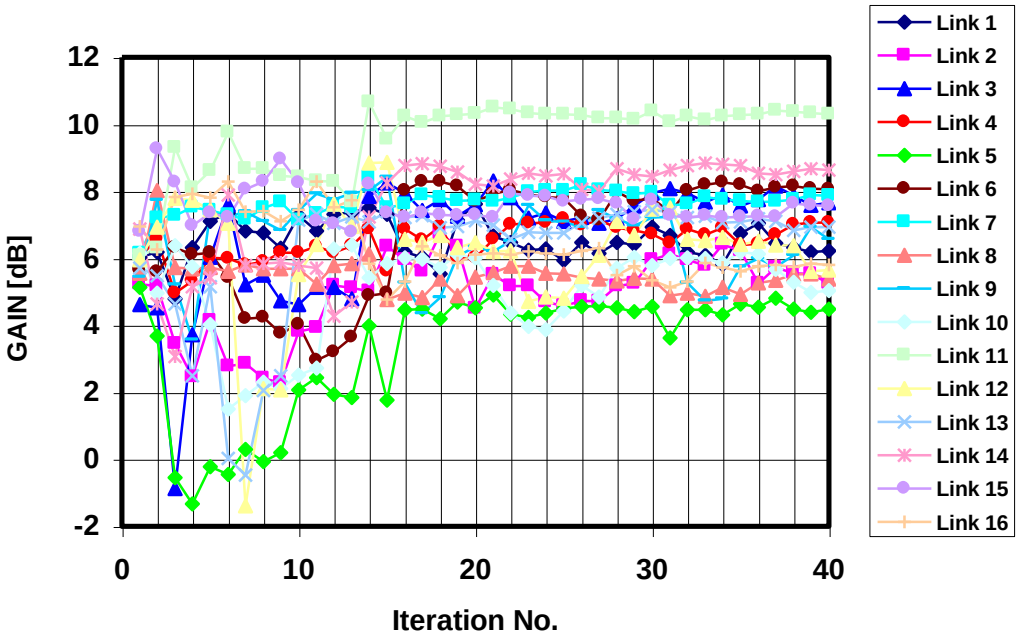

Figure C.2. Gain vs. the number of RLS iterations for 16 links and *M*=4.

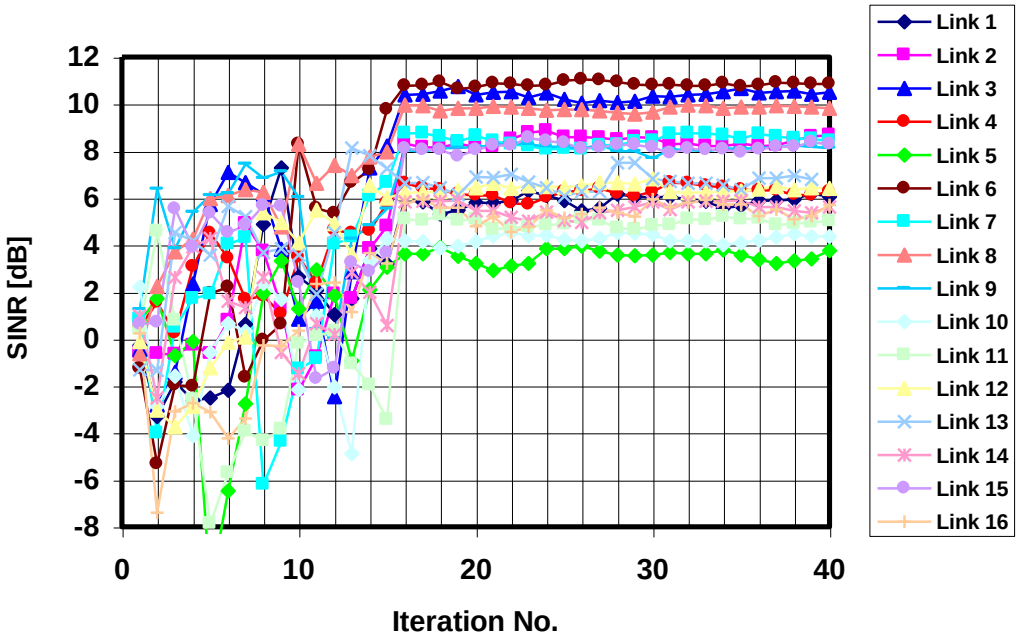

Figure C.3. SINR vs. the number of RLS iterations for 16 links and *M*=12.

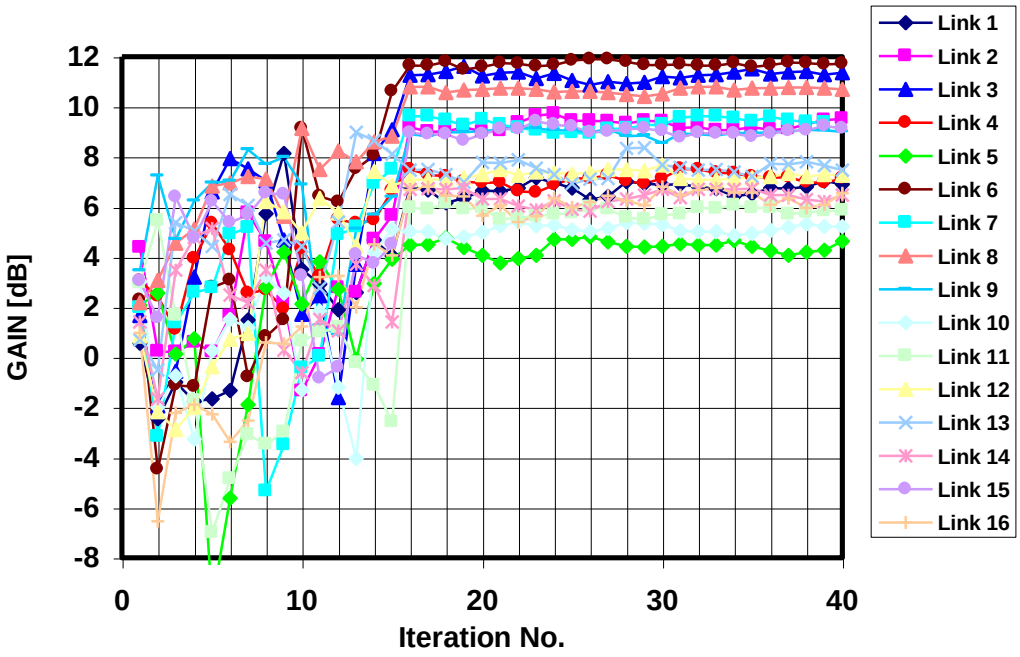

Figure C.4. Gain vs. the number of RLS iterations for 16 links and *M*=12.

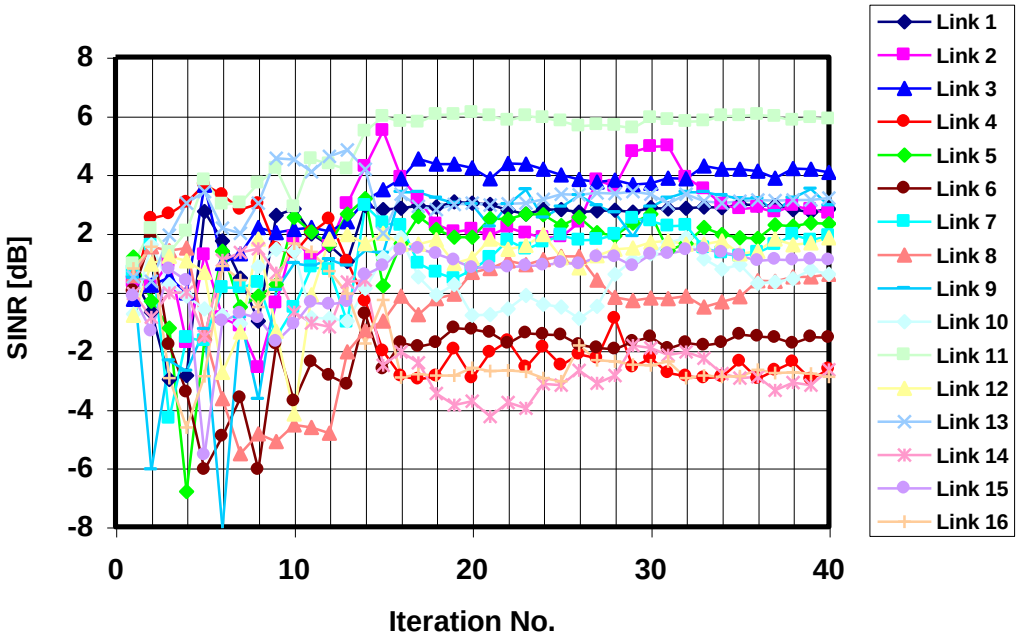

Figure C.5. SINR vs. the number of RLS iterations for 16 links and *M*=6.

References

[Carl86] Carlson,A.B., *Communication Systems*, McGraw Hill, Singapore, 1986.

[CFRR97] Cardona,N., Flores,S., Reig,J., Rubio,L. and Fraile,R., *Mobile Communications* (in Spanish), SPUPV, Polytechnical University of Valencia, Valencia, Spain, 1997.

[ChMO99] Chaudhury,P., Mohr,W. and Onoe,S., "The 3GPP Proposal for IMT-2000", *IEEE Communications Magazine*, Vol. 37, No. 7, Dec. 1999, pp. 72-81.

[DiTa00] Dimitriou,N. and Tafazolli,R. "Quality of Service for multimedia CDMA", *IEEE Communications Magazine*, Vol. 38, No. 7, Jul. 2000, pp. 88-94.

[Fern99] Fernandes,E. (ed.), *UE Radio transmission and reception (FDD)*, 3GPP Technical Specification, No. 25.101, Ver. 3.1.0, Oct. 1999, ftp://ftp.3gpp.org/Specs/December_99/25_series/.

[Fern00] Fernandes,B., *Capturing the Value of UMTS and Driving the New Economy*, Short Course, Instituto Superior Técnico, Lisbon, Portugal, Oct. 2000.

[GiCo00] Gil,J. and Correia,L.M., *Review on Beamforming Adaptive Algorithms*, IST-ASILUM Project, Internal Report IST/TUL/IN/Int./025/0.1, IST, Lisbon, Portugal, Nov. 2000.

[GiCo01] Gil,J.M. and Correia,L.M., "An Implementation of Beamforming Adaptive Algorithms to Particular Mobile Propagation Conditions in UMTS", in *Proc. of Conftele 2001 – 3rd Conference on Telecommunications*, Figueira da Foz, Portugal, Apr. 2001.

[GiMC01] Gil,J.M., Mendez,J.L. and Correia,L.M., "Comparison of Recursive Least Squares and Conjugate Gradient Applied to Adaptive Beamforming in UMTS", in *Proc. of IST-MCS2001 – IST Mobile Communications Summit 2001*, Barcelona, Spain, Sep. 2001.

[Goda97] Godara,L.C., "Application of antenna Arrays to Mobile Communications, Part II: Beam-forming and Direction-of-Arrival Considerations", *Proc. of the IEEE*, Vol. 85, No. 8, Aug. 1997, pp. 1193-1245.

[GoLo96] Golub,G.H. and Loan,C.F. Van, *Matrix Computations*, The John Hopkins University Press, Baltimore, Maryland, USA, 1996.

[Hayk91] Haykin,S., *Adaptive Filter Theory*, Prentice Hall, Upper Saddle River, NJ, USA, 1991.

[Hira00] Hiramatsu,K. (ed.), *Physical channels and mapping of transport channels onto physical channels (TDD)*, Technical Specification Group Radio Access Network, 3GPP Technical Specification, No. 25.221, Ver. 3.4.0, Sep. 2000, ftp://ftp.3gpp.org/Specs/2000-09/R1999/25_series/.

[HoTo00] Holma,H. and Toskala,A., *WCDMA for UMTS*, John Wiley & Sons, London, UK, 2000.

[Ito00a] Ito,K. (ed.), *Spreading and Modulation (TDD)*, Technical Specification Group Core Network, 3GPP Technical Specification, No. 25.223, Ver. 3.4.0, Sep. 2000, ftp://ftp.3gpp.org/Specs/2000-09/R1999/25_series/.

[Ito00b] Ito,K. (ed.), *Spreading and Modulation (FDD)*, Technical Specification Group Core Network, 3GPP Technical Specification, No. 25.212, Ver. 3.4.0, Sep. 2000, ftp://ftp.3gpp.org/Specs/2000-09/R1999/25_series/.

[LiLo96] Litva,J. and Lo,T.K., *Digital Beamforming in Wireless Communications*, Artech House, Norwood, MA, USA, 1996.

[LiRa99] Liberti,J.C. and Rappaport,T.S., *Smart Antennas for Wireless Communications: IS-95 and Third Generation CDMA Applications*, Prentice Hall, Upper Saddle River, NJ, USA, 1999.

[MaCo01] Marques,M.G. and Correia,L.M., "A Wideband Directional Model for UMTS Micro-Cells", in *Proc. of Conftele 2001 – 3rd Conference on Telecommunications*, Figueira da Foz, Portugal, Apr. 2001.

[Marq01] Marques,M.G. "A Wideband Directional Model for Micro-Cells in UMTS", M.Sc. Thesis, IST, Lisbon, Portugal, 2001.

[MGFC01] Marques,G., Gil,J., Ferreira,L. and Correia,L.M., *The COSSAP Radio Channel modules: Models, Implementation and Interface Description*, IST-ASILUM Project, Internal Report IST/TUL/IN/Int./029/0.1, IST, Lisbon, Portugal, Jan. 2001.

[Mous97] Moustakides,G.V. “Study of the transient Phase of the Forgetting Factor RLS”, *IEEE Transactions on Signal Processing*, Vol. 45, No. 10, Oct. 1997, pp. 2468-2476.

[ReMB74] Reed,I.S., Mallett,J.D. and Brennan,L.E., “Rapid Convergence Rate in Adaptive Arrays”, *IEEE Transactions on Aerospace and Electronic Systems*, Vol. AES-10, No. 6, Nov. 1974, pp. 853-863.

[Shew94] Shewchuk,J.R., *An Introduction to the Conjugate Gradient Method Without the Agonising Pain*, Internal Report, School of Computer Science, Carnegie Mellon University, Pittsburgh, PA, USA, Aug. 1994 (available at http://www.cs.cmu.edu/~jrs/jrspapers.html).

[Tosk00] Toskala,A. (ed.), *Physical Layer - General Description*, Technical Specification Group Radio Access Network, 3GPP Technical Specification, No. 25.201, Ver. 3.1.0, Jun. 2000, ftp://ftp.3gpp.org/Specs/2000-09/R1999/25_series/.

[UMTS98a] UMTS Forum, *UMTS/IMT-2000*, UMTS Forum Report No. 6, London, UK, Dec. 1998.

[UMTS98b] UMTS Forum, *Minimum spectrum demand per public terrestrial UMTS operator in the initial phase*, UMTS Forum Report No. 5, London, UK, Dec.1998.

[Vaug88] Vaughan,R.G., “On Optimum Combining at the Mobile”, *IEEE Transactions on Vehicular Technology*, Vol. 37, No. 4, Nov. 1988, pp. 181-188.

[VeBu88] Van Veen,B.D. and Buckley,K.M., “Beamforming: A Versatile Approach to Spatial Filtering”, *IEEE Acoustics, Speech and Signal Processing Magazine*, Vol. 5, No. 2, Apr. 1988, pp. 4-24.

[WaCr94] Wang,Y. and Cruz,J.R., “Adaptive Antenna Arrays for the Reverse Link of CDMA Cellular Communication Systems”, *IEE Electronics Letters*, Vol. 30, No. 13, Jun. 1994, pp. 1017-1018.

[ZoMa00] Zollinger,E. and Marques,M.G., *WDCM and Measurement Campaign*, IST-ASILUM Project, Deliverable D2.1, IST, Lisbon, Portugal, Nov. 2000.